Australian Government

Department of Defence
Defence Science and
Technology Organisation

Contruction Techniques for LC Highpass and Lowpass Filters used in the 1 MHz to 1 GHz Frequency Range

W. Martinsen

DSTO-TN-0531

Australian Government
Department of Defence
Defence Science and
Technology Organisation

Construction Techniques for LC Highpass and Lowpass Filters used in the 1 MHz to 1 GHz Frequency Range

W. Martinsen

Intelligence, Surveillance and Reconnaissance Division
Information Sciences Laboratory

DSTO-TN-0531

ABSTRACT

This technical note describes construction techniques for building passive LC highpass and lowpass filters whose intended use spans several octaves of bandwidth. It examines limitations in the frequency domain of the two basic components, inductors and capacitors, used to build these filters, the unwanted effects of the distributed reactance of opposite sign to the wanted within these components and the electro-magnetic coupling between these components when used to build a filter. The impact these unwanted characteristics have on the filter's overall performance is then examined. Recommendations are given on the various steps that may be taken to reduce these unwanted effects minimising the deviation from a filter's ideal performance.

Published by

DSTO Information Sciences Laboratory
PO Box 1500
Edinburgh South Australia 5111 Australia

Telephone: (08) 8259 5555
Fax: (08) 8259 6567

AR- 012-994
October 2003

APPROVED FOR PUBLIC RELEASE

Construction Techniques for LC Highpass and Lowpass Filters used in the 1 MHz to 1 GHz Frequency Range

Executive Summary

Commercial off-the-shelf and in-house manufactured inductors and capacitors have many unwanted characteristics that alter the manufacturer's indicated component value with frequency. This is reflected as a deviation in a filter's performance from the ideal when it is constructed using these components. A literature search on construction methods to minimise this deviation revealed this issue had not been adequately addressed and thereby motivated an in-house investigation. This investigation was carried out in conjunction with the construction of hardware for the LLISP (Low Latitude Ionospheric Sounding Program) and Perseus projects.

This technical note describes construction techniques for building passive highpass and lowpass filters whose intended use spans several octaves of bandwidth. Its objective is to minimise the difference in response between a filter constructed with ideal components to one using real off-the-shelf or in-house manufactured components. It describes the basic limitations of the real-world components, their impact on the filter's overall response and various techniques that can be employed to improve their performance.

Author

Wayne M. Martinsen
Intelligence, Surveillance and
Reconnaissance Division

Author's CV

Wayne Martinsen was indentured as an apprentice communications technician in 1972 with Transport Communications Pty. Ltd.(Buranda, Qld.). He attended Yeronga Technical College (Brisbane, Qld.) where he received honours in the majority of his subjects. In 1975 his apprenticeship indentures were transferred to The Radio Centre (Archerfield Aerodrome, Qld.) where he was employed as an Air Maintenance Engineer, Category Radio. He was involved in all aspects of repair and maintenance of avionics systems associated with the light aircraft industry. Upon completing his training as an apprentice he sat for and passed various Dept. of Transport Licensed Air Maintenance Engineer (L.A.M.E.) exams. In 1977 he joined the R.A.A.F. and after graduating from their School of Radio, where he received training in military systems, he worked on a wide variety of airborne communications, navigation and anti-submarine warfare systems. In 1986 he was discharged from the R.A.A.F. and applied for a position with D.S.T.O. at Edinburgh. He was offered and accepted the position of Technical Officer (Engineering) with Intelligence, Surveillance and Reconnaissance Division. Here he was tasked with the design and development of R.F. circuits required for tropospheric and ionospheric research.

Contents

1. Introduction

This paper is limited to passive LC lowpass and highpass filters in which the sum of series reactances when multiplied with the sum of the shunt reactances produces an average value of k_{av} which is independent of frequency.

The value of k for a simple second order filter is:-

$$k = X_L X_C = \frac{2\pi fL}{2\pi fC} = \frac{L}{C} \tag{1.1}$$

where: X_C = capacitive reactance (Ω)
X_L = inductive reactance (Ω)
C = capacitance (F)
L = inductance (H)
f = frequency (Hz)

The average value of k_{av} for a filter greater than second order is therefore:-

$$k_{av} = \frac{L_1 + L_2 + L_3 + ...L_n}{C_1 + C_2 + C_3 + ...C_m} \tag{1.2}$$

The Z_O (characteristic impedance) of this filter is:-

$$Z_O = \sqrt{\frac{L_1 + L_2 + L_3 + ...L_n}{C_1 + C_2 + C_3 + ...C_m}} = \sqrt{k_{av}} \tag{1.3}$$

Examples of passive highpass and lowpass LC filters whose value of k_{av} is independent of frequency are:-

Constant k
Gaussian
Bessel or Thomson
Butterworth
Legendre-Papoulis
Chebyshev

It should be noted that filters are not necessarily terminated with their Z_o. Chebyshev filters for example rely on differences between the Z_o and terminating impedances to give a desired slope to the filter skirt. This mismatch also gives rise to a passband ripple. The larger the difference between the Z_o and the terminating impedances, the greater the passband ripple and the steeper the filter's skirt.

Highpass and lowpass filters with the same characteristic impedance (Z_o) and whose combined passbands span several octaves can be assimilated to form one complex filter. For example a 2 MHz highpass and a 30 MHz lowpass can be combined to form a 2-30 MHz bandpass filter. Figure 1.1 describes how the filter's components are connected to form this complex bandpass filter. It should be realised that this is two separate filters that have been combined in a space saving exercise. The product of the summation of the shunt and the summation of the series reactances of this complex filter will still return a k_{av} that is independent of frequency and the square root of which will be the filter's average characteristic impedance.

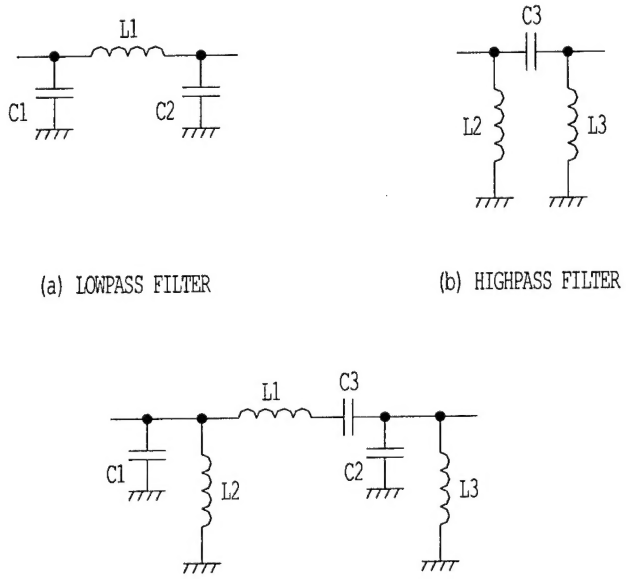

Figure 1.1 *Example of combining a lowpass and a highpas filter into a complex bandpass filter*

Filters whose value of k_{av} is frequency dependent usually employ resonant circuits in the shunt and/or series path. While this technical note is not directly aimed at such filters, the analysis of component limitations and some of the construction recommendations given are relevant. Examples of these filters are:-

Narrow bandpass
Narrow bandstop
Elliptic
m derived.

The component values of an R.F. (Radio Frequency) filter calculated using a software package, look-up tables or from first principles, are lumped components, that is, they are considered to be ideal. In the real world these components occupy three-dimensional space. A consequence of this three dimensional space is the production of components which have unwanted internal distributed resistance, reactance of opposite sign to the wanted, plus unwanted reactive coupling both internally and with other components in their surrounding environment.

For capacitors the main problem areas are distributed plate inductance and the self-inductance of the component connecting leads; in inductors it is the distributed capacitance between turns. Capacitors and inductors have distributed resistance; they also have magnetic and electric coupling both internally and to other surrounding components. Inductors, because of their larger physical size, tend to be more sensitive to their installed environment. Figure 1.2 shows the basic models used for the reactive components throughout this text.

At low R.F. frequencies the unwanted internal reactance is usually swamped by the component's desired characteristics. As the frequency is raised, the desired characteristics are more seriously degraded by the unwanted distributed reactance of opposite sign. A point will eventually be reached where the wanted and unwanted reactances will be equal in magnitude but of opposite sign. This is the component's self-resonant frequency. Raising the frequency beyond the self-resonant point changes the sign of the reactance, i.e. inductors behave like capacitors and capacitors like inductors. This is a very important characteristic of reactive components at R.F. frequencies which has serious ramifications in component selection and in filter construction techniques.

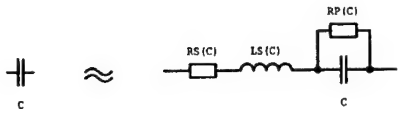

C = TRUE CAPACITANCE
RS(C) = DISTRIBUTED RESISTANCE OF CAPACITOR'S PLATES AND LEADS
LS(C) = SELF INDUCTANCE CAPACITOR'S PLATES AND LEADS
RP(C) = DIELECTRIC LOSS SEEN IN PARALLEL WITH TRUE CAPACITANCE

(A) EQUIVALENT CIRCUIT OF A CAPACITOR

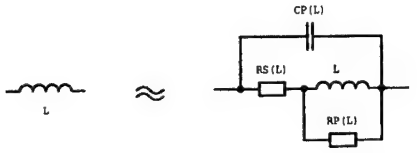

L = TRUE INDUCTANCE
RS(L) = DISTRIBUTED RESISTANCE OF WIRE
CP(L) = DISTRIBUTED CAPACITANCE OF WINDING
RP(L) = LOSS ASSOCIATED WITH INDUCTANCE ENHANCING MATERIAL

(B) EQUIVALENT CIRCUIT OF AN INDUCTOR

Figure 1.2 *Models of equivalent circuits for C and L*

1.1 Changes in a Lowpass Filter with Frequency

Take for example a third order L.P. (Lowpass) filter for use in the H.F. (High Frequency) band comprising a series inductor between two shunt capacitors, figure 1.3(A). In figure 1.3(B) the circuit's components have been expanded to show the lumped and distributed elements. Examining the insertion loss of this filter from the -3dB point upwards in frequency, using the model in figure 1.3(B), will show the expected increase in attenuation until the input frequency reaches the self-resonant frequencies of the individual components. Here, the shunt capacitors will be series resonant providing low impedance paths to ground and the series inductor will become parallel resonant isolating the input from the output with the resonant circuit's high dynamic impedance. The filter's insertion

loss will show unexpected peaks and dips as the input signal generator is swept through these resonances. Increasing the input frequency still further will show a gradual decrease in attenuation.

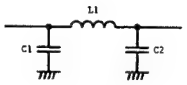

(A)

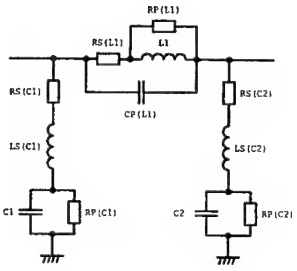

(B)

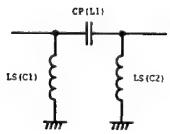

(C)

Figure 1.3 *Change in characteristics of a lowpass filter at high frequencies*

The individual filter components have changed their sign and given the lowpass filter the apparent characteristics of a highpass. This is seen in figure 1.3(C) where only those elements that play a major role in the circuit's behaviour have been shown. With the circuit components changing their characteristics at different frequencies it is possible to observe, over a narrow band, a decrease in the out of passband attenuation to as little as a few dB. Fitting this filter to the front end of a H.F. receiver would not protect the receiver from interference caused by high power V.H.F./U.H.F. television channels, fixed and mobile V.H.F./U.H.F. communications, navigation or radar systems.

The following are the frequency responses of poorly constructed L.P. filters. Figure 1.4 shows the out-of-passband response of a 2 MHz 5th order L.P. filter. It was made using half inch ferrite toroids for the inductors, 350 V silver mica capacitors and housed in a Pomona 3301 box with an internal shield installed between the two coils. Maximum out-of-band attenuation occurs at approximately 5.3 MHz and not at approximately 16 MHz where the shunt capacitors were measured to be series resonant. This discrepancy is due to unwanted coupling between the filter's components, through the incorrect use of shielding, which masked the capacitors' series resonances. Notice the decrease in attenuation with increasing frequency from approximately 5.3 MHz, where attenuation is maximum, up to 320 MHz. From 320 MHz onwards, power is being absorbed by the toroid's ferrite material causing an increase in attenuation with increasing frequency.

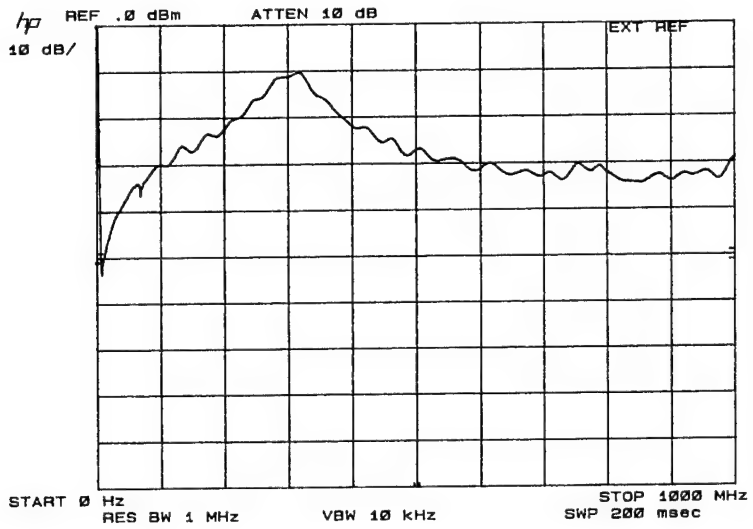

Figure 1.4 *Out-of-band frequency response of a 2 MHz L.P. filter*

Figure 1.5 is a plot of the out-of-passband response of a 28 MHz 5th order L.P. filter. It was made using air wound coils, 350V silver mica capacitors and housed in a Pomona 3301 box with an internal shield installed between the two coils. This is another case of the incorrect use of shielding allowing unwanted coupling between the filter's components. The shunt capacitors' series resonances occur at approximately 122 MHz and not at 95 MHz where the out-of-band attenuation is at a maximum. The absence of power absorption from the coils by inductance enhancing material does allow some of their series resonances at Ultra High frequencies to be observed. These are seen as peaks at approximately 560 MHz, 630 MHz and 940 MHz.

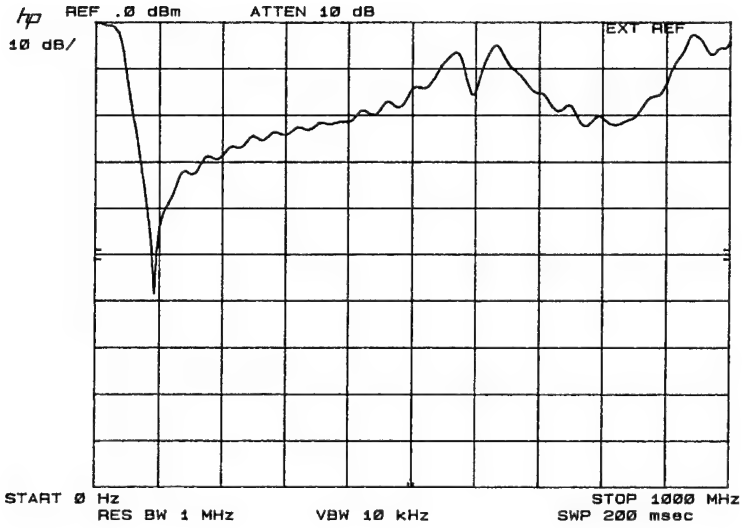

Figure 1.5 *Out-of-band frequency response of a 28 MHz L.P. filter*

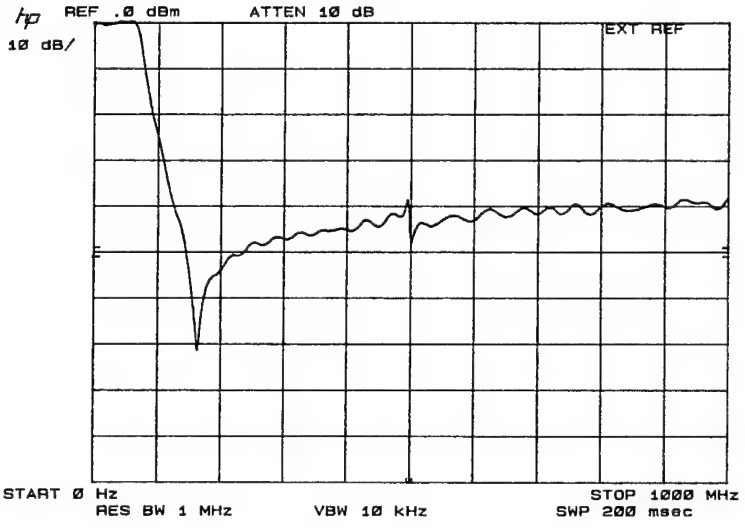

Figure 1.6 *Out-of-band frequency response of a 72 MHz L.P. filter*

Figure 1.6 shows a 72 MHz 5th order L.P. filter with the inductors wound on 0·37 inch toroids and Philips miniature low-K 100VDC NPO capacitors all housed in a Pomona 3753 box with no shielding between the toroidal coils. The measured shunt capacitor's series resonance is at approximately 220 MHz and is being swamped by the unwanted coupling between the filter's components. Power absorbed by the toroids has damped the decrease in attenuation with increasing frequency above 160 MHz in the stop band.

1.2 Changes in a Highpass Filter with Frequency

A third order H.P. (Highpass) filter comprising a series capacitor between two shunt inductors will now be examined, see figure 1.7(A). Figure 1.7(B) is the model used to analyse the circuit's behaviour. The self-resonant frequency of the components used to make H.P. filters are usually well above the -3dB point. Therefore, the out-of-passband response, or frequencies below the -3dB point, will normally be well behaved with attenuation increasing as the frequency is decreased. Increasing the input frequency within the passband from the -3dB point will reveal the expected insertion loss up until the self-resonant frequency of the individual components is approached. The series capacitor becomes series resonant with its distributed inductance and has minimal effect on the insertion loss. At higher frequencies the distributed inductance predominates and makes the capacitor appear as a small series inductor. The series reactance now increases with increasing frequency and increases the through path loss. The shunt inductors become parallel resonant with their distributed capacitance and appearing in shunt with the through path also have minimal effect on the insertion loss. Once the resonant frequency has been traversed the distributed capacitance predominates and starts to shunt to ground a portion of the through path signal. If inductance enhancing material has been used in the coil, the core losses increase the filter's insertion loss by appearing as a resistor in shunt with the distributed inductance associated with the distributed capacitance. This distributed inductance is more commonly known as the coil's one-turn-effect (not shown in the equivalent model in figure 1.2 for simplicity but covered in detail in *Section 3.9.2*) and is not to be confused with the coil's much larger lumped element inductance. Continuing beyond the component's self-resonant frequencies increases the H.P. filter's insertion loss. This loss, which can be in the order of a few dB, is usually seen as an increase in the passband attenuation with increasing frequency and usually starts several octaves above the cut-off frequency. Figure 1.7(C) shows how the circuit appears when the input frequency is higher than the component's self-resonant frequencies.

As noted earlier the distributed capacitance CP(L) of a coil is not as simple as it is shown in figure 1.7(B) but rather complex. This distributed capacitance together with the lumped inductance of the coil form a transmission line which has a high characteristic impedance and appears series resonant at a number of frequencies higher than the lumped inductance L and distributed capacitance CP(L) parallel resonance. Pronounced increases, in the order of several dB, occur in the through path loss at these series resonant frequencies. A point

just below the shunt inductor's lowest series resonant frequency is normally the upper useable frequency limit of a highpass filter. This is covered in more detail in section ***4. Construction Techniques***.

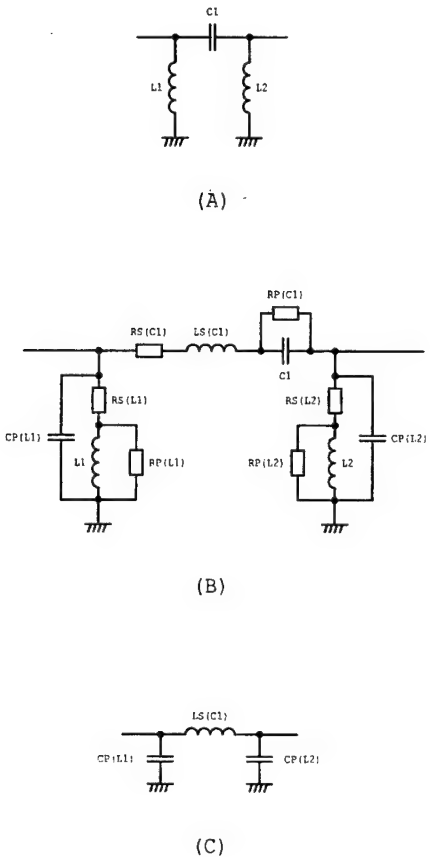

Figure 1.7 *Change in characteristics of a highpass filter at high frequencies*

It can be seen from the above that H.P. filters are generally well behaved below their corner frequency. Their unwanted distributed reactance is progressively swamped by the wanted the further one moves away from the -3dB point into the stopband. Moving away from the -3dB point into the passband and beyond the resonant frequencies of the filter's components, the unwanted distributed reactance of the through path increases the insertion loss through the filter with increasing frequency. The various series resonances of the shunt inductors creates dips in the passband response which also increase the insertion loss. Figure 1.8 is the passband response of a 2 MHz 9th order H.P. filter; note the vertical

scale of 2dB per division. The three dips that occur between 100 MHz and 200 MHz are caused by the parallelling of capacitors with large differences in their series resonant frequencies to obtain the required value of capacitance. This is covered in detail in section *2.3 Effects of Parallelling Capacitors*. Notice the gradual increase in attenuation with increasing frequency and also the dips caused by the various series resonances of the shunt coils. The test set-up in figure 1.10 was used for the measurement.

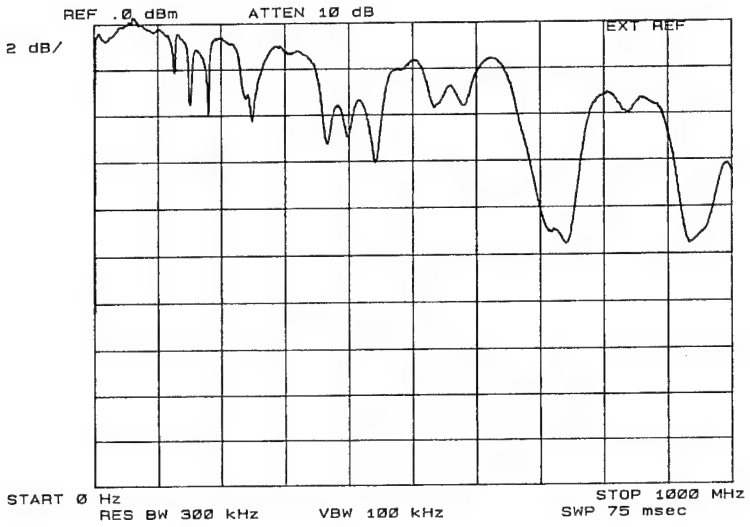

Figure1.8 *In-band frequency response covering 9 octaves of a 2 MHz H.P. filter*

1.3 Changes in Characteristic Impedance with Frequency

Filters are usually designed so that the square root of the product of their series and shunt reactances, which is independent of frequency and is the filter's characteristic impedance (equation (1.3)), matches the impedance of the system it is installed in. Real world components can have many unwanted characteristics one of which is distributed reactances of opposite sign to their wanted which modifies their true values into apparent values. These apparent values change with frequency. The change in components' apparent values with frequency gives a filter's characteristic impedance a frequency dependence and creates a corresponding mismatch between the filter and the installed system. This mismatch increases a filter's in-band through path insertion loss. The increase in loss with an increase in frequency is especially noticeable in high order filters in the V.H.F. range where a component's unwanted distributed reactance is of concern. Such losses, which can be in the order of a few dB, could adversely affect the sensitivity of a receiver if such a filter was installed in the aerial circuit.

1.4 In Summary

Commercial off-the-shelf and in-house manufactured inductors and capacitors have unwanted reactances of opposite sign distributed throughout their length. This unwanted reactance changes the manufacturer's indicated value as a function of frequency and also creates component resonances. The impact this has on a filter's performance can range from minor to catastrophic depending on filter requirements and frequency range. As an example, specific emphasis has to be placed on receiver front end filters to ensure the out of passband attenuation and in-band insertion loss, as predicted, is achieved over a broad range of frequencies. This prevents the degradation of system sensitivity and the generation of spurious in-band signals through an out-of-passband signal mixing with the first local oscillator fundamental or one of its harmonics. A thorough understanding of the two basic components, inductors and capacitors, used in the construction of passive filters and their behaviour at R.F. frequencies is required if the filter's ideal response is to be approached.

All filters used in the examples in this text, except those mentioned in the examples above, have been designed to have minimum through path attenuation, zero in-band ripple and a characteristic impedance of 50 ohms. A special set of normalised values was derived with the aid of ARRL Radio Designer software package. This has been done to better observe the various in-band effects to be described and so as not to confuse them with a filter's designed in-band ripple. The derived normalised values for lowpass filters are tabulated in the appendix. Conversion of normalised lowpass filter values into highpass filters is adequately covered in standard texts on filter design and will not be repeated here. Figures 1.9 and 1.10 are the test set-ups used to measure the filter's through loss characteristics. The 10dB pads were fitted directly at the filter's input/output terminals. Figure 1.11 is the set-up used to measure the filter's Z_{11} parameters.

Figure 1.9 *Test set-up used to measure filter's in-band frequency response*

Figure 1.10 *Test set-up used to measure filter's out-of-band frequency response*

Figure 1.11 *Test set-up used to measure filter's variation in Z_{11} with frequency*

2. Capacitors

Capacitors used in the construction of R.F. filters are usually off-the-shelf devices obtainable in various:-

- dielectrics
- voltage ratings
- shapes
- tolerances, and
- temperature coefficients.

The most common types of capacitors used for R.F. work are polystyrene, mica, ceramic, porcelain and the bush capacitor.

Polystyrene :- Polystyrene has a softening point of 80°C and therefore these capacitors are not suitable in environments where considerable heat is being dissipated; it is also affected by greases and solvents. Polystyrene capacitors are temperature stable, have extremely low series resistance which gives them high Qs and this makes them ideal for filters, timing and tuned circuits. Their rolled construction exposes a section of one of the plates to the external environment. The lead which connects to this plate is usually marked with a band or stripe. When installed in a circuit the lead marked with the band is connected to earth or to the part of the circuit that is closest to earth potential. This minimises unwanted capacitive coupling to the surrounding components. Care has to be taken in the soldering of polystyrene capacitors. Heat from the soldering iron conducted through the component's leads can distort the dielectric film and change the capacitance value. If sufficient heat is applied, a plate to plate short can develop. Polystyrene capacitors have a frequency range up to the upper part of the V.H.F. band.

Mica :- The mica capacitor exhibits excellent characteristics under stress of temperature variations and high voltage applications. They are ideal for transmitter output filters up to low band V.H.F. frequencies. The frequency limitation is due to the finite thickness of sheets that can be readily cleaved from the raw material. This constraint results in the requirement of large plate surface area to overcome the low relative dielectric constant, with a consequential increase in distributed plate inductance and lowering of the self-resonant frequency. Mica capacitors are insensitive to variations in capacitance with applied voltages and exhibit Qs in excess of 1,000. Silver mica capacitors have the highest Qs and are temperature stabilised at approximately 20 parts per million per degree Centigrade.

Ceramic :- Typical applications for the low dielectric constant types (<250) are filters, tuned circuits, timing circuits etc. with a frequency range extending into the V.H.F. range

for wire leads to well into the microwave region for surface mount types. An applied voltage has little effect on the capacitance. Ceramic dielectrics are non-hygroscopic and can operate at relative humidities up to 95 percent. This makes it ideal for use in capacitors for tropical environments. A problem can arise when pure silver is used for the end metallisation of monolithic chip capacitors. When a DC voltage is applied across a silver chip capacitor in the presence of high humidity, the silver in the end terminations migrates across the ceramic dielectric's outer surface decreasing the DC resistance. The introduction of palladium into the end metallisation forms an alloy with the silver and reduces the tendency of the silver to migrate under these conditions. In medium to high dielectric constant types (>250), usually used for R.F. coupling or bypass, the capacitance is sensitive to applied voltage and in some cases show piezoelectric effects.

Porcelain :- Porcelain capacitors are highly stable under extremes of voltage, temperature, time and frequency. Their high Qs make them ideal for high power, high current applications. They are useful well into microwave frequencies when used in the surface mount form to avoid lead inductance.

The Bush Capacitor :- A high voltage R.F. capacitor of the feed-through type which is ideal as a shunt capacitor in a lowpass filter is described in (ref. 18 pp.294) and in detail in (ref. 19). This bush capacitor, which gets its name from the type of construction (figure 2.1), is reported to have Qs in excess of 2500 to 4 GHz and R.F. capabilities at greater than 1 KV and 10A. The capacitor is manufactured in-house, is of bulkhead design using circular metal disks with a low value of resistivity as capacitor plates and TEFLON or ruby mica as the dielectric material. The circular metal disks should be polished on all sides and have rounded edges. This reduces the power loss through ionisation of the air surrounding the outer surface of the plates when operated at high R.F. voltages. The R.F. current fanning out in a 360 degree pattern from the centre terminal provides the shortest path to ground thus keeping the internal distributed inductance low. The bolt used to sandwich the assembly should be of a non-ferrous material of low resistivity such as brass. Capacitance range, typically 20pF to 150pF, is dependent on the geometry of construction, the dielectric constant and thickness of the insulating material used.

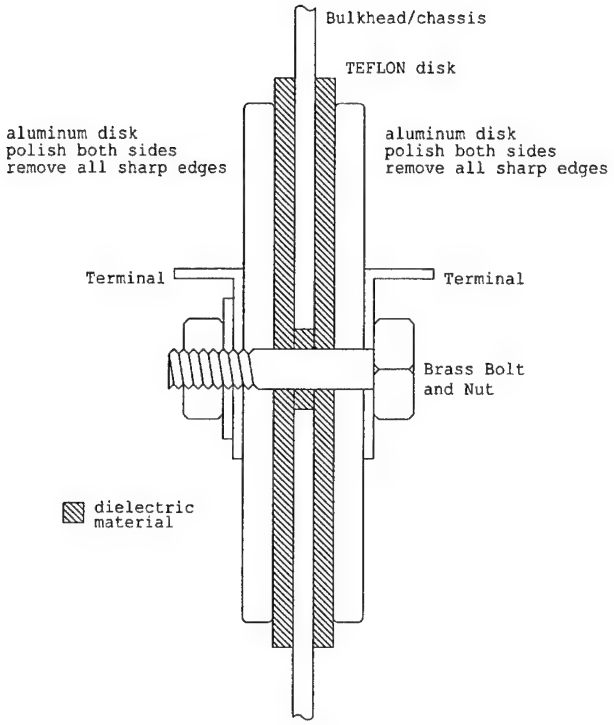

Figure 2.1 *Teflon Bush Capacitor*

2.1 Effects of Distributed Resistance

If a true capacitor connected in series with a low ohmic resistor is placed across the terminals of an LCR bridge, and the bridge's indicated capacitance plotted as the analysing frequency is varied, it will be seen that the capacitance value does not change with frequency, but remains constant. Even increasing the value of resistance to several hundred ohms will have no effect on the capacitance reading of the LCR bridge. The low ohmic resistor is normally distributed throughout the capacitor's plates and connecting leads and the presence of this distributed resistance increases the impedance presented by the capacitor and reduces the capacitor's effectiveness when used in a circuit. If the reactance of the capacitor is many times larger than the value of distributed resistance then the effects of the resistance can be ignored.

The distributed AC and DC resistance of a capacitor may however be of concern when used in power circuits. The voltage rating of an R.F. capacitor at low frequencies is the voltage at which the dielectric breaks down and an arc forms between the two plates. At

higher frequencies the dielectric losses increase, absorbing some of the R.F. energy and dissipating it as heat thereby raising the capacitor's temperature. The capacitor's voltage rating is therefore reduced as the frequency is raised lowering the power absorbed by the dielectric in order to keep the operating temperature of the capacitor below its permissible maximum. If most of the losses are contained within the dielectric material, the voltage rating will be inversely proportional to the square root of the frequency. The increase in A.C. resistance of the capacitor's plates and leads with frequency accelerates the reduction in voltage rating with increasing frequency.

The following equation can be used to calculate the impact the distributed resistance seen in series with the true capacitance has on reducing the effectiveness of a capacitor with increasing frequency. The formula can be derived by considering impedances in the complex plane. Magnitude only is considered due to the second-order nature of the distributed resistance.

$$C_{eff} = \frac{C}{\sqrt{1 + 4\pi^2 f^2 R_{S(C)}{}^2 C^2}} \tag{2.1}$$

where: C_{eff} = capacitance required to obtain a reactance of the same ohmic value as the impedance of a true capacitor and resistor in series at frequency f (F)
C = true capacitance measured at some low frequency (F)
$R_{S(C)}$ = distributed resistance seen in series with C (Ω)
f = frequency (Hz)

2.2 Effects of Distributed Inductance

Parallel plate capacitors have distributed plate inductance and lead inductance if leads are fitted. This distributed inductance and the true capacitance form a series circuit which becomes resonant at some high frequency. Even surface mount or chip capacitors become series resonant if employed at a sufficiently high radio frequency. This is due to their finite physical length plus some inescapable residual inductance inherent in the manufacturing process. The self-resonant frequency, which is very dependent upon the capacitor's body length and the lead length, represent a point where the capacitive reactance has dropped to zero; that is, the component no longer behaves as a capacitor. *Tables 2.1* to *2.3* show the frequency at which various commonly used capacitors become resonant.

Table 2.1: *Measured self-resonant frequency of 350 V SM capacitors 5mm lead length.*

Capacitance (pF)	Frequency (MHz)
120	131
390	62
560	50
680	49
150	32
220	26

Table 2.2: *Measured self-resonant frequency of 350 V red dipped SM capacitors 5mm lead length.*

Capacitance (pF)	Frequency (MHz)
110	135
330	76
510	55
1600	31

Table 2.3: *Measured self-resonant frequency of Philips miniature low K 100 V NPO ceramic capacitors 5mm lead length.*

Capacitance (pF)	Frequency (MHz)
18	422
56	213
100	143

If a capacitor's series resonant frequency is a point where it no longer acts as a capacitor then, between the frequency at which the manufacturer has stated the capacitance value and the frequency of series resonance, there are apparent changes in the value of capacitance. These apparent changes in capacitance with frequency will now be examined.

At low and moderate frequencies the reactance of the distributed inductance associated with the capacitor is negligible, but at very high frequencies it becomes increasingly more significant. The distributed inductive reactance and true capacitive reactance are subtracted to give the apparent reactance at the frequency of interest, equation (2.2).

$$jX_{app} = j2\pi fL_{S(C)} - \frac{1}{j2\pi fC} \tag{2.2}$$

where: jX_{app} = apparent reactance (Ω)
C = true capacitance measured at some low frequency, usually 100KHz (F)
$L_{S(C)}$ = distributed lead and plate inductance seen in series with C (H)
f = frequency (Hz)

This causes the apparent capacitance, deduced purely in terms of the measured reactance value of the series combination of the true capacitance and the distributed inductance as observed at the terminals, to increase markedly above the labelled capacitance value.

Take for example a 1200pF Silver Mica 350 V capacitor with 5mm lead lengths. The self-resonant frequency was measured using an H.P.4191 R.F. Impedance Analyser and found to be 36.3 MHz.

$$X_c = \frac{1}{j2\pi fC} \tag{2.3}$$

where: X_C = capacitive reactance (Ω)
C = capacitance (F)
f = frequency (Hz)

By calculation, equation (2.3), the capacitive reactance of a 1200pF capacitor at 36.3 MHz is 3.654 ohms. However, the reactance at this frequency was measured and found to be zero ohms, signalling the significant impact of the series distributed inductance. A search in frequency on the Impedance Analyser showed that 3.654 ohms reactance pertains at approximately 22.4 MHz. By calculation again, (rearranging equation (2.3)) the capacitance value that will produce a reactance of 3.654 ohms at 22.4 Mhz is 1945pF. This is a 62% increase on the manufacturer's specified value of 1200pF, and demonstrates the impact of the distributed inductance in giving the true capacitance an apparent value of capacitance.

The distributed inductance is readily calculated from the capacitor's series self-resonant frequency where $X_{LS(C)}$ and X_C are equal. X_C was calculated from the manufacturer's stated capacitance. In the case of the 1200pF capacitor, this distributed inductance was approximately 16nH. A 100 times increase in capacitance from that stated by the

manufacture at some low frequency up to a frequency just below the component's series self-resonant frequency is typical. Figure 2.2 is a plot of the measured capacitance versus frequency for the 1200pF capacitor used in the example. This plot shows a change in capacitance from 1200pF at 1 MHz to 0.4uF at approximately 36.2 MHz.

The apparent capacitance seen looking into the two terminals of a capacitor at some frequency below its series self-resonant frequency is (ref.22 pp120):-

$$C_{app} = \frac{C}{1 - 4\pi^2 f^2 L_{S(C)} C} \tag{2.4}$$

where: C_{app} = apparent capacitance (F)
C = true capacitance measured at some low frequency, usually 100KHz (F)
$L_{S(C)}$ = distributed lead and plate inductance seen in series with C (H)
f = frequency (Hz)

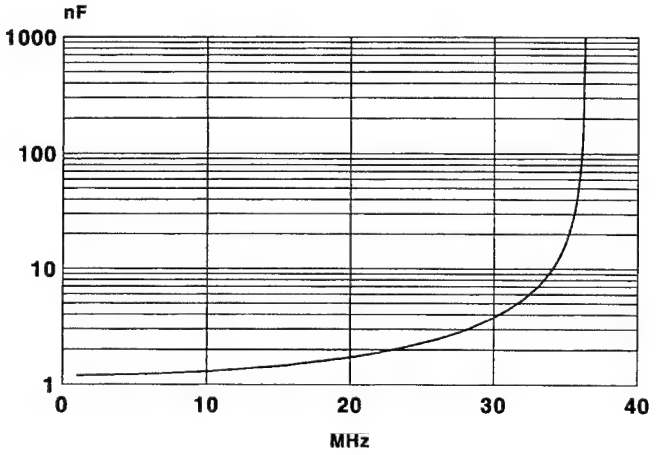

Figure 2.2 *Measured apparent capacitance versus frequency for a 1200pF 350 V 1% Silver Mica capacitor with 16nH distributed inductance (5 mm lead lengths)*

Equation (2.4) was used to generate the plots of figures 2.3 to 2.5. Realistic values of distributed lead and plate inductance have been chosen to highlight typical increases in apparent capacitance versus frequency. This emphasizes the need to measure a capacitor's

value after the component's leads have been cut to the required length at the frequency at which it is being used. For filters, this is normally the cut-off frequency or -3dB point.

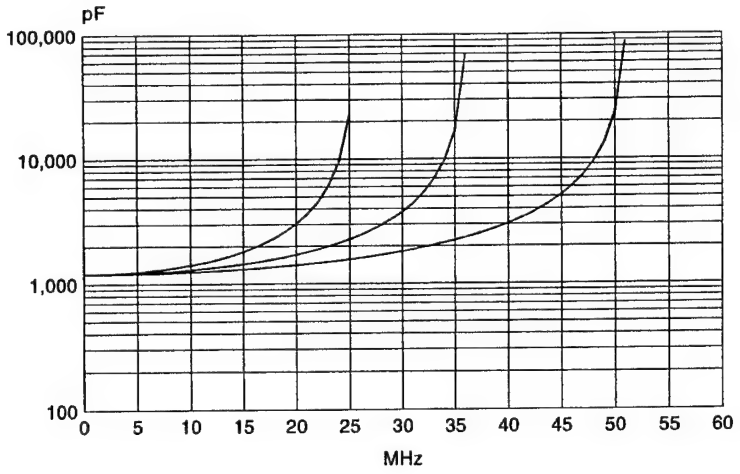

Figure 2.3 *Variation in apparent capacitance of a 1200pF capacitor with (left to right) 32nH, 16nH and 8nH distributed inductance*

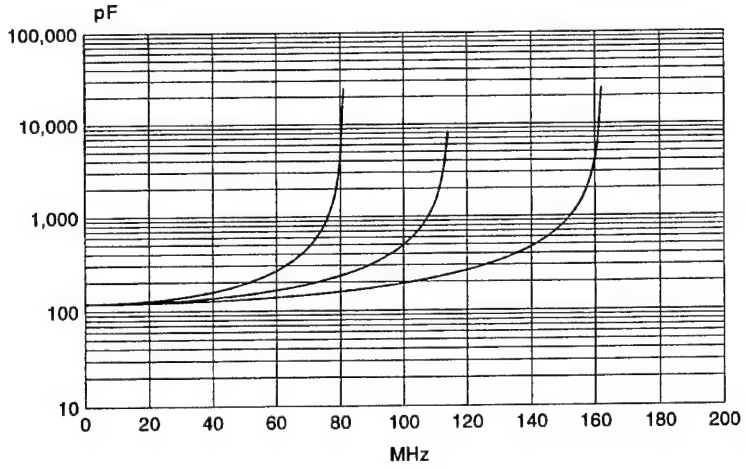

Figure 2.4 *Variation in apparent capacitance of a 120pF capacitor with (left to right) 32nH, 16nH and 8nH distributed inductance*

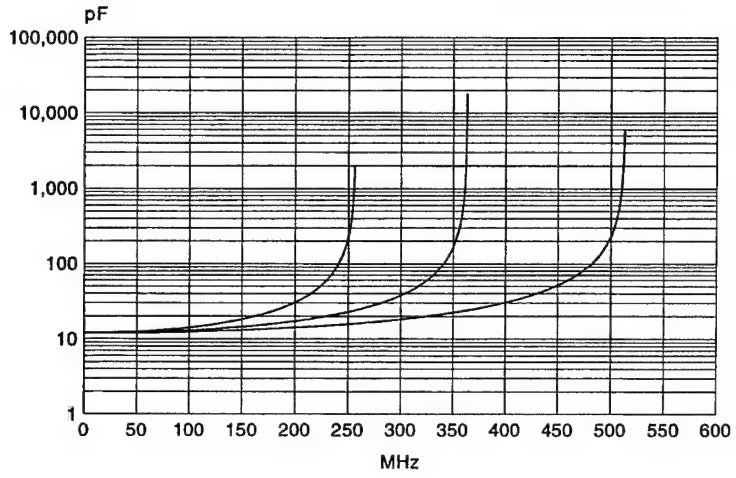

Figure 2.5 *Variation in apparent capacitance of a 12pF capacitor with (left to right) 32nH, 16nH and 8nH distributed inductance*

If an LCR bridge covering the frequency range of interest is unavailable, C_{app} can be estimated with equation (2.4) using the assumption of 20nH per inch for the component's lead length plus a few nH for the distributed plate inductance. Figure 3.2 can also be used to find the self-inductance for various lengths of the average wire diameter (0.82 mm) used by manufacturers in the production of 350 V silver mica R.F. capacitors.

It is not uncommon to see capacitor values being used in real filter circuits above 30 MHz that are less than those called for in the numerical design. This difference, which is caused by the effects the capacitor's distributed inductance has on its true capacitance materializing as an apparent capacitance which changes with an increase in frequency, can be minimised by keeping lead lengths short or by using surface mount components. In either case, if PCB construction is used, attention has to be paid to the distributed inductance of the printed circuit tracks.

2.2.1 Behaviour of capacitors above their self-resonant frequencies

Equation (2.2) was algebraically manipulated to obtained equation (2.5) which is used to calculate the value of inductance presented by a capacitor at frequencies above the capacitor's series self-resonant frequency.

$$L_{app} = L_{S(C)} - \left(\frac{1}{4\pi^2 f^2 C} \right) \tag{2.5}$$

where: L_{app} = apparent inductance (H)
C = true capacitance measured at some low frequency, usually 100KHz (F)
$L_{S(C)}$ = distributed lead and plate inductance seen in series with C (H)
f = frequency (Hz)

2.3 Effects of Parallelling Capacitors

Quite often the component values called for in the numerical design are not preferred values. In such cases, it is common practice to parallel preferred values together to achieve the desired value. This practice, which is frowned on in some texts, is acceptable provided certain precautions are taken. For example, if the design called for a 1100pF capacitor, this could be obtained to within a few percent by parallelling the various capacitors as depicted in *Table 2.4*. The measured series self-resonant frequency of the capacitors used are also listed. A problem arises when using two capacitors with vastly different series self-resonant frequencies.

Figure 2.6(D) is the test set-up used to measure the through path loss of the two capacitors in parallel. Figure 2.6(B) is the model used to examine the frequency response of the circuit. If two identical capacitors being used have the same lead length then they will both have approximately the same series resonant frequency. When the signal generator is swept from some frequency below the series resonance to some frequency above, the two capacitors will change from being capacitive to inductive at about the same frequency. If however there is a difference in the two self-resonant frequencies, then as the signal generator frequency is increased there will be a portion of the sweep where the capacitor with the lowest self-resonant frequency will appear inductive while the other is still capacitive. This creates a parallel resonant circuit as seen in figure 2.6(C) and causes a dip in the frequency response. The size of the dip at parallel resonance is proportional to the L/C ratio which is proportional to the difference between the two capacitors' series self-resonant frequencies. This is clearly seen in *Table 2.4*. A plot of the measured through path loss versus frequency for the 100pF, 1000pF combination is shown in figure 2.7. The signal generator output level was -1dBm.

Table 2.4: *Measured through path loss of the parallel resonant circuit formed by the parallel pairing of capacitors with differing series self-resonant frequencies. Capacitors are 350 VDC silver mica with lead lengths approx. 7mm.*

Capacitance Parallelled (pF)	Self Series Resonant Frequency (MHz)	Combined Parallel Resonant Frequency (MHz)	Through Path Loss at P.R.Freq. (dB)
560	53.41	69.7	-0.05
560	51.5		
470	62	72.58	-0.2
600	51.6		
390	63.24	72.75	-0.82
700	45.33		
270	79.03	82.17	-4.0
820	43.1		
100	134.37	117.8	-8.4
1000	42.33		

The model shown in figure 2.6 (B) indicates a degree of magnetic coupling between the two distributed inductors. The coefficient of coupling "*k* " is dependent upon the proximity of the two capacitors with respect to one another. The closer the two capacitors are the larger the value of "*k* ". Typical values for "*k* " are in the range of 0.2 to 0.3. This mutual magnetic coupling between the two capacitors has the effect of lowering the distributed inductance and increasing the components' series self-resonant frequencies. This is readily seen in *Table 2.4* in the first four entries where the combined parallel resonance is higher than the highest series self-resonant frequency of either of the two capacitors in parallel. In the 100pF,1000pF combination, if there was no coefficient of coupling, parallel resonance would occur at approximately 100 MHz and not 117.8 MHz where it was measured.

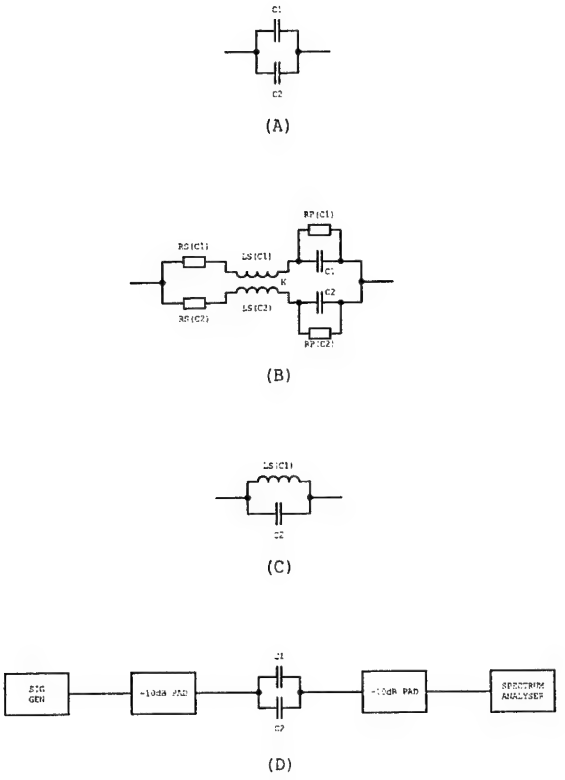

Figure 2.6 *Model and test set-up used to measure through path loss of capacitors in parallel*

Equations (2.4) and (2.5) can be used to find the L_{APP}/C_{APP} ratio of the parallel resonant circuit keeping in mind the reduction in $L_{S(C)}$ via "k", the coefficient of coupling. The value of mutual inductance (L_M), which is subtracted from the distributed inductance ($L_{S(C)}$) is found using equation (2.6).

$$L_M = k\sqrt{L_{S(C1)}L_{S(C2)}} \tag{2.6}$$

where: L_M = mutual inductance
k = coefficient of coupling (for capacitors intentionally mounted in very close proximity, usually between 0.2 to 0.3)
$L_{S(C1)}$ = distributed inductance seen in series with C1
$L_{S(C2)}$ = distributed inductance seen in series with C2

If the 100pF,1000pF combination was used in a low pass filter in the H.F. band where it was required to shunt to ground the out of passband signals, a localised decrease in attenuation would occur at approximately 117.8 MHz. If this same combination was used as a highpass filter from somewhere in the H.F. band upwards, a localised increased in the through path attenuation would occur at approximately the same frequency. *Table 2.4* shows that only preferred values within one increment of each other possessing the same distributed inductance should be parallelled together and that caution should be used if any other combination is used. Figure 1.8 is an example of a 2 MHz Highpass filter in which three localised unwanted increases in passband attenuation occur between 100 MHz and 200 MHz. These dips in the response are caused by the paralleling of capacitors with large differences in their series self-resonant frequencies.

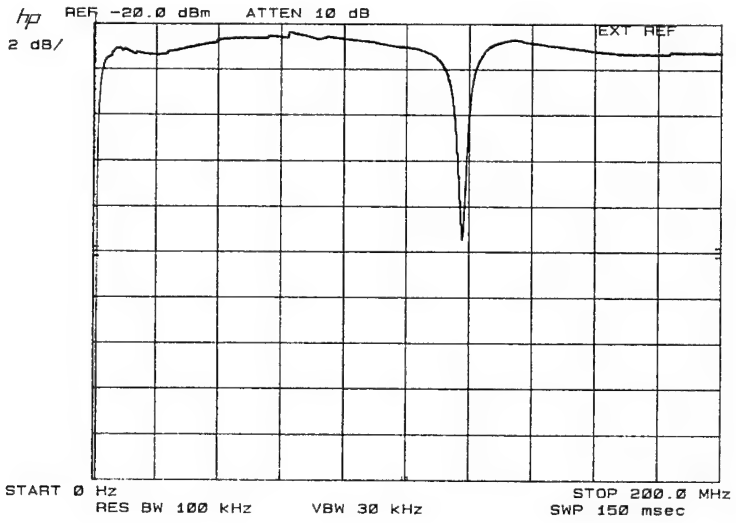

Figure 2.7 *Measured through path loss of a 100pF and 1000pF capacitor in parallel*

2.4 Effects of Capacitors in Series

Theory shows that it is possible to connect capacitors in series to obtain non-preferred values. It has already been demonstrated, via equations (2.4) and (2.5), the impact distributed inductance has on the true capacitance. Connecting capacitors in series effectively doubles the distributed inductance. The effect this has on the true capacitance of capacitors connected in series is best seen by comparison. Figure 2.8 is a plot of the measured changes in apparent capacitance with frequency for three methods of obtaining the value of 110pF; all capacitors are 350 V silver mica with 5 mm lead lengths.

Moving from left to right, the first trace, which goes through resonance at approximately 106 MHz, is two 220pF capacitors connected in series, the next is a single 110pF capacitor and the third is two 56pF in parallel. Of the three techniques used to obtain the value of 110pF, connecting capacitors in series is by far the most undesirable. It exhibits the lowest series resonance and hence undergoes the greatest change in apparent capacitance for a given frequency range than the other methods. This is due to the summation of the distributed inductance of both capacitors. It is interesting to note that of the techniques presented, the two parallel capacitors of equal value with the highest possible coefficient of magnetic coupling between them have the best performance. This is due to the negative mutual inductance between both components lowering each others distributed inductance.

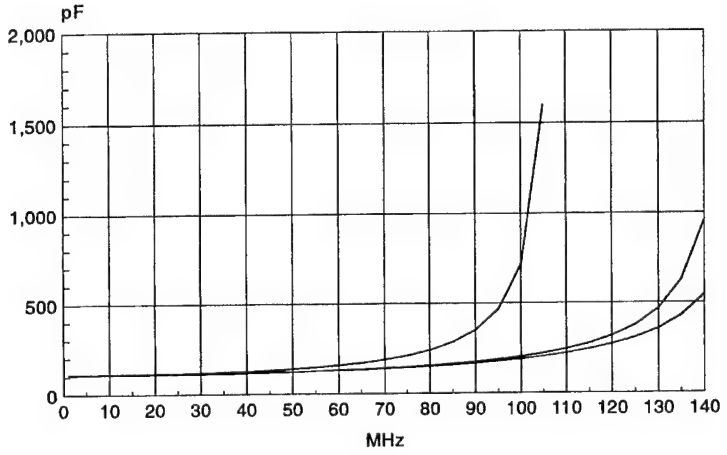

Figure 2.8 *Comparison of three methods of realising a 110pF capacitor. Left 2x220pF in series, centre 110pF, right 2x56pF in parallel*

2.5 Summarising Capacitors

All capacitors are supplied from the manufacturer with their true capacitance, measured at some low frequency, indicated on them. This true capacitance is modified in the frequency domain by the component's distributed resistance and inductance. The distributed resistance is usually extremely small and is swamped by the effects of the distributed inductance. Most of this inductance is contained in the leads. Unless there are specific reasons for having leads a particular length, (for example, enhancing out-of-band rejection at a particular frequency by making a shunt capacitor series resonant) all lead lengths

should be kept as short as possible. This includes any PCB tracks or wiring used to connect the capacitor to the rest of the circuit.

Connecting capacitors in series to obtain a non-preferred value is to be discouraged. It increases the distributed inductance, lowers the series self-resonant frequency and has adverse affects on the apparent capacitance with frequency.

All capacitors used in the construction of R.F. filters should have their apparent capacitance measured at the filter's cut off frequency (-3dB point) after the component's leads have been cut to length. If an LCR bridge is unavailable, equation (2.4) can be used to estimate the capacitance at this frequency.

Capacitors connected in parallel to obtain non-preferred values should be:-

a. Equal in value or within one increment in preferred value of each other. This minimises the spot frequency attenuation of through path signals brought about by the formation of a parallel resonant circuit in series with the path.

b. Installed as close together as possible in order to maximise the magnetic coefficient of coupling. This has the effect of reducing the distributed inductance through mutual induction, raising the series self-resonant frequency of the individual capacitors and lowering the apparent capacitance to bring it closer to the true capacitance. If chip capacitors are used they should be pyramidally stacked, that is, the smaller of the two sitting on top of the larger. The reasons for this will be covered in section ***4. Construction Techniques***.

As a rough rule-of-thumb, a capacitor can only be trusted to have its labelled capacitance value for frequencies less than approximately one third the frequency of its series resonance.

3. Inductors

Unlike capacitors which are usually off-the-shelf components, inductors are normally fabricated in-house to meet requirements. Some of the factors which influence the physical design are:-

- size constraints dictated by the filter order and maximum volume the filter can occupy.
- required inductance.
- power handling capability.
- the desired Q.
- frequency range of operation.
- inductance enhancing materials used, iron powder or ferrite.
- reduction in μ (permeability) of inductance enhancing materials used by passing D.C. currents through the inductor windings. e.g. remote active antennas or mast head pre-amplifiers.
- temperature stability.
- self-capacitance of coil.

An understanding of the physical nature of inductance is required when constructing coils for any LC filter. This then will be the starting point. More detailed information can be obtained from the various cited references.

The following laws and rules relating to magnetic flux have been reproduced here for convenience. They will be found useful in understanding the effects time varying magnetic fields have on conducting mediums.

Faraday's law: The voltage induced in a circuit is proportional to the rate at which the magnetic flux linkages of the circuit are changing.

Lenz's law: The current induced in a circuit due to a change in its magnetic flux is in such a direction as to oppose the change in flux.

Left-hand rule for a current-carrying wire: If the fingers of the left hand are placed around the wire in such a way that the thumb points in the direction of electron

flow, the fingers will be pointing in the direction of the magnetic field produced by the current flow in the wire.

Left-hand rule for induced currents: The thumb and fingers of an open left-hand are placed at right angles on the same plane. If the fingers point in the direction of the magnetic lines of flux and the palm is facing the direction in which the lines of flux are travelling as if it were pushing the lines of flux in that direction, then the extended thumb points in the direction of the induced electron current flow.

3.1 Magnetic Field Surrounding a Wire

A quantum of charge travelling at constant velocity, relative to a stationary observer, is surrounded by concentric circles of magnetic lines of flux centred on the trajectory and perpendicular to it. An electron is a quantum of charge and therefore, it is reasonable to say that an electron travelling at constant velocity is surrounded by magnetic lines of flux.

A conductor is a material inside which electric charges can flow freely. In the absence of an electric field, the directions in which the electrons move is completely random. The summation of the lines of magnetic flux from the thermal agitation of the random motion of electrons is a zero average magnetic field. When an electric field (E) is placed across the ends of the conductor, the electrons modify their random motions in such a way that they drift slowly, with an average drift velocity, in the opposite direction to that of the applied electric field. This drift velocity is much less than the effective average velocity of the electrons in random motion. The drift in the random motion of electrons, brought about by the electric field, gives rise to an electric current (i). This current in turn produces concentric circles of magnetic lines of flux perpendicular to the applied E field.

The concentric circles of magnetic lines of flux surrounding a wire in which a current is flowing, as seen in most text books, are not as simple as the diagrams might imply. These magnetic lines are contour lines connecting equipotential points where the summation of the various lines of flux centred on their corresponding electrons moving under the influence of an E field are equal. The magnetic field surrounding a conductor is therefore the summation of the magnetic fields surrounding every electron that is free to move and is also under the influence of an applied E field.

The magnetic field (H) surrounding a cylindrical wire is:-

$$dH = i\frac{ds \times r}{r^3} \tag{3.1}$$

In the terms of the notation of Figure 3.1.

$$dH = i\frac{\sin\theta ds}{r^2} \tag{3.2}$$

where: i = current flowing in element ds of wire.
ds = vector element of length along the wire.
r = distance between ds and point P where H is being determined.
θ = angle between r and element ds.

Equations (3.1) and (3.2) are known as the Biot-Savart law. The two points to note in equation (3.2) are the magnetic field is proportional to i and inversely proportional to the square of the distance.

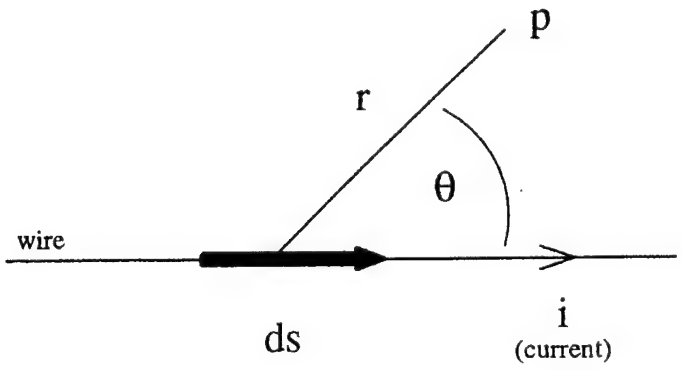

Figure 3.1 *Definitions of terms used in equation (3.2)*

3.2 Self-Inductance of a Straight Wire and a Single Turn Loop

The self-inductance of a round wire can be calculated using the following formulas obtained from (ref.9 pp.261). It shows that inductance is dependent upon wire diameter and length and is almost independent of frequency.

$$L = 0.002l\left[\log_e \frac{2l}{r} - \frac{3}{4}\right] \qquad \text{at low frequencies} \qquad (3.3)$$

$$L = 0.002l\left[\log_e \frac{2l}{r} - 1\right] \qquad \text{at high frequencies} \qquad (3.4)$$

where: L = inductance in μH
l = length in centimetres
r = radius of round wire in centimetres

The self-inductance of a 0.82 mm diameter copper wire at various lengths was calculated using equation (3.4) and the results are seen in figure 3.2. This is the average diameter of lead wires used by various manufacturers of high voltage (350 V) mica and ceramic capacitors. Figure 3.2 can therefore be used to estimate the capacitor's lead inductance.

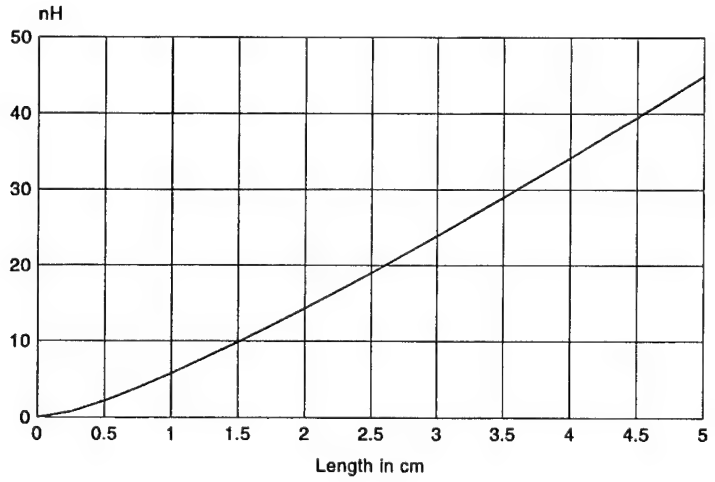

Figure 3.2 *Calculated inductance of a 0.82 mm dia. wire*

The self-inductance of a single turn circular loop can be calculated using the following equation (3.5) obtained from ref. 30 pp6-9.

$$L = \frac{r}{254}\left(3.193 Log_e \frac{16r}{d} - 6.386\right) \tag{3.5}$$

where: L = inductance (uH)
r = mean radius of single turn loop (cm)
d = diameter of wire (cm)

3.3 Inductance of Coils

A coil is normally constructed of circular loops of wire connected in series on a common axis and mutually coupled to one another. Factors that influence the inductance of coils are:-

- wire gauge and type,
- coil diameter and length,
- turns per inch,
- core permeability,
- proximity of surrounding enclosure used for shielding,
- distributed capacitance both internal and to other components.

Inductors differ from capacitors in that they are more susceptible to their installed environment. This is primarily due to their larger physical size which increases the electric and magnetic coupling both within themselves and to their surrounding components. It is for this reason that the high frequency resistance and inductance of coils cannot be accurately calculated and should be measured at the desired frequency, ideally in a simulation of its installed environment. Any formula used to calculate inductance should therefore be treated as a guide, an approximation only. There have been many attempts to minimise the error between calculated and measured inductance over time yielding equations that become quite tedious; ref.1 being a good example.

3.4 Air Wound Coils

Equation (3.6) is Wheeler's formula for calculating the approximate low frequency inductance for short air wound coils in which the values of l are between one tenth of r

and two thirds of r. Note the inductance varies as the square of the turns, i.e. if the number of turns is doubled, for a given l and r, the inductance is quadrupled.

$$L = \frac{0.394 r^2 n^2}{\left(9 - \frac{r}{5l}\right) r + 10l} \tag{3.6}$$

where: L = low frequency inductance (uH)
r = coil radius (cm)
l = coil length (cm)
n = number of turns

Where l is greater than two thirds of r equation (3.6) simplifies to:

$$L = \frac{0.394 r^2 n^2}{9r + 10l} \tag{3.7}$$

Wheeler's formula does not take into account the variation in a coil's inductance with wire thickness. The formula given below, due to Reyner (ref. 28), gives the inductance of normal air wound coils to within a few percent. If the wire used to construct the coil is of appreciable thickness an additional correction factor is introduced by the second part of the expression.

$$L = \frac{0.2 n^2 D^2}{3.5D + 8l} \times \frac{D - 2.25t}{D} \tag{3.8}$$

where: L = low frequency inductance (uH)
D = outside diameter of coil (inches)
l = coil length (inches)
n = number of turns
t = winding thickness (inches)

3.5 Effects of Distributed Resistance

The D.C. and A.C. resistance of a coil seen in series with the true inductance increases the effective inductance with decreasing frequency. Coils used for filters in the H.F. and V.H.F. bands are usually made from short lengths of wire and the wire gauge is chosen to maximise the Q. The resistance of the wire is therefore small and the effect it might have on an inductor with frequency is swamped by the coil's distributed capacitance. It is only at M.F. frequencies and below where long lengths of fine wire are used to manufacture coils that the effects of distributed resistance need be considered. The following formula can be derived by considering impedances in the complex plane. Magnitude only is considered due to the second-order nature of the distributed resistance.

$$L_{eff} = L\sqrt{1+\frac{R_{S(L)}{}^{2}}{4\pi^2 f^2 L^2}} \tag{3.9}$$

where: L_{eff} = inductance required to obtain a reactance of the same ohmic value as the impedance of a pure inductor and a resistor in series at frequency f (H)
L = true inductance (H)
$R_{S(L)}$ = distributed resistance both D.C. and A.C. seen in series with L (Ω)
f = frequency (Hz)

3.6 Effects of Distributed Capacitance

The distributed capacitance of an inductor, both internal between the windings and to the surrounding components, changes the apparent measured inductance with frequency. Equation (3.10), (ref.30 pp13-17), can be used to show the variation in measured apparent inductance with frequency. It assumes the self parallel resonant frequency of the coil, from which the distributed capacitance can be calculated, and the true inductance, measured at some low frequency where the distributed capacitance has minimal effect, are known.

$$L_{app} = L\left(\frac{1}{1-4\pi^2 f^2 L C_{P(L)}}\right) \tag{3.10}$$

where: L_{app} = apparent inductance (H)
L = true inductance measured at some low frequency (H)
$C_{P(L)}$ = distributed capacitance seen in parallel with inductor L (F)
f = frequency (Hz)

Equation (3.10) becomes quite inaccurate for frequencies closer than half an octave below self-resonance. It does not take into account the reduction in inductance to zero at the self-resonant frequency. This can be corrected by applying equation (3.11) to the results of equation (3.10).

$$L_{appc} = L_{app} - \left(\frac{L_{app}}{1 + Q^2 \left(\frac{f_r}{f} - \frac{f}{f_r} \right)^2} \right) \tag{3.11}$$

where: L_{appc} = corrected apparent inductance (H)
L_{app} = apparent inductance derived from equation (3.10), (H)
Q = figure of merit of the self parallel resonant circuit formed by the distributed capacitance $C_{P(L)}$ and the true inductance L
f = frequency used to calculate L_{app} (Hz)
f_r = self-resonant frequency of inductor (Hz)

The variation in apparent inductance with frequency becomes noticeable in highpass filters where inductors are connected in shunt to the through path. If the inductance required is measured at the cut off frequency, the apparent inductance will increase with increasing frequency causing a subtle change in characteristic impedance of the filter the further one moves into the passband. This mismatch in impedances between the filter and its terminations, which results in a small increase in expected in-band insertion loss normally seen as an increase in in-band ripple with increasing frequency, can be reduced by measuring the inductance of the coils to be used at a frequency approximately one to two octaves into the passband. This usually results in a coil whose apparent inductance at the cut off frequency is slightly less than the numerical design. The improvement in passband performance normally outweighs the subtle changes that occur in the filter's cut off frequency. A coil's distributed capacitance can be reduced by winding the shunt coils with finer wire and slightly increasing the turns spacing. This will raise the coil's self-resonant frequency and extend the useful upper frequency response of the highpass filter.

Fine adjustment of the inductance of an air wound coil is usually carried out through compressing or stretching the turns. This has the effect of changing the length l in equation (3.6) and hence altering the inductance. Figure 3.3 shows the variation in measured inductance of a 5 mm diameter coil of 15 turns when l was varied between 9 mm to 25 mm. It can be seen that the greatest change in inductance occurs when the turns are close together. This is due to the inverse square law nature with distance of the magnetic field surrounding the wire used to construct the coil, equation (3.2). Mutual coupling

between the individual loops of the coil is therefore the greatest when the turns are separated by the wire's enamel insulation only.

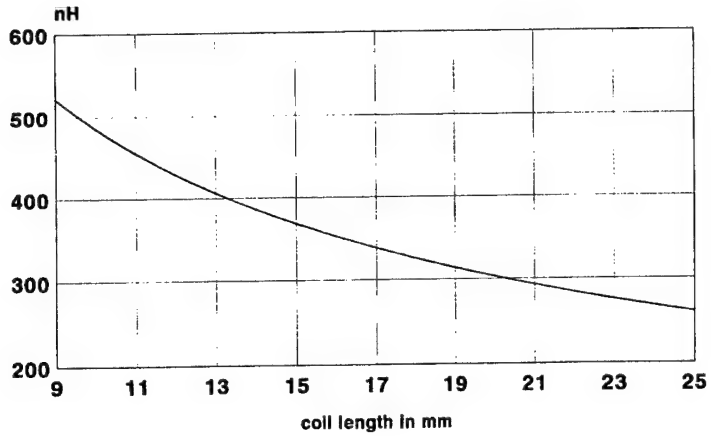

Figure 3.3 *Variation in measured inductance of 15 turns of 0.51 mm wire 5 mm dia coil of varying length. Test frequency 10 MHz*

A coil originally designed for a low phase noise VFO in the H.F. band will be used to demonstrate the effects predicted in equations (3.10) and (3.11). This coil would also be ideal for use in a 2 MHz fifth order medium power L.P. filter. The dimensions of the coil are given in figure 3.4 and these were used in equations (3.7) and (3.8) to calculate the inductance. The calculated inductance was 6.696uH and 6.576uH respectively as opposed to the measured 6.235uH at 1 MHz. Figure 3.4 is a plot showing the measured effects with frequency the 1.233pF of distributed capacitance has on the inductance of the 6.235uH air wound coil. Capacitive coupling to the surroundings was kept to a minimum. Figure 3.5 is the results of equation (3.10) when applied to the 6.235uH inductor with 1.233pF distributed capacitance. This capacitance was calculated from the inductance measured at 1 MHz and the coil's self-resonant frequency. Note the similarity of figure 3.5 to figure 2.2 which depicts the change in apparent capacitance of a capacitor with frequency. Figure 3.6 shows the correlation between the measured apparent inductance (HP-4191A) and the results of equation (3.11). The difference between the two plots is attributed to the limitations of the test equipment. The Q of the parallel self-resonant circuit was calculated from a measurement of the dynamic resistance (R_D) at resonance and the reactance of the true inductance (X_L) at this frequency. The relationship between the two to obtain the value of Q is:-

$$Q = \frac{R_D}{X_L} = \frac{15{,}300}{2{,}248} = 6.8 \qquad (3.12)$$

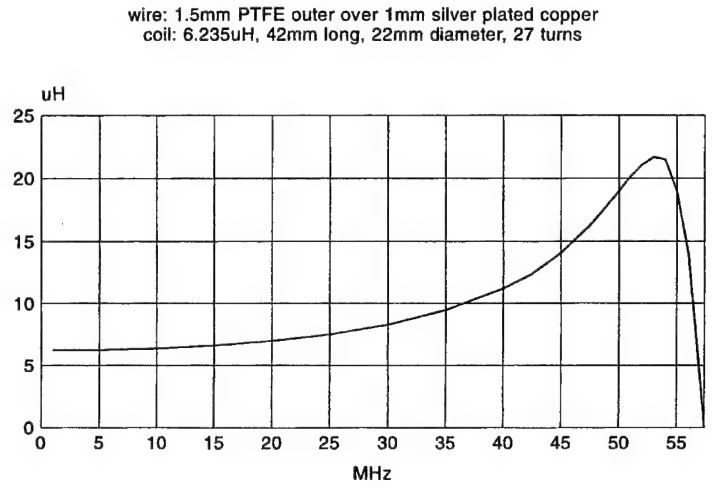

Figure 3.4 *Variation in measured apparent inductance with frequency of an air wound 6.235uH coil with 1.233pF distributed C*

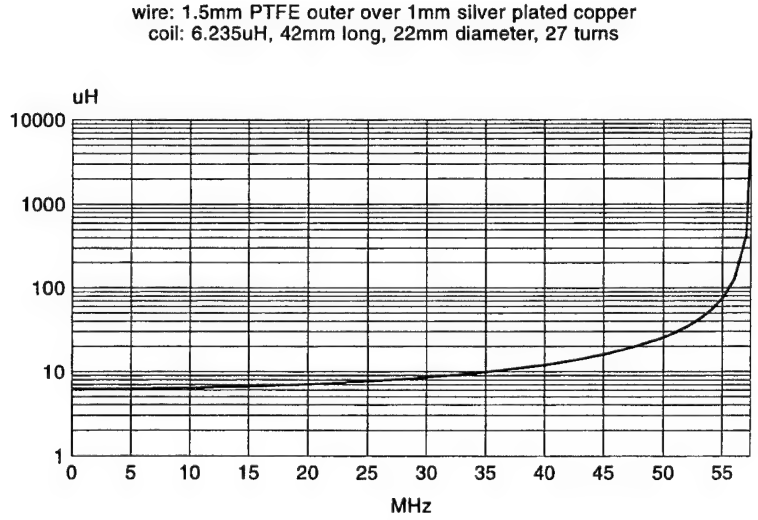

Figure 3.5 *Variation in apparent inductance with frequency of a 6.235uH coil as calculated using equation (3.10)*

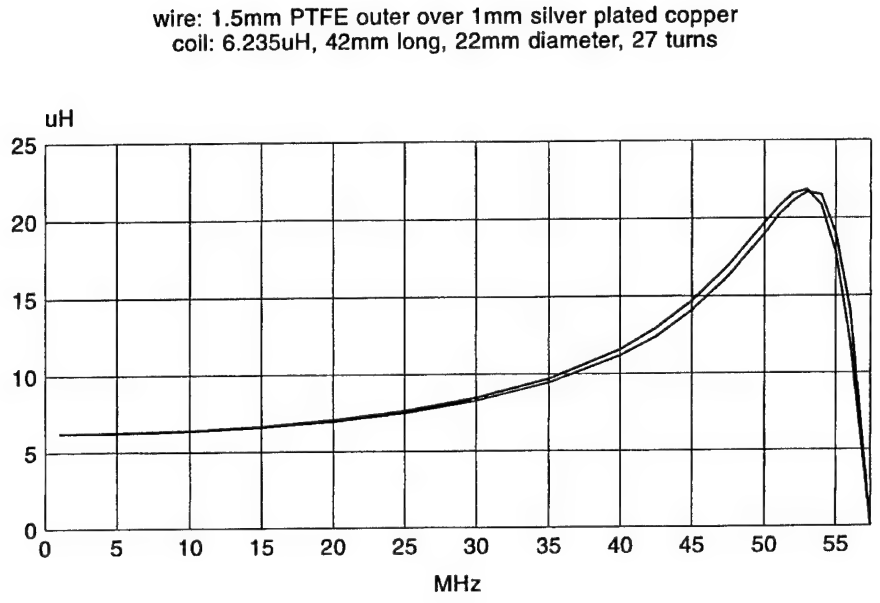

Figure3.6 *Comparison between measured and calculated apparent inductance using equations (3.10) and (3.11)*

Figure 3.7 shows the measured variation in effective series resistance, measured under the condition of resonance, and the calculated Q with frequency for the 6.235uH coil used in this example. The measured resistance between 5 MHz and 20 MHz is primarily due to the proximity effects of adjacent turns of the coil. Beyond 20 MHz the effects of the coil's self resonance predominate. Figure 3.8 is a universal resonance curve for a parallel resonant circuit. At parallel resonance there is a high dynamic pure resistance in the order of tens of kilo-ohms whose decay from resonance is frequency and Q dependent. This is seen as the resistance component curve in figure 3.8. The change in slope of R_{series} in figure 3.7 at frequencies higher than 20 MHz is due to this increase in the dynamic resistance with frequency which maximizes at the coils parallel resonance.

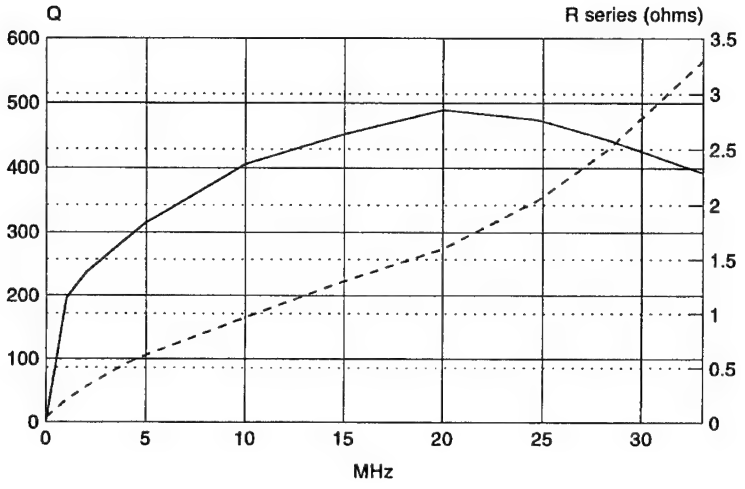

Figure 3.7 *Variation of Q (solid line left axis) and R series (dashed line right axis) with frequency for the 6.235uH coil*

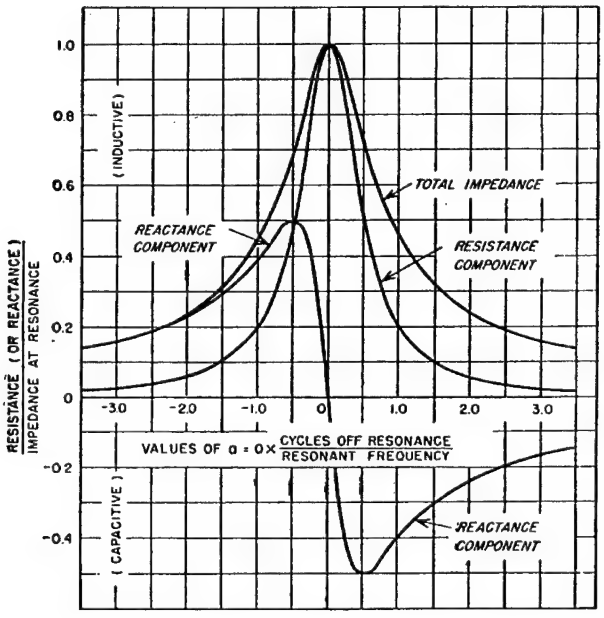

Figure 3.8 *Universal Parallel Resonance Curve obtained from (ref. 22)*

3.7 Effects of Q on a Filter's Response

The Q of a coil used in a filter has a direct effect on the filter's characteristics. Using coils with low Qs has the following effects on a filter's performance.

- Increase in insertion loss,
- Decrease in the rate of attenuation roll off with some reduction in attenuation at the highly attenuated frequencies,
- Attenuation at the cut-off frequency is greater than -3dB,
- The response around the cut-off frequency becomes more rounded, and
- Reduction in desired in-band ripple of Chebyshev filters.

Coils possessing the highest Qs should therefore be used. This can be achieved if the following construction guidelines for air cored coils are adhered to.

(1) Use a conducting material with a wire gauge that has the lowest possible D.C. resistance per unit length that is manageable with the size of coil to be constructed. At V.H.F. frequencies and above tubular conductors are effective in reducing the A.C. resistance of coils.

(2) The optimum spacing of the turns, defined by the ratio d/s (wire diameter/distance between centres of adjacent turns) is between 0.5 and 0.7 for short coils (length is less than the diameter), between 0.6 and 0.8 where the length is approximately twice the diameter and finally between 0.75 and 0.9 for long coils.

(3) For a given coil diameter and wire spacing, the maximum Q increases rapidly at first as the coil length is increased, however further improvement is small if the length is made greater than the coils mean diameter.

A good compromise is to make the length to diameter ratio of the coil somewhere between 1/1 and 3/1 and then to choose the wire diameter to make the ratio d/s approximately 0.7. Close wound coils, where the d/s ratio is less than 0.5, should be avoided. This is because the maximum Q obtainable from a coil versus frequency is related to the coil's self-resonant frequency and the proximity effect of adjacent turns. The higher the self-resonant frequency for a given inductance the greater will be maximum obtainable Q. Close wound coils increase the distributed capacitance between turns and hence lower

the self-resonant frequency. At the same time the closeness of the turns also increases the A.C. resistance of the wire; this is the proximity effect. As a general rule, make the air wound coils as large as is consistent with any shielding being used. The relationship between coil diameter and shield dimensions with respect to a lowpass filter's terminating impedances will be covered in section ***4. Construction Techniques***.

3.7.1 A Word About Measuring the Q of Coils

It has been this author's experience that the accurate measurement of a coil's Q using modern Impedance or LCR Bridges can be fraught with difficulties. The results tend to be instrument specific and are generally unreliable for the frequencies and purposes under consideration in this Tech Note. To avoid such anomalies, this author prefers the more traditional technique of obtaining values of Q at specific frequencies of interest by resonating the coil at each measurement spot with a high quality external capacitor. The measurement technique using these instruments is as follows.

The coil's reactance is cancelled by placing a capacitor, with a reactance equal to but of opposite sign to the coil, in series with it, thus reducing the combined imaginary components (reactance) to zero. This is the condition of resonance. A reading is then made on the real or resistive component. The measured resistive component is then divided into the inductive reactance of the coil's true inductance at the measurement frequency, not the apparent inductance. This procedure has to be repeated for every frequency at which Q is to be measured. Only high quality capacitors possessing high Qs should be used to cancel the reactance of the coil. This ensures the Q of the coil is measured and not the Q of the inserted capacitor used to cancel the reactance. Silver mica capacitors are ideal for this purpose as their Qs are typically greater than 1000. The ability of the impedance analyser to measure low ohmic values accurately should be checked by measuring the values of various low ohmic resistors of known value. *Table 3.1* lists the measured values of effective series resistance and calculated Q for the 6.235uH air wound coil under the condition of resonance at the measurement frequency.

Table 3.1: *Measured values of effective series resistance and calculated values of Q for the 6.235μH air wound inductor described in Section 3.6. Measurements were carried out on the HP-4191A RF Impedance Analyser using the resonant method.*

Frequency MHz	Resistance ohm	Resonant Q
1	0.2	195
2	0.33	237
4	0.54	290
5	0.62	315
10	0.965	405
15	1.3	452
20	1.6	489
24.8	2.05	473
28.3	2.5	443
33.1	3.3	392

3.8 Air Wound Coils in High Power Filters

This discussion on air wound coils is limited to coils used in series with the through path of passive lowpass filters. Air wound inductors are:-

- non-saturable,
- relatively stable with time and temperature when compared with cored inductors,
- linear, i.e. inductance does not change with respect to flux density,
- such that permeability is independent of frequency, changes in inductance with frequency are due to the effects of distributed capacitance,
- the preferred coil for power circuits.

A pure inductor does not dissipate power as heat. It is the inductor's distributed resistance that warms it when used in power circuits. Air wound coils used in the through path of power circuits should therefore be designed to achieve the maximum obtainable Q. This ensures the distributed D.C. and A.C resistance is small, keeping the heat generated within the coil's wire to a minimum. Most insulations used on wires are poor conductors of heat and impede the dissipation of heat generated within the wire to its environment. It is therefore recommended that only bare wire be used for power coils. It may be necessary

to employ forced air cooling to keep the coil's temperature within tolerable limits. Attention also needs to be given to the peak currents and voltages generated under extremes of S.W.R. and the impact they have on the heat generated by the coil, voltage breakdown between turns and voltage breakdown between the coil and surrounding components.

Large air wound coils as used in power filters are surrounded by intense R.F. magnetic fields when the filter is in service and the transmitter is operating. Shielding is normally used to protect personnel and other electronic equipment from the effects of these fields. The resistivity of the enclosure used as a shield must be low in order to ensure shielding effectiveness and to keep induction heating of the shield to a minimum. The mechanism of shielding is covered in section ***4.3 Shielding***.

3.8.1 Coils Used in Shunt With the Through Path

Coils used in shunt with the through path, i.e. highpass filters, are mainly subjected to voltage stresses between adjacent turns and are not normally required to shunt to ground large amounts of R.F. currents. Most of the current will be flowing through the capacitors in the through path. Wire with high temperature insulation such as TEFLON can therefore be used to increase the breakdown voltage between turns keeping in mind the increase in distributed capacitance and the lowering of the coils' parasitic resonances. Finer wire can also be used to help offset the increase in capacitance between turns.

3.9 Toroidal Coils

The inductance of a toroidal coil, uniformly wound with a single layer of fine wire (ref.27 pp21) is:-

$$L = \frac{0.004\pi N^2 \mu_o \mu_r A_c}{l_e} \tag{3.13}$$

where: L = inductance (uH)
N = number of turns
μ_o = permeability of free space (1.257×10^{-6} H/m)
μ_r = relative permeability of core material
A_c = cross-sectional area of core (cm^2)
l_e = effective length of core (cm)

μ_r, A_c and l_e are obtained form the manufacturer's data sheets. Most manufacturers combine μ_o, μ_r, A_c, l_e and any other constants that influence inductance into a single quantity called the *inductance index* (A_L) for a given core. This greatly simplifies calculations by reducing equation (3.13) to:-

$$L = N^2 A_L \tag{3.14}$$

The values of A_L for the various toroids can be obtained from the manufacturer's data sheets. Iron powder cores A_L are usually quoted in uH/100 turns. The number of turns needed for a required inductance is:-

$$N = 100\sqrt{\frac{L}{A_L}} \tag{3.15}$$

where: N = number of turns
L = desired inductance (uH)
A_L = inductance index of the toroid (uH/100turns)

Table 3.2 summarises the characteristics of iron powder materials available from Amidon. In powdered iron material, a higher Q will be obtained in the upper portion of a material's frequency range when smaller cores are used. Likewise, in the lower portion of a material's frequency range, higher Q can be achieved when using the larger cores.

Table 3.2: *Property Chart of Amidon Iron Powder Materials obtained from Reference 15.*

Best Q freq. range (MHz)	μ	Material	Temperature stability (ppm/°C)	Colour code
0.05 - 0.5	35	3	370	grey
0.1 - 2.0	25	15	190	red/white
0.5 - 5.0	20	1	280	blue
2.0 - 30.0	10	2	95	red
5.0 - 35.0	9	7	30	white
10.0 - 50.0	8	6	35	yellow
30.0 - 100.0	6	10	150	black
50.0 - 200.0	4	17	50	blue/yellow
100.0 - 300.0	1	0	0	tan

The permeability of ferrite is generally much higher than iron powder and the A_L value is usually quoted in mH/1000 turns. The number of turns for a required inductance on a ferrite toroid is:-

$$N = 1000\sqrt{\frac{L}{A_L}} \tag{3.16}$$

where: N = number of turns
L = desired inductance (mH)
A_L = inductance index of the toroid (mH/1000turns)

Equations (3.15) and (3.16) do not make allowances for variation in inductance with wire gauge and therefore should be used as a guide only. A smaller diameter wire will return a larger value of inductance than for a larger diameter of wire with the same number of turns on the same toroid. This is very useful when using ferrite material with large permeability where compressing and stretching the turns has minimal effect on the inductance and the required inductance is more than the number of turns on the toroid but less than adding one more turn. Under such conditions either use the same number of turns using a smaller diameter wire or use a larger diameter wire adding the extra turn. The inductance of toroids, like that of air wound coils, should be measured at the filter's cut-off frequency.

3.9.1 Electromagnetic Flux Surrounding Toroidal Coils

There appears to be two common misconceptions about toroidal coils.

1. They are inherently self-shielding and this is due to the magnetic flux being constrained within the core, and

2. there are no magnetic lines of flux in the hole in the centre of the toroid.

Table 3.3 lists the changes in inductance of two short lengths of wire of different diameters when they were held against the inner and outer surfaces of 0.5 inch toroids of various relative permeabilities ranging from 1 to 2000. The first entry is the measured self-inductance in air and is used as a reference to which the increase in inductance is compared. Notice the inductance of the wire at most only doubles when held against the outside perimeter of the toroid as the permeability was increased from 1 to 2000. A measurement carried out on the two adjacent sides showed similar results. The same wires held against the inside surface of the toroid returned a large increase in self-inductance as the permeability was increased. From this it can be deduced, the inductance of a toroid is relatively evenly distributed around the individual turns of the winding for cores with low

permeability and is progressively concentrated on the part of the turns that passes through the centre of the toroid as the core's permeability is increased to high levels.

Table 3.3: *Increase in the self-inductance of a 4.7 mm length of 0.16 mm and 0.6 mm diameter ECW (enamel covered wire) measured at 1MHz when held against the inside and outside boundaries of 0.5 inch (OD) toroids of varying μ. Permeabiliy of 1 is phenolic, 3 to 20 are iron powder, 40 and above are ferrite.*

μ	Inductance of 0.16 mm wire		Inductance of 0.6 mm wire	
	Outside (nH)	Inside (nH)	Outside (nH)	Inside (nH)
air	4.3		2.5	
1	4.3	4.3	2.5	2.5
3	6.2	6.7	3.4	5.2
6	7	9.7	3.9	7.2
10	7	12	4.1	9.6
20	8	18.2	4.6	16
40	8.3	32.3	4.8	29.4
125	8.4	79.2	4.9	76.2
850	8.5	351	5	339
2000	8.7	1141	5.1	1137

Table 3.4: *Self-inductance of 6T of 0.4 mm ECW close wound on sample 0.5 inch toroids with various permeabilities.*

μ	Inductance
air	141nH
1	139nH
3	291nH
6	379nH
8	460nH
10	527nH
20	768nH
40	1.31μH
125	3.02μH
850	12.54μH
2000	41.1μH

Six turns of 0.4 mm wire were close wound on 0.5 inch toroids of various permeabilities and their measured inductances at 1 MHz are given in *Table 3.4*. These toroids will be used to examine the magnetic field distribution both in the hole in the centre of the toroid and beyond the outer perimeter. Figures 3.10 and 3.11 show the test set-up used to measure the magnetic fields.

A one turn pick-up loop described in figure 3.9 was used to measure the relative magnitudes of the magnetic fields. The axis of the one turn loop was held parallel to the axis of the six close wound turns with side AD of the one turn loop centrally located between that part of turns three and four of the six turns that passes through the centre of the toroid. The centre of side BC of the one turn loop lies on an imaginary line at a right angle to the axis of both loops which starts at the axis of the six turn loop, passes between turns three and four cutting side AD of the one turn loop and continues on to pass through the centre of side BC. Very fine wire, 39SWG, for the one turn loop and a test frequency of 1 MHz were chosen to minimise the capacitive coupling between the two loops. The two parts of the one turn loop that will have voltages induced into them from the six turn loop are lengths AD and BC. Length AD will be used to measure the relative magnitudes of the magnetic flux by measuring the induced voltage. The induced voltage will be proportional to H and its rate of change (Faraday's Law). The magnitude of H will follow an inverse square law with distance provided that all mediums that H traverses have a relative permeability of one, equation (3.2) the Biot-Savart Law. If the attenuation of the 1 MHz test signal, via the inverse square law with distance, is kept large between AD and BC then the voltage induced into AD will be representative the magnitude of H at the point where AD resides. The maximum distance from the perimeter of the six turn loop over which the measurements will be made is 18.75 mm. Side AD and BC have to be displaced many times this distance in order to keep the voltage induced in BC small enough so it can be ignored. A distance of 106 mm was found to satisfy this requirement. Measurements made at points (A), (B) and (C) were carried out by unsoldering the wire of the one turn loop from the termination resistor, threading the wire through the toroid then resoldering and tensioning the wire.

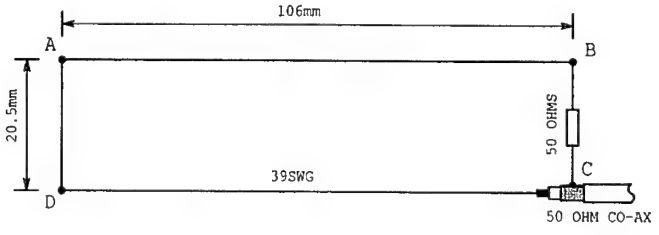

Figure 3.9 *Single turn pick-up loop*

A phenolic toroid which has a permeability of one, the same as air, was used to set the distances of measurement points (C) to (F) relative to distance between (A) and (B), the inner radius of the toroid. The six turn loop was driven from a 50 ohm source at a frequency of 1 MHz and side AD of the one turn loop placed at position (A) lightly pressed between turns 3 and 4. A spectrum analyser was used to measure the level of induced signal into the single turn pick-up loop. This was the reference level to which all other measurements were made for a given toroid. The one turn loop was then moved so that side AD was at the centre of the toroid, position (B), and the deviation in dB of the induced signal was recorded. Measurement point (B) is sufficiently removed from the six turn loop to counter any proximity effects, i.e. the difference in distance between side AD of the one turn loop and the six individual close wound turns is small. Point (B) is at the centre of curvature of the six turn loop and therefore is equidistant.

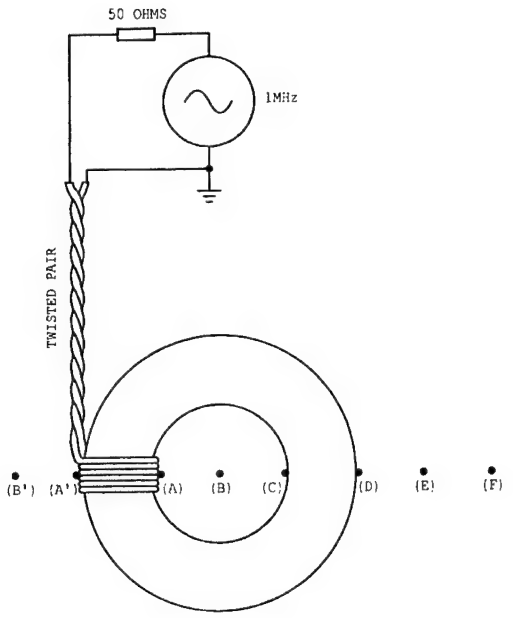

Figure 3.10 *Excitation set-up of toroidal 6 turn loop*

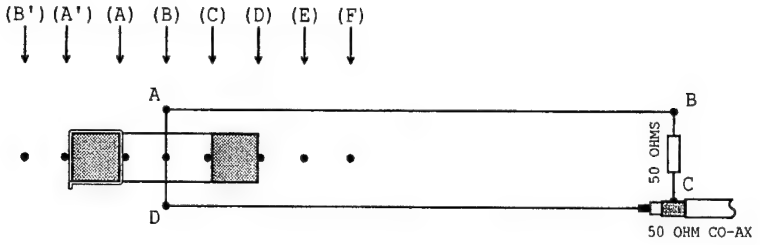

Figure 3.11 *Relative positioning of test loop with respect to the toroidal winding. Side AD of the one turn loop shown at test point (B)*

The one turn loop was then moved away from (B) until the induced signal was 6dB less than it was at (B). This becomes position (C). For the 0.5 inch phenolic toroid position (C) is diametrically opposed to (A) and was just on the inside boundary. The distance between (B) and (C) was measured and found to be 3.75 mm. If this distance is doubled, the induced signal should be reduced by a further 6dB relative to position (B) provided the attenuation with distance follows the inverse square law. With this in mind the expected attenuation values in dB with respect to the distance between (B) and (C) was calculated for multiples of this distance. These figures are tabulated in the first entry of *Table 3.5*. Side AD of the one turn loop was moved away from the six turn loop from (C) 3.75 mm to (D). The induced signal was measured and found to be -23.1dB, approximately 6dB less than (C). The distance between (B) and (D) is 7.5 mm. Moving side AD of the one turn loop 7.5 mm away from (D), doubling the distance from reference point (B), should produce a further 6dB decrease in the induced signal. This is measurement point (F). A measurement made at (F) reveals a 0.3dB difference between the expected and measured. The measured attenuation between (B) and (F) was -18.3dB which compares favourably with the expected -18dB and confirms the measurement technique and the Biot-Savart Law. Measurement point (E) equidistant between (D) and (F) was included. The inverse square law indicates there should be a 3dB difference in the induced signal between (E) and the adjacent points (D) and (F).

The one turn loop was rotated 180° about AD and AD was placed at measurement point (A') lightly pressed between turns three and four of the six turn loop on the outer perimeter. The induced signal was measured and found to be -1.1dB, lower than expected. It should be the same as measurement point (A). Closer inspection of the six turn loop reveals the turns are splayed from the inner to outer perimeter of the toroid. Compressing the turns on the outer perimeter with a pair of non-metallic tweezers increased the induced signal to the expected 0dB, the same as (A). The tweezers were removed, the turns splayed and the level of induced signal fell back to -1.1dB. Side AD was then moved to point (B') and the level of induced signal recorded. All the recorded measurements for the

phenolic toroid are tabulated in *Table 3.5* for a μ_r (relative permeability) of one. A check was then made on the permeability of the toroid. The toroid was broken with a pair of side cutters and the core removed from the six turn loop with as little disturbance to the loop as possible. The six turn loop was then air cored and the measurements at the stated distances repeated. There was no significant difference between the air core reading and the phenolic toroidal core. This confirms the permeability of the phenolic toroid was the same as air. Measurements were carried out on the remaining toroids listed in *Table 3.4*. The results are also tabulated in *Table 3.5*.

Figure 3.12 displays the data in graphical form. It can be seen that the strength of the signal external to the toroid at D, E and F is relatively the same for permeabilities one to ten. There is very little difference in the magnetic flux external to the toroid relative to the same coil air cored. It is only when high permeability cores are used that the toroid shows signs of self-shielding. Low permeability cores with windings covering 90% of the toroid were also tested for magnetic flux external to the core. While some improvements in the measured isolation between point A, the centre of the winding as with the six turn loop, and the area external to the toroid out to a distance of 18.75 mm was noticed, it was not deemed significant. In fact the field generated by the one-turn-effect added an extra orthogonal dimensional plane on which external magnetic flux could be measured.

Table 3.5: *Attenuation in dB measured with respect to position A, using a one turn rectangular loop 106 mm x 20.5 mm; test frequency 1 MHz.*

μ_r	B′ 3.75 mm′	A′ 0 mm′	A 0 mm	B 3.75 mm	C 7.5 mm	D 11.25 mm	E 15 mm	F 18.75 mm
expected	-11.2dB	0dB	0dB	-11.2dB	-17.2dB	-23.2dB	-26.2dB	-29.2dB
1	-12.5dB	-1.1dB	0 dB	-11.2dB	-17.2dB	-23.1dB	-26.6dB	-29.5dB
3	-12.2dB	-3.2dB	0 dB	-8.7dB	-14.1dB	-22.4dB	-26.9dB	-30dB
6	-14.6dB	-4.9dB	0 dB	-7.1dB	-11.3dB	-21.6dB	-26.5dB	-29.8dB
8	-15.2dB	-5.9dB	0 dB	-6.3dB	-9.8dB	-22.2dB	-27dB	-30.1dB
10	-16.7dB	-6.9dB	0 dB	-5.2dB	-8.7dB	-22.5dB	-27.1dB	-30.1dB
20	-20.7dB	-9.7dB	0 dB	-3.1dB	-4.8dB	-24.1dB	-28.8dB	-32.4dB
40	-25.5dB	-15.7dB	0 dB	-1.7dB	-2.5dB	-28.5dB	-33.3dB	-36.9dB
125	-33.9dB	-23.9dB	0 dB	-0.6dB	-0.9dB	-36.6dB	-41.8dB	-45.7dB
850	-51.5dB	-41.3dB	0 dB	-0.06dB	-0.08dB	-52.7dB	-58dB	-61.5dB
2000	-56dB	-47dB	0 dB	-0.02dB	-0.04dB	-58.8dB	-63.2dB	-66.2dB

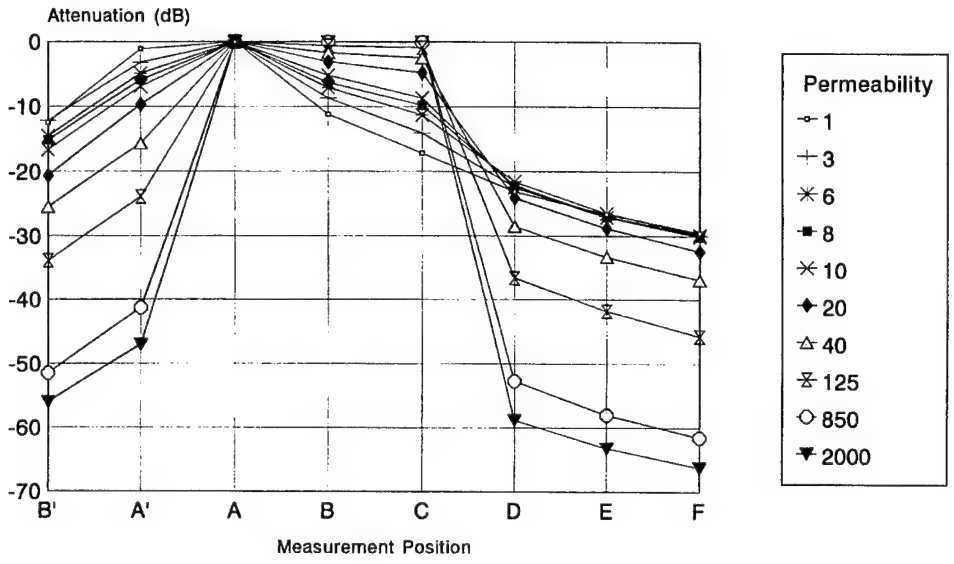

Figure 3.12 *Level of signal induced into side AD of the one turn loop at indicated positions*

It is erroneous to think a coil is self-shielding merely because it has the form of a toroid. Most toroids used in filters in the H.F./V.H.F. bands will have permeabilities less than 20. The data in *Table 3.5* shows magnetic flux external to the toroidal coil on low permeability cores to be comparable to the same coil air cored. Placement of toroidal inductors with respect to other components is therefore just as critical as if the coils were air wound.

The data in *Table 3.5* shows the magnetic field in the hole in the centre of the toroid follows an inverse square law when the cores permeability is the same as air, unity. It also shows the lines of flux become more uniform with distance in direct proportion with increases in the core's permeability. A permeability of 2000 shows an almost uniform distribution of lines of flux as opposed to a permeability of one in which it follows an inverse square law.

3.9.1 The One-Turn-Effect of Toroidal Coils

Figure 3.13 (A) is a toroidal coil of 10 turns in which the turns have been manipulated to form a one turn loop on the outer perimeter commonly known as the one-turn-effect. In reality the one turn is evenly distributed throughout the winding of the coil approximating a tubular conductor that surrounds the core for the length of the coil. The self-inductance of the one turn loop is relatively independent of the core's permeability being similar to the wire held against the outside boundary of the toroidal core as in *Table 3.3*. The

orientation of the magnetic field of the one turn loop generated by an R.F. current passing through the helical coil is orthogonal to the normal field of the coil. Measurements of the magnetic field generated by the one turn loop external to the toroid using the pick-up loop of figure 3.9 showed a field which followed an inverse square law with distance and an intensity that was relatively independent of the core's permeability. This agrees with the self-inductance of the one turn loop being almost independent of the core's permeability. The loop formed by the one-turn-effect is approximately equivalent to a single turn loop in free space. Mutual coupling can exist between the toroid via the one-turn-effect and components in the surrounding environment provided the components are not situated in the one turn loop's null points.

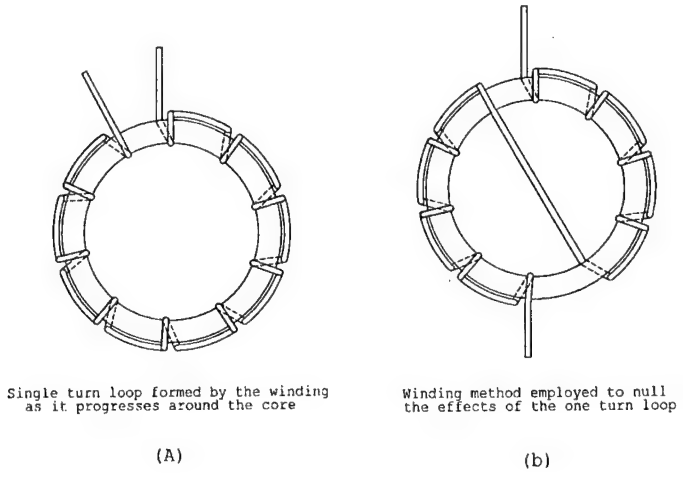

Figure 3.13 *Illustrating the one-turn-effect*

Figure 3.13 (B) shows a winding method used to null the field generated by the one-turn-effect. The magnetic fields generated by each half of the one turn loop are equal but of opposite direction, their net sum being zero. Mutual coupling will still exist between components that are not approximately equidistant from both halves of the loop, i.e. components adjacent to one half of the winding. Attention to component placement is therefore still required. The part of the winding that passes through the centre of the toroid on a slant suffers an increased A.C. resistance due to circulating eddy currents within this part of the winding and lowers the toroidal coil's Q. The decrease in Q is most pronounced in low permeability cores where the flux gradient through the hole in the toroid is the greatest. Winding the coil with larger diameter wire increases the dimensions of copper over which the flux gradient has an influence and induces larger circulating eddy currents, increasing the total A.C. resistance, not decreasing it as one might expect. The toroidal coil's Q is reduced by 10 to 25 percent and is dependent on core size, core

permeability, wire gauge and angle of slant of wire relative to the direction of travel of the lines of flux in the hole in the centre of the toroid. The reduction in Q is generally not sufficient to adversely affect a filter's performance. This winding technique lowers the coil's distributed capacitance and hence raises the parallel self-resonant frequency. Also, this technique is not recommended for filters employing resonant circuits as it lowers the circuits Q, i.e. elliptical, *m*-derived, notch, and tuned narrow band filters.

3.9.2 Toroids in High Power Filters

Iron powder, as opposed to ferrite, is the preferred toroidal material in the H.F. and V.H.F. bands. It has lower losses, can withstand higher flux densities and is more stable over a wide range of flux levels and temperatures. Ferrite or powdered iron toroids, to be used in power circuits, should be first covered with glass-electrical tape, such as 3M-27, before winding, to prevent arcing to the core. In high power toroids where considerable heat is being generated, it is recommended that PTFE or 'Thermoleze' insulated winding wire be used. In power toroids however, consideration needs to be given to the peak flux density relative to the chosen core's saturation flux density and the distortion products generated. The peak flux density combined with the hysteresis losses heat the core material. Equations for calculating the flux density and heat management together with worked examples can be found in References 15 and 27 and will not be repeated here.

The non-linear relationship between B and H of the core material distorts the flux density with respect to the alternating magnetising force. The distortion is usually seen as third order products. At low signal levels, say, less than one Watt, the distortion is so small that it can be ignored. At higher power levels, the induced distortion may be of concern. In spot frequency transmitters where a lowpass filter employing toroids is installed at the transmitter's output to attenuate the harmonics, the out-of-passband third order distortion products (third harmonic) generated by the toroids within the filter are attenuated by the action of the filter itself just as it attenuates the harmonics of the transmitter. The shunt capacitors to ground at either side of the toroid provide a low impedance path, relative to the source and load impedances, between the ends of the windings. A filter with a low out-of-passband impedance is therefore preferred to one whose impedance is high.

A toroidal filter fitted to the output of a broadband transmitter needs special consideration. Take for example a 2 to 30 MHz high power transmitter to which a 30 MHz lowpass roofing filter employing toroids has been fitted at the output. The third order products (third harmonic) generated by the toroids within the filter by a single tone between 2 to 10 MHz will not be attenuated by the components within the filter, namely the shunt capacitors to ground. The toroids will behave like signal generators of third order products effectively in series between the output impedance of the power amplifier and the load impedance presented by the antenna, thus offering a ready path for the radiation of unwanted harmonics.

The generation of third order intermodulation products within the filter is dependent partly on the differences in the hysteresis of the toroidal material measured at the frequencies of the two tones and also on the variation of permeability with the strength of the cores' magnetic flux (frequency dependent). As an example, two pure high power tones separated by 10 KHz placed anywhere in the 2 to 30 MHz range presented at the input of the high power filter may have an acceptable third order intercept at the filter's output. However, displace the same two tones by a frequency greater than say, 1 MHz, and the output intercept of the filter may show unacceptable third order intermodulation distortion levels.

4. Construction Techniques

There are two impedances that need to be considered when building LC filters. The first is the filter's characteristic or the lumped element impedance (*Section 1*, equation (1.3)). The second is the reactance presented by the distributed elements that appear in the in-band through path, that is, elements that are seen in series with the through path by the lumped elements occupying three dimensional space. For highpass filters it is the distributed inductance of the in-line series capacitor's plate and lead inductance and any lead or PCB tracks used for routing. For lowpass filters it is the distributed inductance of the one-turn-effect of large air wound coils used in series with the through path. Techniques used to convert the unwanted distributed inductance into a transmission line will now be examined for highpass and finally lowpass filters.

4.1 Highpass Filters

At frequencies well into the passband, the inductive reactance of the shunt inductors is large when compared to the filter's terminating impedances and therefore can be deemed as an open circuit. The coils' distributed capacitance will be considered later. At the same time, the lumped capacitive reactance of the series capacitors is very small when compared to the filter's terminating impedances and, being in series with the filter's through path, can therefore be represented as a very low impedance or a short circuit. This then leaves the capacitors' distributed lead and plate inductance. A filter's total in-line distributed inductance, which can be in the order of tens of nH, is dependent on capacitor construction, lead length, filter configuration (pi or Tee) and the order of the filter. This inductance, which is in series with the filter's through path, and has an increasing reactance with increasing frequency, can become an appreciable percentage of the filter's source and load impedances and start to affect the insertion loss of the filter.

If the right amount of distributed capacitance is added to the in-line distributed inductance, then the in-band through the path of the filter would look like a transmission line whose characteristic impedance is independent of frequency. If this characteristic impedance was tailored to match the filter's terminating impedances, then an in-band signal passing through the filter would be subjected to minimum attenuation. In the real world however, there are parasitic resonances in the shunt inductors as well as ohmic losses of any inductance enhancing material used. The filter's in-band response would be relatively independent of frequency up until these effects become noticeable. There are two ways of adding the required distributed capacitance.

1. adding distributed discrete capacitors to the through path, or
2. converting the through path into a transmission line.

4.1.1 Adding Discrete Capacitors

First it is necessary to calculate or measure the distributed inductance of the through path of the filter. Then using equation (1.3) from *Section 1* find the total distributed capacitance required to give the desired characteristic impedance. Subtract from this value the self-capacitance of the shunt inductors and the already existing capacitance to ground of the through path. The result is the value of capacitance that has to be added to the through path. Divide this capacitance into equal discrete preferred values and evenly distribute them in shunt with the through path for the length of the filter. The distributed inductance of the through path together with the added shunt discrete capacitors to ground form a high frequency lowpass filter. This lowpass filter creates a useable low loss upper frequency limit to the highpass filter. This technique is ideal for power filters where physically large components are used to keep losses to a minimum. These large components, especially the shunt inductors to ground, generally have parasitic resonances that affect a filter's performance before the cut-off frequency of the lowpass filter is reached.

4.1.2 1.875 MHz Highpass Filter

Figure 4.1 is a 1.875 MHz H.P. filter which will be used to demonstrate this technique. The filter was constructed in a Pomona diecast box whose inside dimensions are 53x24x19 mm. The through path of the filter will be the long dimension. The two 350 V silver mica 1000pF capacitors were connected point to point between input and output BNC connectors. A distributed lead and plate inductance of 36.4nH of the two capacitors connected in series was calculated from the network's series resonant frequency of 37.3 MHz. The required distributed shunt capacitance to ground for a 50 ohm system is 14.6pF. The measured distributed capacitance to ground of the two capacitors when installed in the box was 2.6pF. The three shunt coils were made using Amidon T-37-2 toroids and 0.25 mm enamel covered wire. Total distributed capacitance of the three shunt coils calculated from their respective parallel resonant frequencies is approximately 2.2pF. *Table 4.1* lists the various resonant frequencies of the coils used. The lowest series self-resonant frequency at 378 MHz for the two larger inductors will create a localised increase in the through path loss of the filter. This will place a limit on the filter's useful in-band upper frequency response of approximately 300 MHz. Fine winding wire (0.25 mm) was used to make these coils in order to:-

- decrease the distributed capacitance and raise the series self-resonant frequencies in order to maximise the useable upper frequency response, and

- increase the A.C. resistance at the series self-resonance to lower its Q and dampen its shunting of the through path signal to ground. The A.C. resistance at the out-of-passband signals, being much lower in frequency, will be significantly smaller and therefore should not appreciably affect the out-of-band attenuation.

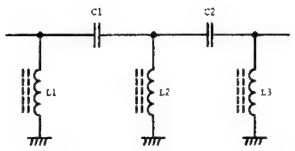

C1 = 1000pF L1,L3 = 4.03uH
C2 = 1000pF L2 = 1.922uH
4.03uH = 31T of 0.25mm wire on T-37-2
1.922uH = 21T of 0.25mm wire on T-37-2

Frgure 4.1 *1.875 MHz highpass filter*

Table 4.1: *Measured parallel and lowest series resonant frequencies of toroidal coils used in the 1.875 MHz Highpass filter.*

Inductor (μH)	Parallel self-resonant frequency (MHz)	Lowest series self-resonant frequency (MHz)
4.03	91.3	378
1.92	142.3	513

The parallel resonant frequencies of the coils were measured in the absence of any shielding. The presence of shielding will slightly increase the coils' distributed capacitance, say 0.5pF total for the three coils. Total shunt capacitance to ground is approximately 2.6+2.2+0.5 = 5.3pF. This is 9.3pF less than the 14.6pF required. There are three convenient points in which to add extra shunt capacitance and that is in the general area of the three coils. The 9.3pF shortfall divided by three is 3.1pF. This is between the preferred values of 2.7pF and 3.3pF supplied by most manufacturers. It was shown in section 2.2 *Effects of Distributed Inductance* how distributed inductance in capacitors increases their apparent capacitance with frequency. By choosing the preferred value of 2.7pF over 3.3pF for these three capacitors allowance is made for this increase as well as any external capacitive coupling to the installed environment.

Figure 4.2 is the frequency response of the filter before the three 2.7pF capacitors were added. The top trace is the input signal from the signal generator, the bottom the filter's output, their difference being the insertion loss. Note the general increase in attenuation from the cut off frequency (1.875 MHz) into the passband. Also note the dips in the response at the coils' series self-resonant frequencies as tabulated in *Table 4.1*. Figure 4.3 is the associated Z_{11} plot spanning 3 MHz to 1 GHz, markers are at 100 MHz increments, 3 MHz is at the 50 ohm point.

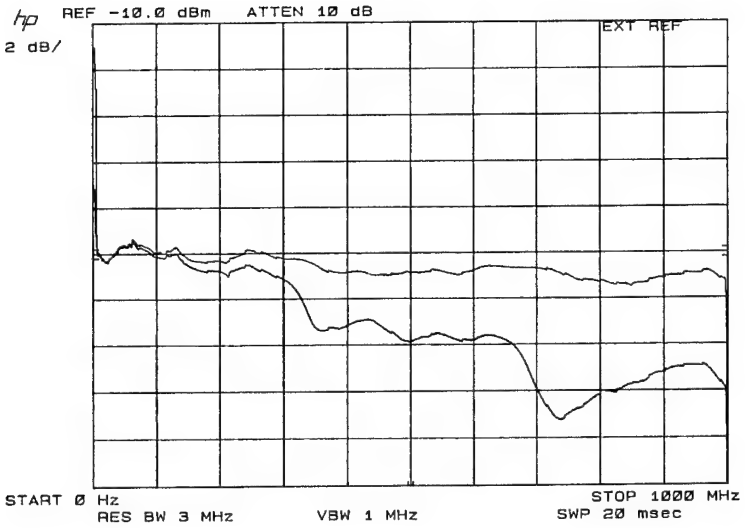

Figure 4.2 *Insertion loss of the 1.875 MHz H.P. filter in Pomona box*

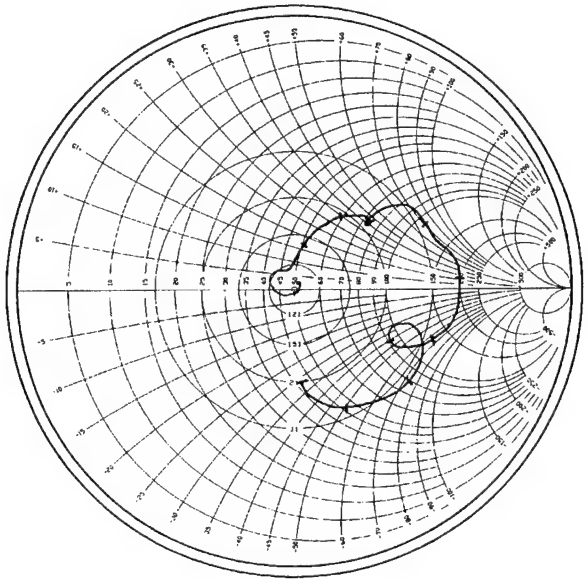

Figure 4.3 *Z_{11} plot 3 MHz to 1 GHz of 1.875 MHz H.P. filter in Pomona box, 100 MHz markers*

Figure 4.4 is the frequency response after the three 2.7pF capacitors were fitted. Note the general lifting of the filter's response towards the input level of the signal generator. The dips caused by the series resonances of the shunt inductors are still present with an improvement in the dip at approximately 756 Mhz (the slight frequency shift is attributed to disturbing the coils when installing the capacitors). The through path distributed inductance and the installed discrete 2.7pF capacitors together with the coils' distributed capacitance form a lowpass filter whose cut off frequency is approximately 1.4 GHz. This is well above the 375 MHz series resonance of the larger coils. Figure 4.5 is the Z_{11} plot spanning 3 MHz to 500 MHz. Note the improvement in SWR from 4:1 at 500 MHz (marker just above 200 ohms on the R line in fig 4.3) to less than 1.4:1 in figure 4.5. Figure 4.6 is the Z_{11} plot spanning 3 MHz to 1 GHz.

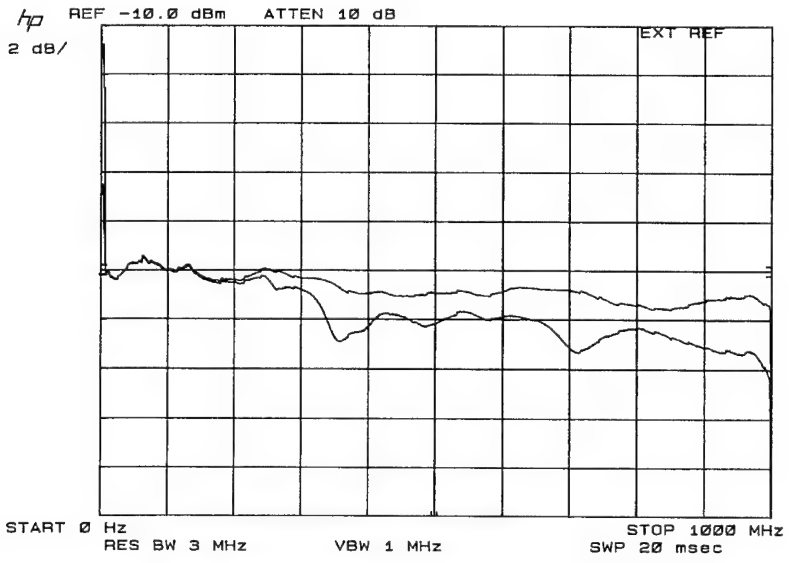

Figure 4.4 *Insertion loss of 1.875 MHz H.P. filter in Pomona box with the three 2.7pF shunt capacitors installed*

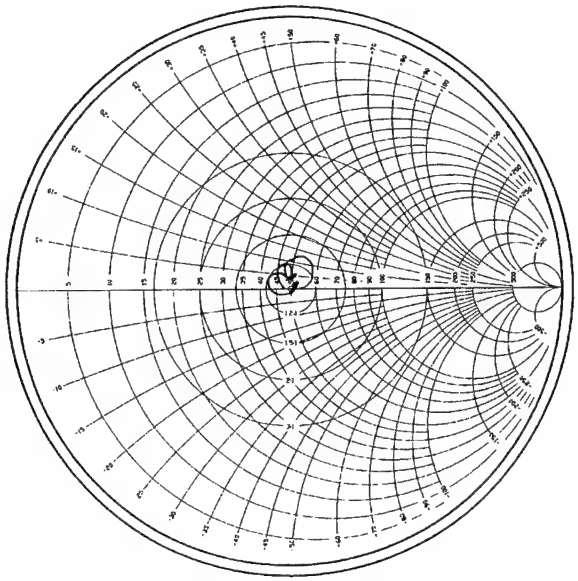

Figure 4.5 *Z_{11} plot 3 MHz to 500 MHz of the 1.875 MHz H.P. filter in Pomona box with the three 2.7pF shunt capacitors installed*

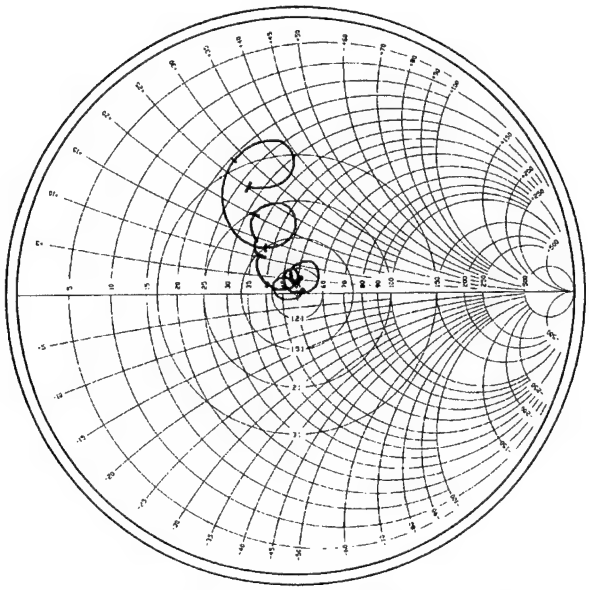

Figure 4.6 *Z_{11} plot 3 MHz to 1 GHz of the 1.875 MHz H.P. filter in Pomona box with the three 2.7pF shunt capacitors installed*

The cut-off frequency of this filter was chosen to so that the coils' self-resonant frequencies were within the upper frequency limit of the test equipment being used. This was done to show how the series resonance of the shunt coils affects the frequency response creating an upper frequency limit on the low loss usefulness of a highpass filter. Unfortunately, the low series resonance is superimposed on the increased insertion loss created by the distributed inductance of the through path and also the power being absorbed in the toroidal material used to make the coils. The parasitic resonance and power absorption losses are masking the gains that can be obtained in this construction technique. In order to highlight the losses of toroidal material versus air core and to show the effectiveness of the construction technique, a second H.P. filter with a cut-off frequency of 27.5 MHz was constructed in the same enclosure. This higher cut-off frequency for the same through path length means the reactance of the distributed inductance can reach an appreciable percentage of the terminating impedances before the limiting effects of the parasitic resonances of the coils are seen. The largest coil's series self-resonant frequency was at approximately 1.3 GHz. The useful low loss upper frequency limit of the filter should be approximately 1 GHz.

4.1.3 27.5 MHz Highpass Filter

A 27.5 MHz highpass filter, Figure 4.7, was constructed using 68pF 350 V silver mica capacitors in the through path and the same technique as above. The series self-resonant frequencies of the coils are just above 1 GHz and therefore will not be seen using the current test equipment. Figure 4.8 is the frequency response of the filter when constructed using point to point wiring and toroidal coils in the same Pomona box as before. Note the expected decrease in attenuation as the frequency is increased from the -3dB point into the passband then an increase in attenuation caused by the distributed inductance in the through path. Figure 4.9 is the associated Z_{11} plot spanning 3 MHz (+j8 ohms on circumference of Smith chart) to 1 GHz. The length of the through path is the same as in the 1.875 MHz example, therefore the amount of distributed capacitance needed will be approximately the same. Three 2.7pF capacitors were added in shunt with the coils and the frequency response remeasured. Figure 4.10 shows the improvement in insertion loss between the filter's cut-off frequency and 800 MHz. Note the 1 GHz cut-off frequency of the lowpass filter formed by the distributed inductance of the through path and the coil's distributed plus 2.7pF added shunt capacitance to ground. Figure 4.11 is the Z_{11} plot spanning 3 MHz to 1 GHz, markers are at 500 MHz and 1 GHz. A more even distribution of smaller capacitors, four 2.2pF instead of three 2.7pF, would raise the corner frequency of the lowpass filter formed by the introduction of the discrete shunt capacitors to ground thus raising the useable upper frequency.

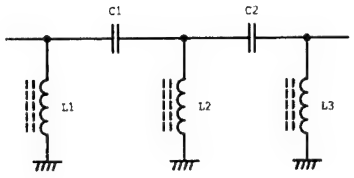

C1 = 68pF L1,L3 = 380nH

C2 = 68pF L2 = 146nH

TOROIDAL

380nH = 10T of 24SWG wire on T-37-6

180nH = 6T of 26SWG wire on T-37-6

AIR WOUND

380nH = 12T of 24SWG wire 5mm ID

180nH = 6T of 26SWG wire 5mm ID

Figure 4.7 *27.5 MHz highpass filter*

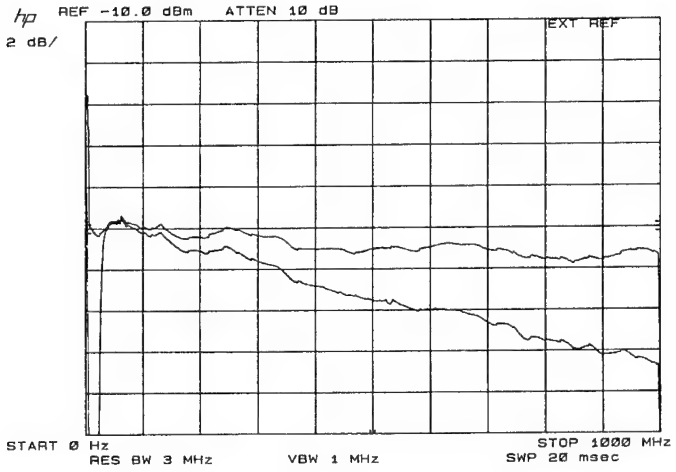

Figure 4.8 *Insertion loss of the 27.5 MHz H.P. filter in Pomona box*

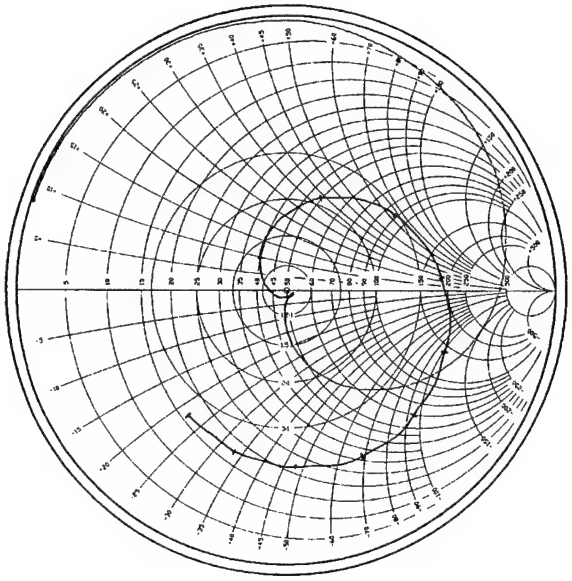

Figure 4.9 *Z_{11} plot 3 MHz to 1 GHz of 27.5 MHz H.P. filter in Pomona box, 100 MHz markers*

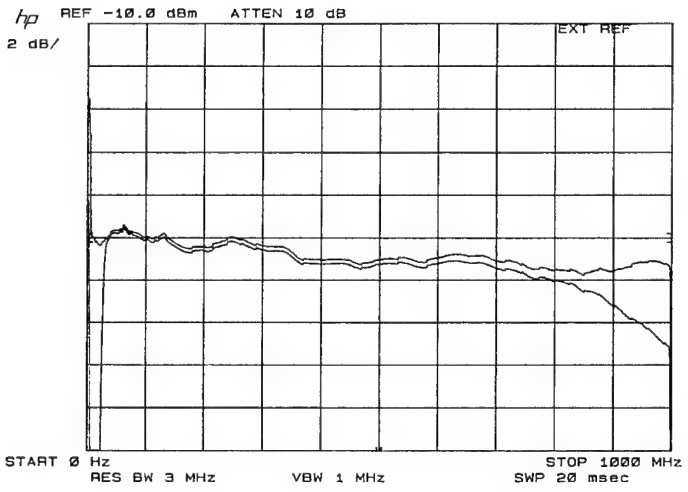

Figure 4.10 *Insertion loss of 27.5 MHz H.P. filter in Pomona box with the three 2.7pF shunt capacitors installed*

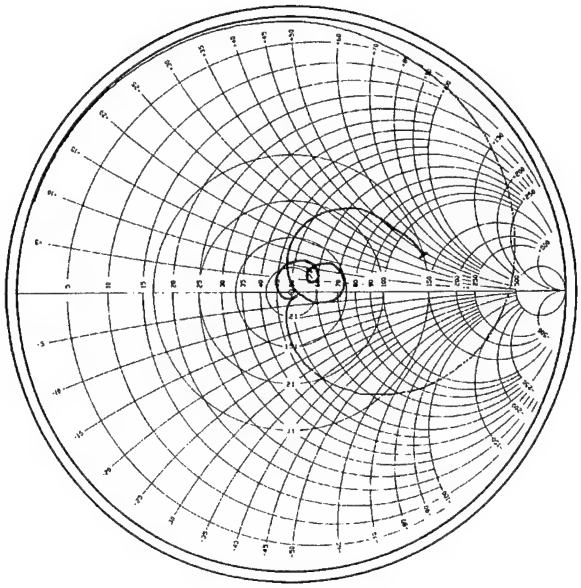

Figure 4.11 *Z_{11} plot 3 MHz to 1 GHz of the 27.5 MHz H.P. filter in Pomona box with the three 2.7pF shunt capacitors installed, markers 500 MHz and 1 GHz*

4.1.4 Converting the Through Path into a Transmission Line

This is achieved by increasing the distributed shunt capacitance to ground of the capacitor leads by laying them in line with a microstrip line designed to the filter's characteristic impedance. The capacitor is soldered in place on top of the line straddling a gap that has been cut in the through path. The diameter of the capacitor's leads is usually several times less than the width of the microstrip line and therefore has negligible effect on the line's distributed capacitance. The increase in thickness of the line caused by the capacitor's leads does alter the distributed inductance. This variation in inductance is usually small and can be ignored. This technique suits PCB layout with the added bonus that the capacitors' connecting leads become part of a transmission line and as such their length is not critical. Chip capacitors are ideally suited to microstrip work and are the preferred component for low power filters. Their width is usually chosen to be the same size or just a little smaller than the width of the microstrip line. If two chip capacitors are required to make a non-preferred value, they should be pyramidally stacked, that is the smaller of the two sitting on top of the larger, across the gap in the line. Had the capacitors been placed side by side, the line would have to have been widened at the connection point to allow adequate pad area to accommodate the components and the solder fillets. This creates a small discontinuity in the line. The summation of these discontinuities in a high order highpass filter can affect the through path insertion loss at the higher passband frequencies before the parasitic effects of the shunt inductors become noticeable. By stacking the components their footprint and solder fillets are equal to or are just within the

confines of the microstrip track width. This minimises the line discontinuity. Smaller sized chip capacitors can be placed side by side so long as their total width is equal to or just within the confines of the microstrip track.

The same H.P. filters using the same components will be used to demonstrate this technique so that a direct comparison can be made. A 48 mm long 50 ohm microstrip line was constructed from double sided FR-4 fibreglass P.C.B. material using the method described in *4.1.7 Microstrip Line*. Two gaps were placed in the line dividing it into thirds. These gaps were made wide enough to allow a chip capacitor to be soldered across it at some later time.

4.1.5 1.875 MHz Highpass Filter using Microstrip

The two 1000pF 350 V silver mica capacitors as used in the 1.875 MHz filter were disconnected from the Pomona box, from a previous demonstration, and installed soldered on top of the line each straddling a gap cut in the line. The capacitors' lead lengths were unaltered. The three shunt inductors were also removed and installed at the mid point of the respective one third microstrip lines and ground.

Figure 4.12 is the frequency response of the 1.875 MHz filter. Note the presence of the dips in the response caused by the series resonance of the coils and their slight improvement. Figure 4.13 is the Z_{11} plot spanning 3 MHz to 1 GHz. The large 350 V mica capacitors were removed and replaced with 1000pF ceramic chip capacitors. Figure 4.14 is the frequency response of the filter using chip capacitors. Note there is very little difference between using the physically large mica capacitors with leads and the small leadless ceramic chip capacitors.

There is a discrepancy between the measured insertion loss of the filter and the measured SWR as seen in the Z_{11} plot. Equation (4.1) was used to generate the plot in Figure 4.15 which shows the expected insertion loss of an ideal lossless filter for a given SWR.

$$dB_{Loss} = 10Log_{10}\left|1-\left(\frac{SWR-1}{SWR+1}\right)^2\right| \tag{4.1}$$

where: dB_{Loss} = Through path transmission loss of filter
SWR = Standing Wave Ratio at input of filter with ideal termination at filter output

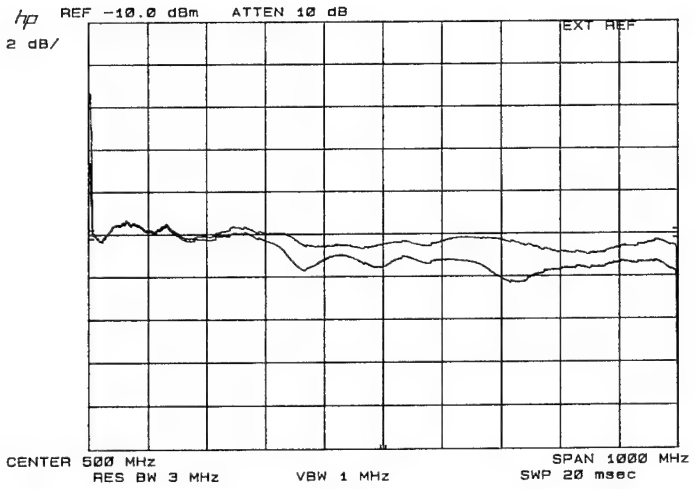

Figure 4.12 *Insertion of 1.875 MHz H.P. filter on microstrip, 350 V silver mica capacitors*

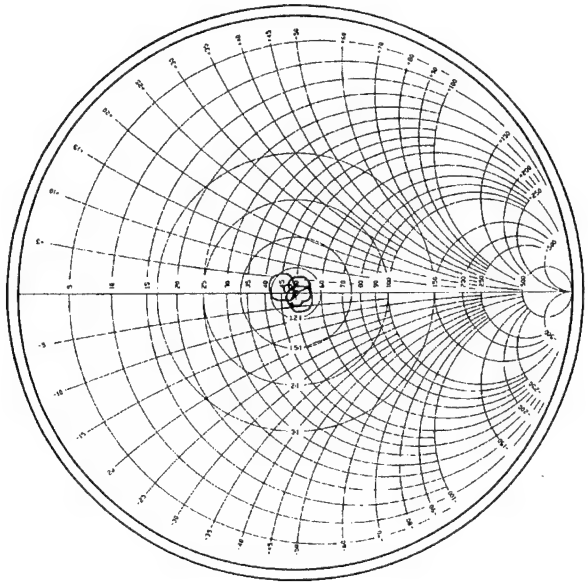

Figure 4.13 *Z_{11} plot 3 MHz to 1 GHz of the 1.875 MHz H.P. filter on microstrip, 350 V silver mica capacitors*

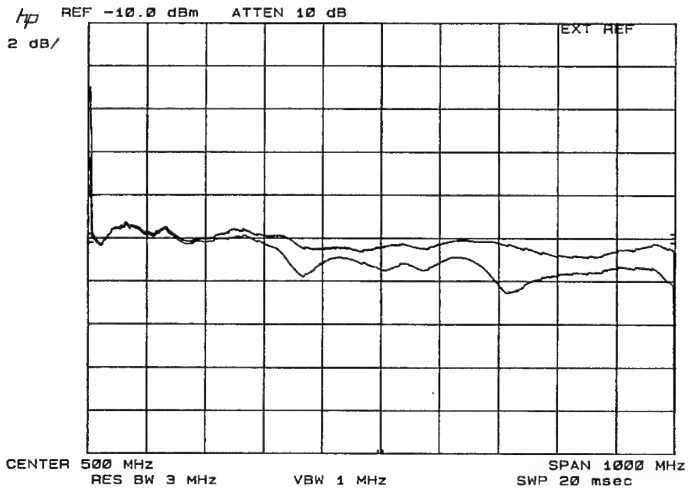

Figure 4.14 *Insertion loss of 1.875 MHz H.P. filter on microstrip, using chip capacitors*

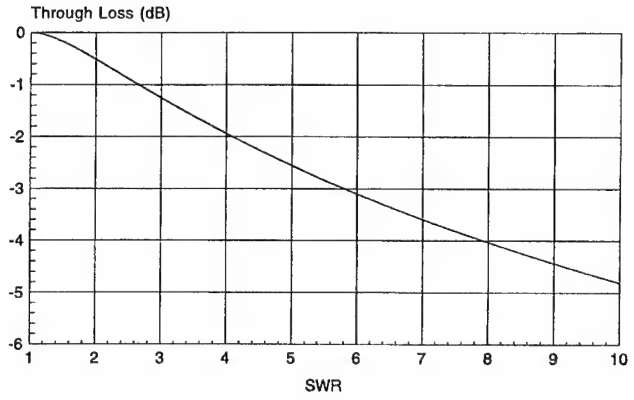

Figure 4.15 *Filter transmission loss versus SWR for an ideal LC filter with no distributed R*

Comparing the expected insertion loss versus SWR (Fig. 4.15) with the Z_{11} plots (Fig. 4.13) and the through path loss (Fig. 4.12) indicates that power is being absorbed by the filter, most likely by the toroidal material used in the coils. Air wound coils needed to confirm this through substitution would be too large for the space provided. Therefore, this loss into the core material will be demonstrated in the 27.5 MHz H.P. filter.

4.1.6 27.5 MHz Highpass Filter using Microstrip

The components used in the 27.5 MHz filter constructed in the Pomona box were removed and installed on the microstrip line described in figure 4.22. The distributed plate inductance of the in-line capacitors was incorporated into the transmission line by adding the appropriate amount of distributed capacitance using the following method. A small piece of brass shim approximately the same size as the capacitor was soldered vertically on the earth plane adjacent to each capacitor. This is the area of the PCB indicated by 'A' in figure 4.22. The mounting method is shown in more detail in figure 4.23 (A). Bending this shim towards and away from the capacitor adjusts the distributed capacitance appearing between the capacitor's plate and ground. Adjustment of this shim is best carried out in conjunction with the filter alignment and using a network analyser. An alternative method is shown in figure 4.23 (B) in which the capacitor is mounted in the same plane as the area of PCB indicated by 'A'. Adjustment of distributed capacitance is controlled by moving the component relative to the ground plane. In both methods note that the leads of the capacitors are soldered near the edge of the microstrip track that is closest to the area of PCB indicated by 'A'. By placing the capacitor on the line edge, the shim does not lean over the microstrip line upsetting its characteristic impedance. Incorporating the capacitor's lead and distributed plate inductance into the transmission line nulls the effects this inductance would have on the true capacitance with frequency. There will be very little change in the value of the silver mica 68pF capacitors from the filter's cut-off frequency up to the measurement limit of 1 GHz. The only concern will be the variation in inductance of the shunt coils with frequency. Figure 4.16 is the new measured insertion loss.

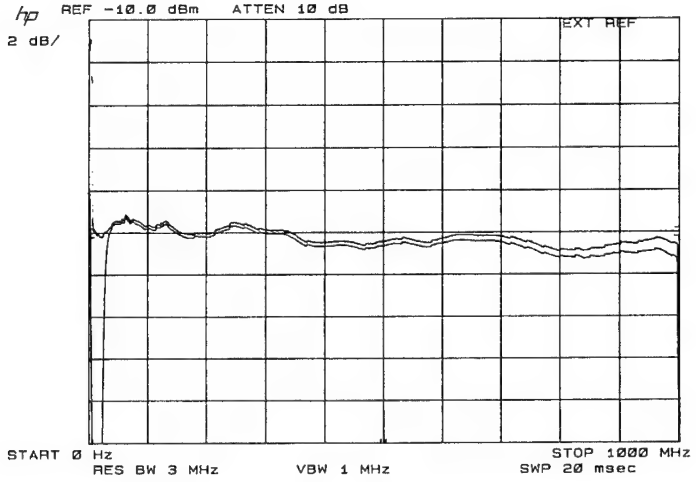

Figure 4.16 *Insertion loss of 27.5 MHz H.P. filter on microstrip, toroidal coils*

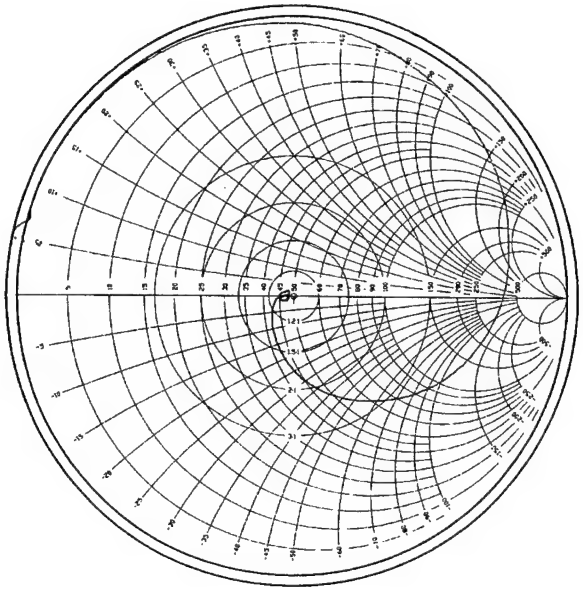

Figure 4.17 *Z_{11} plot 3 MHz to 1 GHz of the 27.5 MHz H.P. filter on microstrip, toroidal coils*

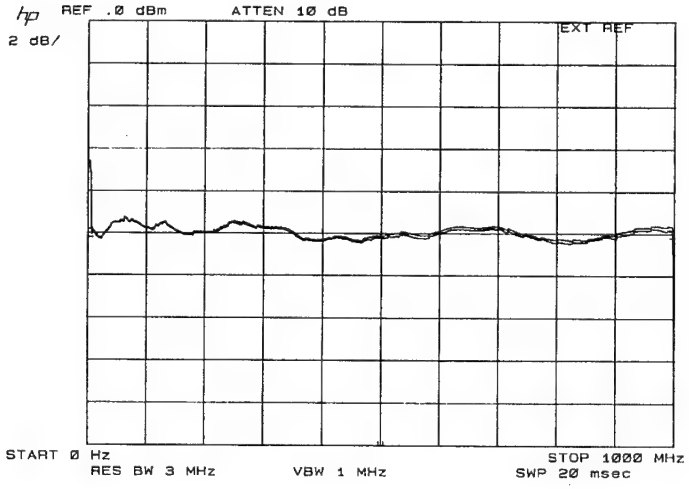

Figure 4.18 *Microstrip line insertion loss*

Comparing this plot with figure 4.8 will show an improved insertion loss from just above the cut off frequency up to the measurement limit of 1 GHz. Also comparing with figure 4.10 shows the improved response above 800 MHz where the added 2.7pF discrete capacitors created a L.P. filter with the distributed in-line inductance. Comparing the Z_{11} plot figures 4.9 and 4.11 to 4.17 shows the progressive improvement in passband SWR. Figure 4.18 is the insertion loss of the microstrip line before it was modified to accommodate the filters. Comparing this figure with figure 4.16 shows the loss attributed to the inductance enhancing material used in the toroidal coils.

In-band R.F. currents travelling through the distributed capacitance of the coil on the way to ground are affected by losses. These losses appear as resistance in series with the distributed capacitance and in shunt with the distributed inductance (coil one-turn-effect) associated with the distributed capacitance. The overall effect this has on the insertion loss of the filter is dependent on:-

- Core Losses of inductance enhancing material which appears in shunt with the one-turn-effect inductance (frequency dependent),
- A.C. resistance of the wire that forms the distributed capacitance (frequency dependent), and
- distributed capacitance of coil windings.

Figure 4.19 describes the transformation of the 27.5 MHz highpass filter into a lowpass as the frequency is raised from the cut-off frequency into the passband. The model shown in (B) is the one used in *Section 4.1.1* for calculating the required additional shunt capacitance. In (C), the current example, the series through path distributed inductance has been incorporated into a transmission line and hence only the line's ohmic losses are of concern. For simplicity it will be assumed that these losses are so small that they can be ignored. The impedance presented by the three shunt circuits, representing the high frequency model of the parasitic elements of a toroidal coil, has to be many times larger than the terminating impedances if the through path loss is to be kept low. The coil's distributed capacitance has a 1/f reactive characteristic, its impedance decreases with increasing frequency. Its effect is to increase the filter's dissipative and non-dissipative through path insertion loss with increasing frequency by:-

- the shunting of signal to ground through the coils distributed capacitance (CP),
- increasing the coupling with frequency of the A.C. resistance (RS AC) part of the distributed capacitance between the line and ground, and
- increasing the losses associated with the distributed inductance (LD) part of the distributed capacitance (CP), magnetically coupling to the toroidal losses (RP

CORE) by increasing the coupling of these losses via the decrease in capacitive reactance of CP(L) as the frequency is raised.

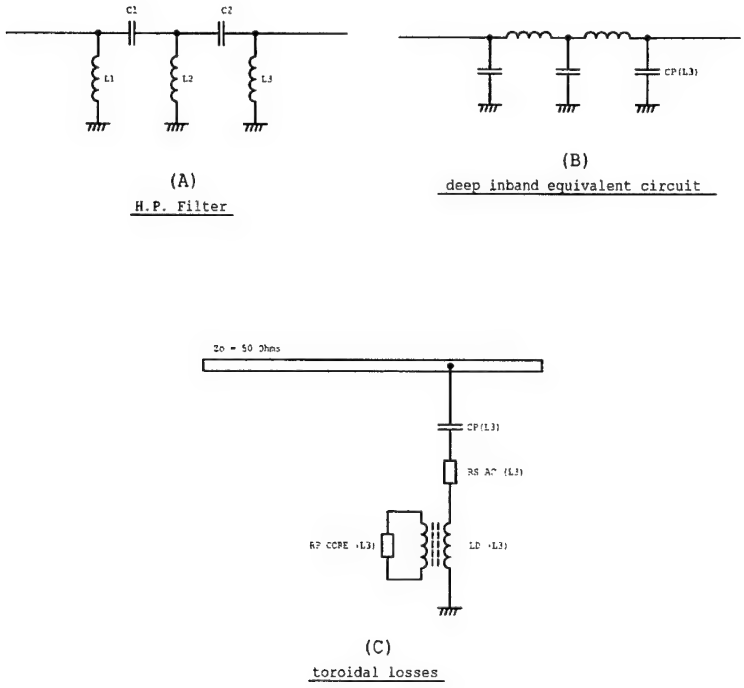

Figure 4.19 *Transformation of 27.5 MHz H.P. filter into a L.P. as in-band frequency is raised*

Steps that can be taken to reduce the distributed capacitance whether the coil is air wound or toroidal are:-

- keep a reasonable spacing between turns, don't compress the turns to the point where they are almost touching,
- elevate the coil away from the microstrip ground plane or any shielding, and
- use a thinner gauge wire than would normally be used for a high Q coil. The use of a thinner gauge wire has the added benefit of increasing the A.C. resistance of the path thus increasing the overall shunt impedance. The increase in A.C. resistance with frequency helps to offset the corresponding decrease in capacitive reactance.

Losses attributed to the inductance enhancing material appear as RP CORE in figure 4.19(C) (for simplicity only the losses associated with L3 have been shown). LD is the distributed inductance (coil one-turn-effect) of the distributed capacitance and is magnetically coupled to RP CORE. The RP CORE apparent resistance is very high around the filter's cut-off frequency falling to a much lower value as the frequency is raised into the passband. This effect is seen as the increase in insertion loss with frequency in figure 4.16. Power lost into the material is proportional to frequency and flux density. The flux density in the core material is proportional to frequency and the distributed capacitance. Any steps taken to reduce the distributed capacitance will also reduce the losses into the core material.

The three toroidal coils were replaced with air wound inductors and the improvement in insertion loss is seen in figure 4.20. Very little difference can be seen between the in-band insertion loss of figure 4.20 and the insertion loss of the microstrip line in figure 4.18. The major losses now appear to be associated with the microstrip. Figure 4.21 is the Z_{11} plot from 3MHz (outer perimeter of circle) to 1 GHz (at 50 ohms) using the air wound coils. The series self-resonant frequencies of the larger air wound coils are at approximately 1.2 GHz and places a low loss upper frequency limit of approximately 1 GHz..

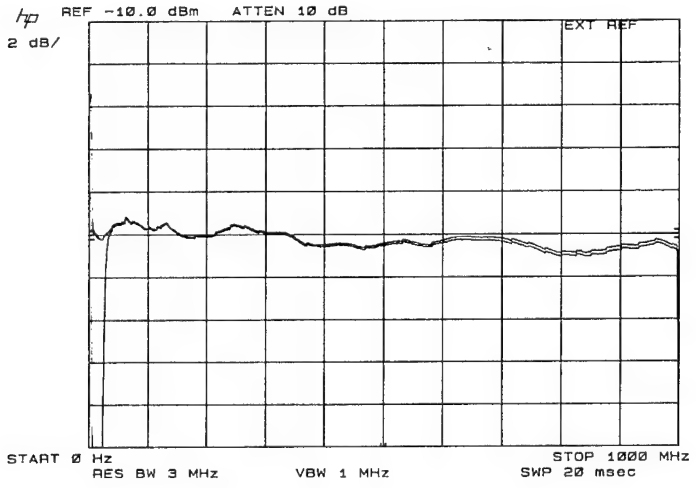

Figure 4.20 *Insertion loss of 27.5 MHz H.P. filter on microstrip using air wound coils*

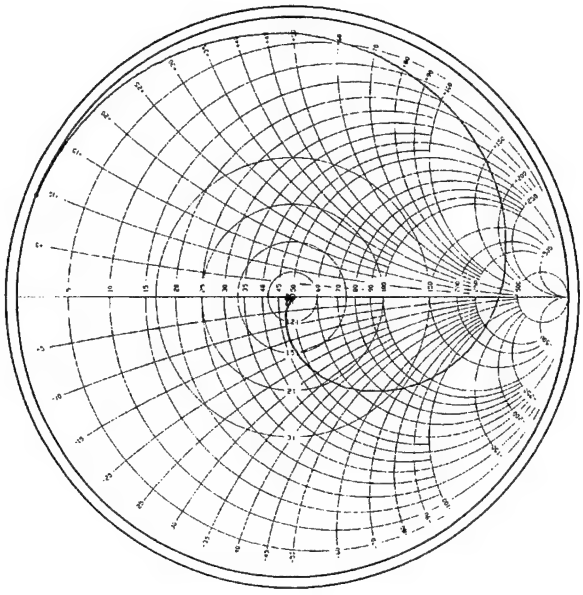

Figure 4.21 *Z_{11} plot 3 MHz to 1 GHz of the 27.5 MHz H.P. filter on microstrip, using air wound coils*

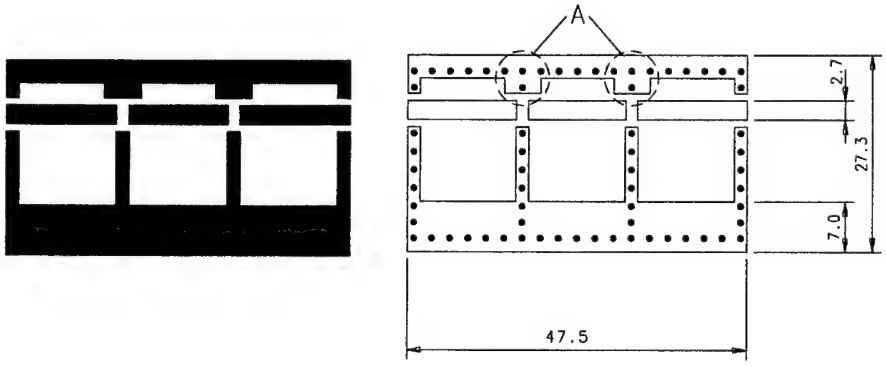

Figure 4.22 *Microstrip line used in 5th order H.P. filters*

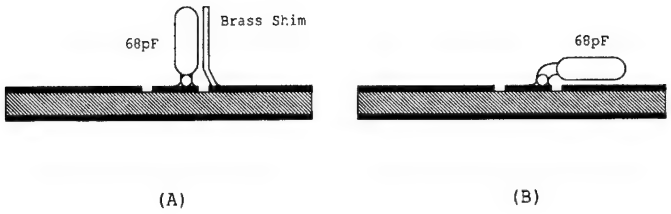

Figure 4.23 *Two methods of mounting the capacitors on a microstrip line to compensate for the internal distributed plate inductance*

4.1.7 Microstrip Line

The width of a microstrip line for a desired characteristic impedance can for most practical purposes be calculated using the following method. The dielectric constant of the PCB substrate, if unknown, can be calculated by measuring the capacitance of a sample of the double sided PCB material from which the microstrip is to be manufactured. Measurements made at different points on various shaped samples at 1 MHz and 100 MHz and the difference in apparent capacitance between these two frequencies with the view to finding a method that has the least impact on the true capacitance revealed the following. It is recommended the sample be rectangular in shape with an aspect ratio in the range of 2:1 to 3:1 (25 mm x 60 mm being typical). The capacitance measurement is made across the midpoint of the shorter side. Applying *the left hand rule for induced currents* to the current flowing in the two parallel plates of the P.C.B. capacitor will show the mutual inductive coupling between the parallel plates to be negative. The effect the plates' distributed inductance has on the true capacitance is reduced and a more accurate reading is obtained. The frequency at which the measurement is made has to be low in order to measure the true capacitance between the plates and not the apparent capacitance. Any bonding wires used to make a connection to the plates are for this reason to be kept extremely short. Equation (4.2) can be used to find the relative dielectric constant.

$$\varepsilon_r = 113C\frac{h}{A} \tag{4.2}$$

where: ε_r = relative dielectric constant
C = capacitance of sample material (pF)
h = thickness of dielectric material between the metallic plates (mm). This is the total thickness of the PCB material (including the copper and adhesive) minus the total thickness of the copper. The thickness of 1oz copper is 0.03556 mm.
A = area of one plate (mm^2)

The characteristic impedance of a microstrip line in a homogeneous medium, air above the line and air between the line and the ground plane is:-

where $w/h \leq 1$

$$Z_{o(\varepsilon_r=1)} \approx 60 Log_e\left(\frac{8h}{w}+\frac{w}{4h}\right) \tag{4.3}$$

where $w/h \geq 1$

$$Z_{o(\varepsilon_r=1)} \approx \frac{377}{\frac{w}{h}+1.393+0.667 Log_e\left(\frac{w}{h}+1.444\right)} \tag{4.4}$$

where: $Z_{o\,(\varepsilon r=1)}$ = characteristic impedance in homogeneous medium (ohm)
w = width of track (mm)
h = height of dielectric material between the metallic plates (mm)

The effective relative dielectric constant which is the average between air and PCB dielectric constants is:-

where $w/h \leq 1$

$$\varepsilon_{r(eff)} = \frac{\varepsilon_r+1}{2}+\left(\frac{\varepsilon_r-1}{2}\right)\left(\frac{1}{\sqrt{1+\frac{12h}{w}}}\right)+0.04\left(1-\frac{w}{h}\right)^2 \tag{4.5}$$

where $w/h \geq 1$

$$\varepsilon_{r(eff)} = \frac{\varepsilon_r+1}{2}+\left(\frac{\varepsilon_r-1}{2}\right)\left(\frac{1}{\sqrt{1+\frac{12h}{w}}}\right) \tag{4.6}$$

where: $\varepsilon_{r\,(eff)}$ = effective relative dielectric constant
ε_r = relative dielectric constant
w = width of track (mm)
h = height of dielectric material between the metallic plates (mm)

The characteristic impedance of the microstrip line with air above the line and PCB substrate between the line and the ground plane is:-

$$Z_{o(\varepsilon_r)} = \frac{Z_{o(\varepsilon_r=1)}}{\sqrt{\varepsilon_{r(eff)}}} \tag{4.7}$$

where: $Z_{o\,(\varepsilon r)}$ = characteristic impedance
$Z_{o\,(\varepsilon r=1)}$ = characteristic impedance in a homogeneous medium
$\varepsilon_{r\,(eff)}$ = effective relative dielectric constant

Equations (4.3) to (4.7) were obtained from Reference 25 pp.10.

4.1.8 Summarising Highpass Filters

The distributed inductance of the through path of a highpass filter causes a gradual increase in insertion loss with increasing frequency from the cut-off frequency into the passband. Point to point wiring can be used only if the reactance of the distributed inductance of the through path is very much less than the terminating impedances at the highest frequency of interest. If the distributed inductance does pose a problem, there are two courses of action open.

1. Convert the distributed inductance of the through path into a transmission line by adding enough evenly placed discrete shunt capacitors to ground to give it the same distributed characteristic impedance as the filter's terminations. This technique is more suited to power transmitter filters where the internal distributed inductance and the lower parasitic series resonances of the larger high voltage/ high current components places an upper frequency limit on the filter. The cut-off frequency of the lowpass filter formed by adding evenly distributed discrete capacitors is usually higher than the lowest parasitic series resonances of the largest shunt coils.

2. Build the filter around a modified transmission line, such as a microstrip. By straddling the capacitors across a gap cut in the line and soldering the leads on top of the line, the components' lead length becomes incorporated within the

transmission line and as such their length is not critical. This technique suits both leaded and leadless capacitors commonly used in filters for low power R.F. transmitters and receivers. The useful upper frequency limit is still limited by the parasitic series resonance of the shunt inductors. The smaller size of low power inductors, compared to high power ones wound with much heavier gauge wire, have proportionally smaller distributed capacitance and therefore higher parasitic resonant frequencies.

Series resonance of the shunt inductors usually places an upper frequency limit to the usefulness of a highpass filter. Because the shunt inductors represent a high impedance to the in-band signal, much finer wire than would normally be used if the coil was in series with the through path, can be used in the construction of the coils. The use of finer wire lowers the distributed capacitance, raises the frequency of the series parasitic resonances, helps to reduce the losses into the core and increases the upper frequency usefulness of the filter. Air wound coils are preferred as these have the least amount of internal dissipative losses.

4.2 Lowpass Filters

In *Section 3.6* it was shown how the distributed capacitance in an inductor changes the true inductance with frequency. The physical size of inductors, especially the air wound type, makes them susceptible to internal and external capacitive coupling. Inductors are usually manufactured in-house and the distributed internal capacitance is usually a trade-off between power handling capability, required Q, inductance enhancing material used, wire gauge and any insulation used on both the wire and the coil former. There are several experimental methods that can be used to find the parallel self-resonant frequency of a coil and hence the distributed capacitance. Having found the distributed capacitance, the apparent inductance at the filter's cut-off frequency can then be calculated and appropriate measures taken to achieve the required inductance.

The internal and external capacitive coupling between a coil's turns and between coils in the through path affect the out-of-passband response of a lowpass filter. The capacitive coupling presents a lower impedance path, as the frequency is raised, around the high inductive reactance of the coils. This appears as a decrease in out-of-passband attenuation with increasing frequency. Capacitive coupling between coils can be controlled by installing Faraday shields next to the filter's shunt capacitors between the coils. This greatly improves the out-of-passband attenuation. Faraday shields however, do not prevent in-band mutual coupling between a lowpass filter's through path coils.

4.2.1 The Effects of Mutual Coupling

Any current flowing through a coil sets up a magnetic field around it. If the current is time varying, the magnetic field surrounding the coil will also be varying in sympathy. Time varying magnetic fields induce voltages into conducting mediums that are under their influence causing currents to flow if the conducting medium is part of a closed loop. Currents flowing in this closed loop change the impedance of the circuit generating the magnetic field, especially if the closed conducting loop is the same loop as the current that created the magnetic field. In the case of a lowpass filter where the through path coils are in-line and there is mutual coupling between coils, the characteristic impedance of the filter will either increase or decrease, depending on the sign of mutual inductance, in sympathy with an increase in the co-efficient of coupling. Mutual inductance between the in-line coils also affects the filter's cut-off frequency.

Mutual coupling also exists between the in-line coils and the shunt capacitors. This has the effect of altering the apparent capacitance in sympathy with the coefficient of coupling. In *Section 3.9.1* it was shown how low permeability toroids are surrounded by magnetic fields both from the coil winding and the one-turn-effect. Capacitors that are mounted in close proximity to these toroids will have their distributed inductance altered through mutual coupling. The distributed inductance of the capacitor is proportional to the physical size, therefore the larger the physical size the greater the coefficient of coupling and hence a commensurate impact on the apparent capacitance. Large high voltage silver mica capacitors are susceptible to the effects of mutual coupling, especially from air wound coils. All shunt capacitors used in lowpass filters should be installed in such a way that the flow of current through them is on the same line as the direction of travel of the varying magnetic field from the coils used in the through path. This ensures mutual coupling between shunt capacitors and through path inductors is kept to a minimum. If a filter is constructed using *Bush Capacitors* and air wound coils, the capacitors should be mounted on the end sections of the shielding with the axis of the blots used to sandwich the capacitor's components lying on the axis of the air wound coil. The induced circulating current from the coil, as seen in the end section of figure 4.66, will be at right angles to the current travelling from the centre of the disk to its outer perimeter.

In order to highlight the effects of mutual coupling between coils, all shunt capacitors used in the following lowpass filters were the physically small Philips low K 100 V NPO ceramic capacitors with lead lengths kept as short as possible. This ensured the mutual coupling between the coils and capacitors was kept to a minimum.

4.2.2 Reducing the Effects of Mutual Coupling Through Separating Unshielded in-line Coils

To demonstrate this effect a 33 MHz lowpass 7th order filter, figure 4.24, with a characteristic impedance of 50 ohms was constructed in a 3301 Pomona box 105x69x42.5 mm fitted with BNC connectors. The through path was the longest dimension. L2, the centre coil, has 5 mm lead lengths. L1 and L3 each have 5 mm lead lengths on one end and 19 mm on the other. All coils were air wound, 12.7 mm outside diameter. The filter was initially constructed with the 5 mm lead length of L1 and L3 on the input and output side of the filter. The separation between L1 and L2 as well as L2 and L3 was 21 mm.

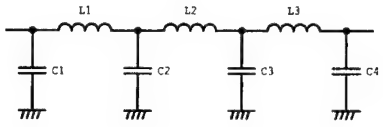

C1 = 62pF	22pF and 39pF in parallel
C2 = 186pF	82pf and 100pF in parallel
C3 = 186pF	82pf and 100pF in parallel
C4 = 62pF	22pF and 39pF in parallel
L1,L3 = 369nH	1.2mm dia. silver plated wire
	8T, 12.7mm OD, 15mm long
	5mm and 19mm lead length
	Air wound
L2 = 489nH	1.2mm dia. silver plated wire
	10T, 12.7mm OD, 19mm long
	5mm lead lengths
	Air wound

Figure 4.24 *33 MHz 7th order lowpass filter*

Figure 4.25 is the Z_{11} plot showing the characteristic impedance of the filter is 50 ohms and no non-dissipative insertion loss. Coils L1 and L3 were then removed and re-installed with their 19 mm lead lengths connected to the input and output. The distance between L1

and L2 was 8 mm and likewise L2 and L3. Figure 4.26 is the Z_{11} plot showing the increase in the filter's characteristic impedance caused by the magnetic coupling between the coils. The characteristic impedance is the centre of the mismatch circle which lies on the R line above 50 ohms. A measurement was made and the characteristic impedance found to be 52.7 ohms. Referring to equation (1.2) which is used to calculate the characteristic impedance of a filter, if the value of C remains unchanged yet the Z_o has increased to 52.7 ohms, then L must have increased via the effects of the coefficient of coupling between the coils.

The value of mutual inductance between two coils is:-

$$\pm L_{M12} = k\sqrt{L_1 L_2} \tag{4.8}$$

where: L_{M12} = mutual inductance between L_1 and L_2, can be positive or negative depending upon circuit configuration
k = coefficient of coupling (for adjacent in-line air wound coils mounted in close proximity as used in this example, in the vicinity of 0.1)
L_1 = self-inductance of coil 1
L_2 = self-inductance of coil 2

Where L_M is positive, as in the current example, the inductance of the coils has increased to:-

$$L_{1_{M12}} = L_1 + L_{M12} \tag{4.9}$$

$$L_{2_{M123}} = L_2 + L_{M12} + L_{M23} \tag{4.10}$$

$$L_{3_{M23}} = L_3 + L_{M23} \tag{4.11}$$

The coefficient of coupling between L1 and L3 is very small due to the distance between the coils and can be ignored.

The increase in inductance of the three coils in the lowpass filter has increased the characteristic impedance which is seen as the mismatch circle in figure 4.26. This mismatch circle indicates that an insertion loss ripple now exists in the passband. At first glance it would appear that the increase in inductance of the coils by the value of L_M would lower the cut-off frequency of the filter, the values of shunt Cs being unaffected, and all that is

required is to reduce the coils' inductance by their respective values of L_M and the filter would behave as predicted. Comparing figure 4.26 with 4.25 confirms the increase in the filter's characteristic impedance and hence the increase in inductance of the coils. However, the filter's cut-off frequency does not decrease as one might expect, it increases in sympathy with the coefficient of coupling between the coils. Reducing the inductance through the manipulation of the turns will lower the filter's characteristic impedance to the required 50 ohms but at the cost of raising the cut-off frequency still further. Comparing figure 4.25 to 4.26 also indicates that there is a minimum ratio of distance between adjacent coils, installed unshielded on a common axis, to coil diameter which reduces the unwanted effects of mutual coupling between coils. A minimum ratio of 1.75:1 is suggested. In order to examine these effects in more detail a higher order filter will be constructed to take advantage of the accumulation of coupling effects. A reference filter needs to be built first so comparisons can be made.

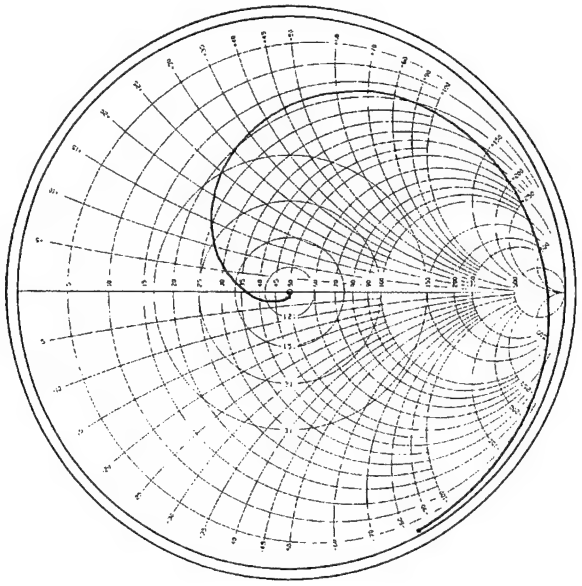

Figure 4.25 *Z_{11} plot 3 MHz to 50 MHz of the 33 MHz L.P. 7th order filter, 21 mm between air wound coils*

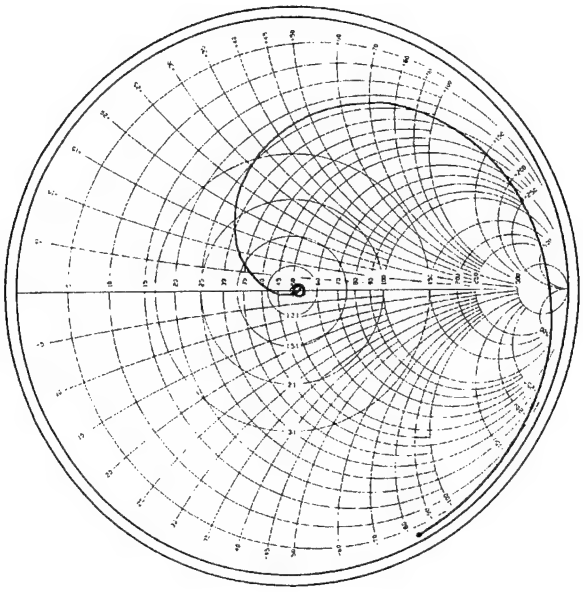

Figure 4.26 *Z_{11} plot 3 MHz to 50 MHz of the 33 MHz L.P. 7th order filter, 8 mm between air wound coils*

4.2.3 Converting an Air Wound Coil's One-Turn-Effect Inductance into a Transmission Line Using a Fully Enclosed Square Section Conducting Shield

The one-turn-effect inductance of air wound and toroidal coils is not to be confused with the coil's much larger lumped element inductance. The one-turn-effect inductance approximates that of a solid tubular conductor whose length and inner and outer diameter are the same as that of the coil and co-exists with the coil's lumped inductance; the coil being viewed as a slow wave structure. The magnitude of the inductance of the one-turn-effect is proportional to the length of a typically wound coil. Inductance enhancing material used in toroidal coils greatly reduces the length of wire required; this in turn lowers the coil length and the one-turn-effect inductance. The one-turn-effect inductance of toroidal coils is therefore usually small and can for the most part be ignored. Only when a large number of turns are wound on a very low permeability core should it be of concern. The use of very low permeability cores indicates the operating frequency is very high. Other unwanted parasitic elements that appear at these frequencies usually predominate and swamp its effects.

This unwanted one-turn-effect inductance can be made transparent by adding an appropriate amount of distributed capacitance making it part of a transmission line whose distributed impedance is tailored to match that of the filter's terminating impedances. This is achieved in an unbalanced lowpass filter by surrounding the in-line coils at an appropriate distance with an earthed conducting medium, usually an R.F. shield.

The ratio of the distance between the parallel surfaces of the insides of a square shield to the coil outer diameter of 2.25 to 1 was used. This ratio is based on the propagation of a TEM wave in a 50 ohm system travelling between the confines of the inside surface of the filter enclosure and the coil's outer surface for the length of the coil. It was found empirically using the filter described in figure 4.27 installed in the enclosure of figure 4.28. For most lowpass filters using air wound coils the improvement in the in-band performance through adherence to this ratio in a 50 ohm system is small when compared to other unwanted characteristics and is therefore usually masked. It is good practice however to counter any effects that can alter a filter's performance to prevent them from compounding. An accumulation of such effects in high order filters can adversely affect a filter's performance, especially if the filter is designed to have an in-band ripple. The following equation, obtained from (ref. 24 pp57), has been modified and is offered as a guide to calculate the ratio of inner distance between the parallel surfaces of a square shield to the outer diameter of an air wound coil whose wire diameter to distance between centres of adjacent turns ratio is in the vicinity of 0.7.

$$Z_o = 138 Log_{10} \frac{1.023D}{d} \tag{4.12}$$

where: Z_o = filter's characteristic impedance
D = distance between parallel surfaces of a square shield
d = outside diameter of air wound coil

The distance (s) between the shield end sections and the ends of the coil relative to equation (4.12) is:-

$$s = \frac{D-d}{2} \tag{4.13}$$

The effect the distributed impedance has on a filter's overall response is best seen on an expanded central region of a Z_{11} Smith chart of a correctly terminated high order lowpass filter whose cut-off frequency is above 30 MHz. If the distributed impedance is higher than the filter's characteristic impedance, the Z_{11} response will show a small residual series

inductance in the passband before the effects of the lumped elements become significantly reactive and start to attenuate the through path signal. And likewise if the distributed impedance is lower, the Z_{11} response will show a small residual shunt capacitance in the passband. The residual reactance, whether inductive or capacitive, will slightly increase the in-band through path attenuation with increasing frequency before the effects of the lumped elements are seen as the cut-off frequency is approached.

4.2.4 Reducing the Effects of Mutual Coupling Through Shielding

A 33 MHz 9th order lowpass filter was built to highlight the effects of mutual coupling between coils on a higher order filter. Two different diameter air wound coils (a) and (b) were tried to examine the effects of the co-efficient of coupling between coils. The circuit described in figure 4.27 using coils (a) was built in a fully enclosed PCB box, shown in figure 4.28, with complete shielding between the coils. Coils (a) diameter and the distance between parallel surfaces of the square shield of the P.C.B. enclosure were designed via equation (4.12) to have a distributed impedance of 50 ohms.

The performance plots of the filter using air wound coils in a fully enclosed shield were taken and will be used as a reference to which comparisons will be made. Figure 4.30 is the Z_{11} plot from 3 MHz (chart centre) to 26 MHz showing the characteristic impedance of the filter is 50 ohms. Figure 4.29 is the Z_{11} plot from 3 MHz (chart centre) to 50 MHz. Figure 4.31 is the in-band insertion loss compared with the level of input signal. The -3dB point was measured at 32.5 MHz. Figure 4.32 is the out-of-band response. The plateau between 50 and 100 MHz is due to in-band distortion products of the spectrum analyser. The analyser noise floor can be seen at -75dBm. The two peaks appearing about 860 MHz are due to the series resonance of coils L2 and L3. Series resonances of coils L1 and L4 appear almost coincidental at 750 MHz. The enclosure resonances are well above 1 GHz and are not displayed.

The filter components were removed from the shielded enclosure and mounted above a PCB ground plane. The outer perimeters of the coils were 9 mm above the ground plane and 11 mm between adjacent coils. Figure 4.33 is the Z_{11} plot showing the increase in the characteristic impedance of the filter brought about by mutual coupling between the coils. Figure 4.34 is the in-band response. Note the increase in the cut-off frequency with respect to figure 4.31. Using equation (4.1) on the data displayed in figure 4.33 shows a 0.01dB ripple now exists in the passband.

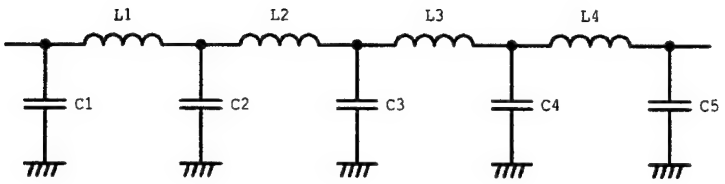

33MHz L.P. Filter

C1,C5 = 53pF — 2 x 27pF in parallel

C2,C4 = 170pF — 100pF and 68pF in parallel

C3 = 191pF — 120pF, 68pF and 5.6pF in parallel

L1,L4 = 327nH — 1.6mm dia. silver plated wire

(a) 17.7mm OD, 16mm long, 6 turns

(b) 22mm OD, 16mm long, 5 turns

(c) 8T 26SWG T-50-6 Toroidal

L2,L3 = 466nH — 1.6mm dia. silver plated wire

(a) 17.7mm OD, 21mm long, 8 turns

(b) 22mm OD, 20mm long, 6 turns

(c) 9T 26SWG T-50-6 Toroidal

Figure 4.27 *33 MHz lowpass 9th order filter*

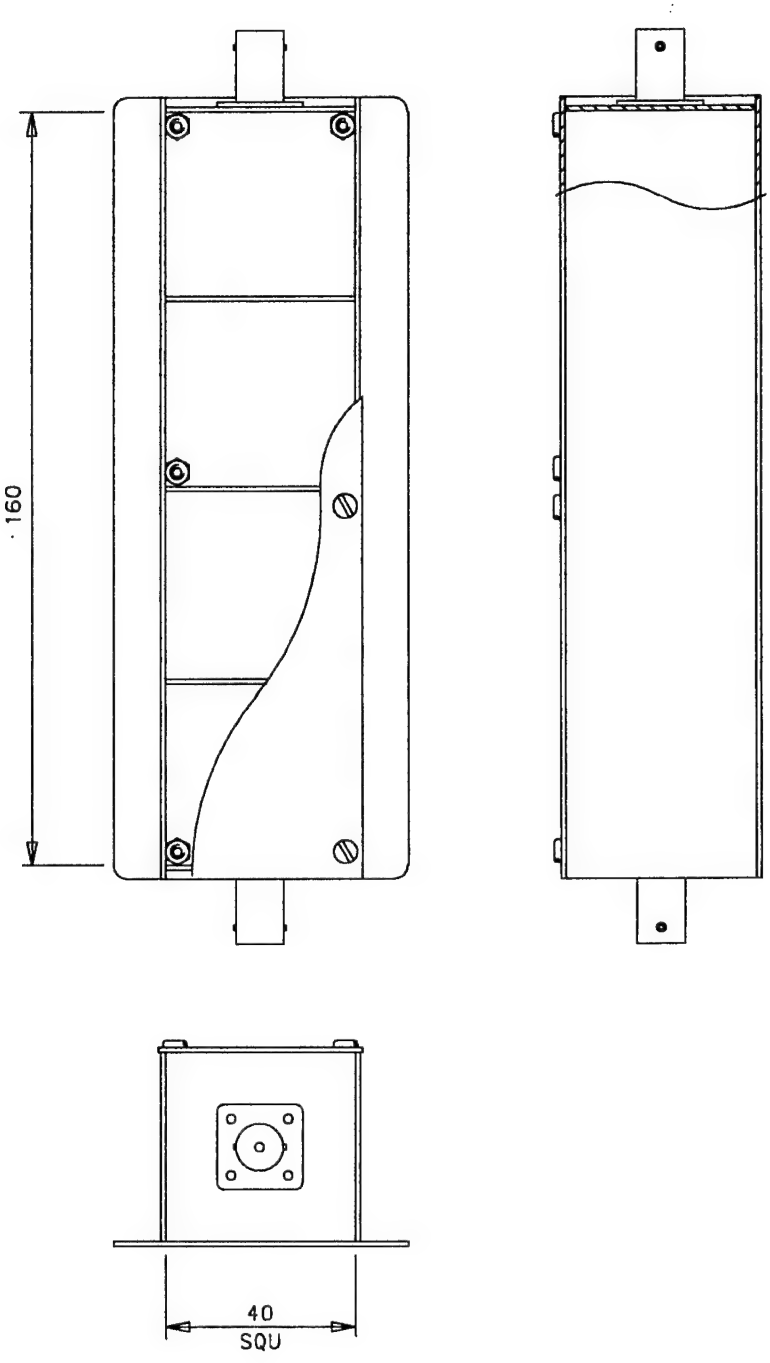

Figure 4.28 *PCB enclosure for 9th order lowpass filter*

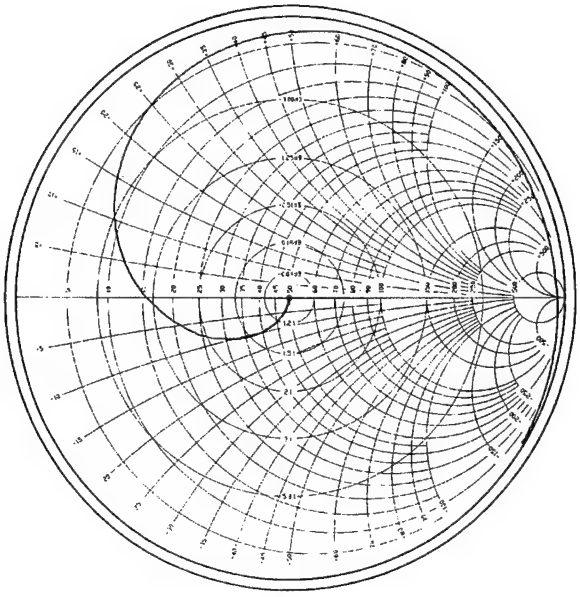

Figure 4.29 *Z_{11} plot 3 MHz to 50 MHz of the 33 MHz L.P. 9th order filter 17.7 mm air wound coils in P.C.B. enclosure*

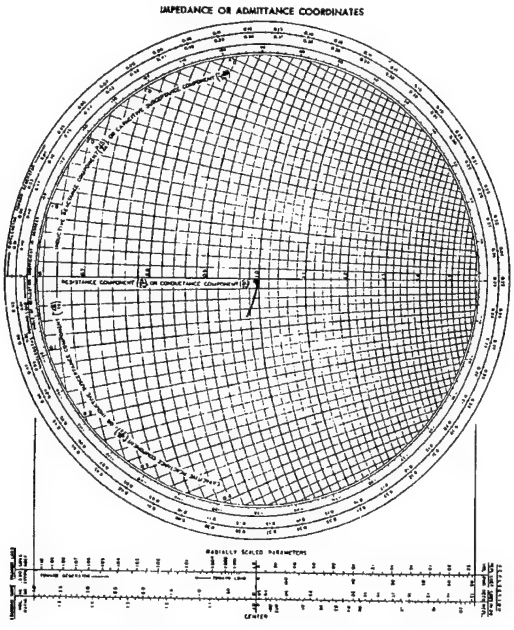

Figure 4.30 *Expanded Z_{11} plot 3 MHz to 26 MHz of the 33 MHz L.P. 9th order filter 17.7 mm air wound coils in P.C.B. enclosure*

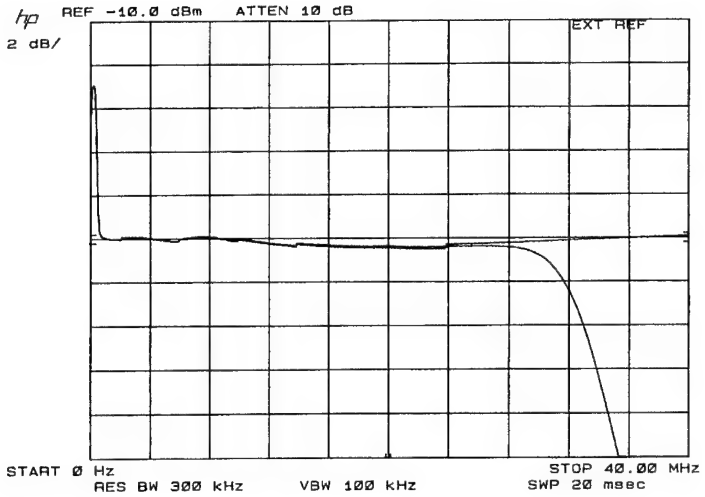

Figure 4.31 *In-band response of 33 MHz L.P. 9th order filter 17.7 mm air wound coils in P.C.B. enclosure*

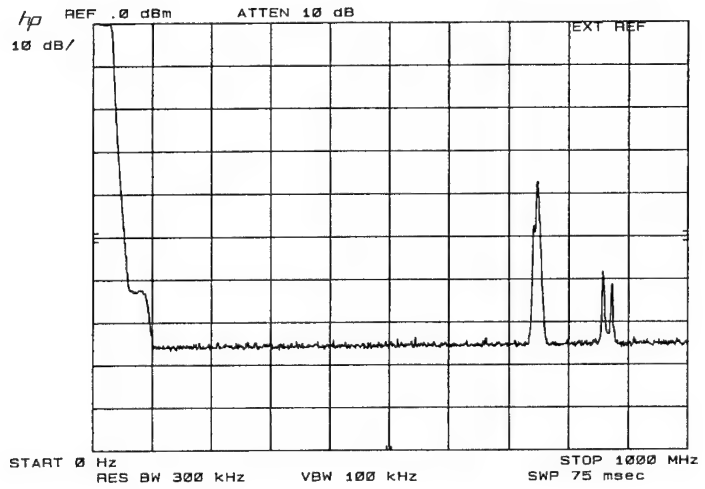

Figure 4.32 *Out-of-band response of 33 MHz L.P. 9th order filter 17.7 mm air wound coils in P.C.B. enclosure*

This figure may seem trivial, but when this ripple caused by mutual coupling between in-line coils is combined with a filter designed to have a passband ripple their accumulative effects can be disastrous. A quick demonstration will be used to illustrate this point. The component values of the 9th order filter have been re-engineered to form a 32.5 MHz Chebyshev filter with 0.01dB bandpass ripple. A ripple that appears on the low side of 50 ohms when viewed on a Smith chart was chosen. Coil length, diameter and distance between coils have been kept the same. The inductance of each coil was carefully measured and adjusted on a HP-4191 R.F. Impedance Analyser at the filter's cut-off frequency before being installed in the circuit. Z_{11} plot and frequency response figure 4.35 and figure 4.36 were recorded. Notice the 1dB plateau in the in-band frequency response of Figure 4.36 just prior to the cut-off frequency supported by the corresponding Z_{11} plot of figure 4.35. The combined effects of the two 0.01dB ripples has resulted in an approximate 0.5dB increase in insertion loss as the cut-off frequency was approached.

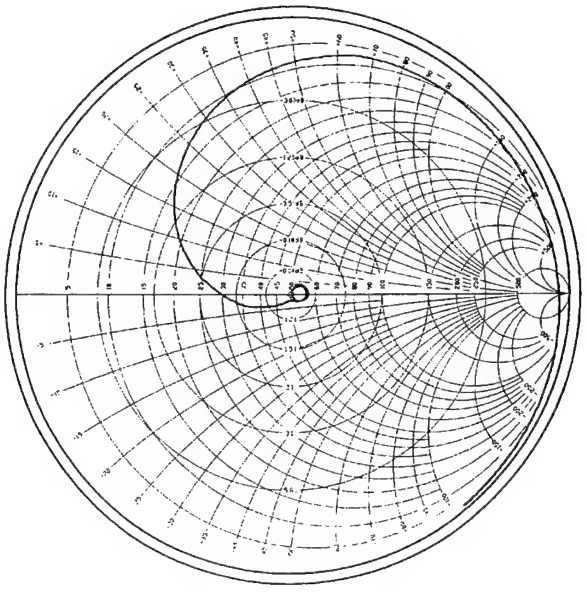

Figure 4.33 *Z_{11} plot 3 MHz to 50 MHz showing the increase in characteristic impedance through mutual coupling between coils*

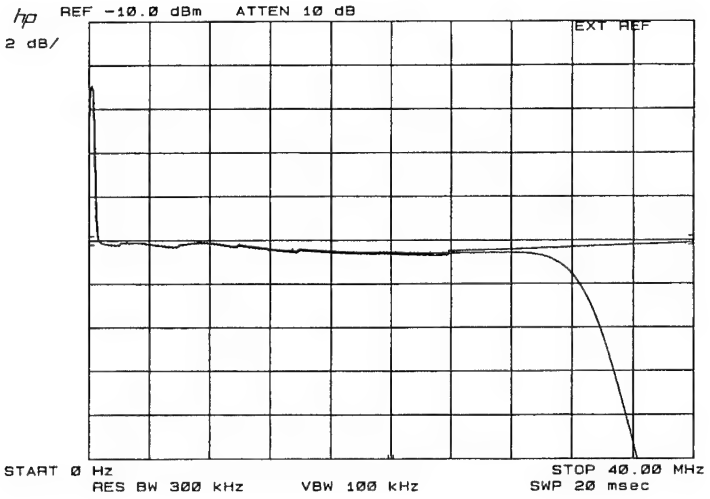

Figure 4.34 *In-band response showing the increase in cut-off frequency through mutual coupling between coils*

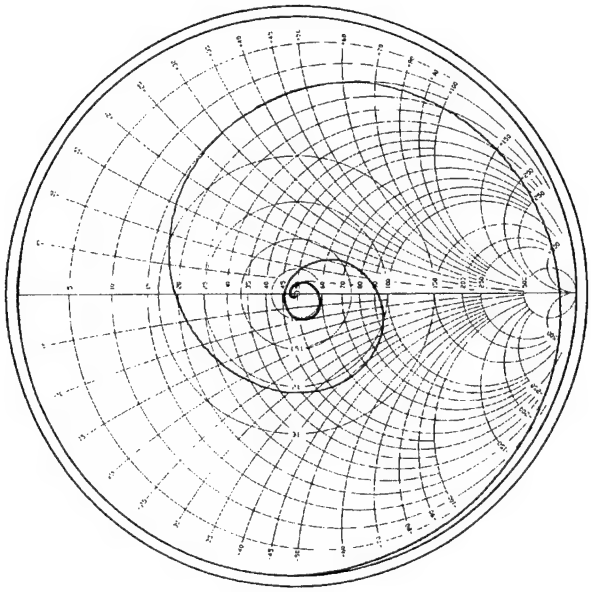

Figure 4.35 *Z_{11} plot 3 MHz to 50 MHz of a 32.5 MHz L.P. 9th order 0.01dB Chebyshev filter with mutual coupling between air wound coils*

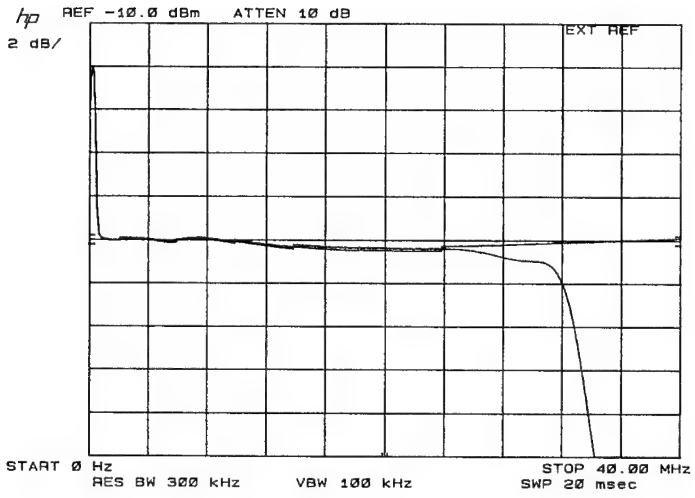

Figure 4.36 *In-band response of a 32.5 MHz L.P. 9th order 0.01dB Chebyshev filter with mutual coupling between air wound coils*

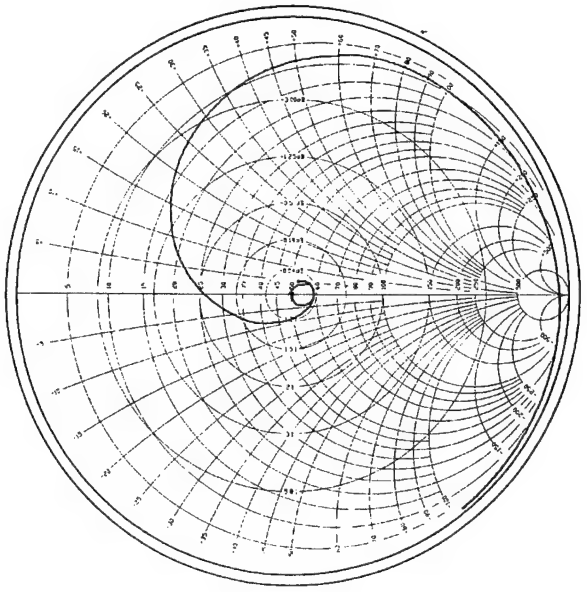

Figure 4.37 *Z_{11} plot 3 MHz to 50 MHz of the 33 MHz L.P. 9th order filter 22 mm air wound coils*

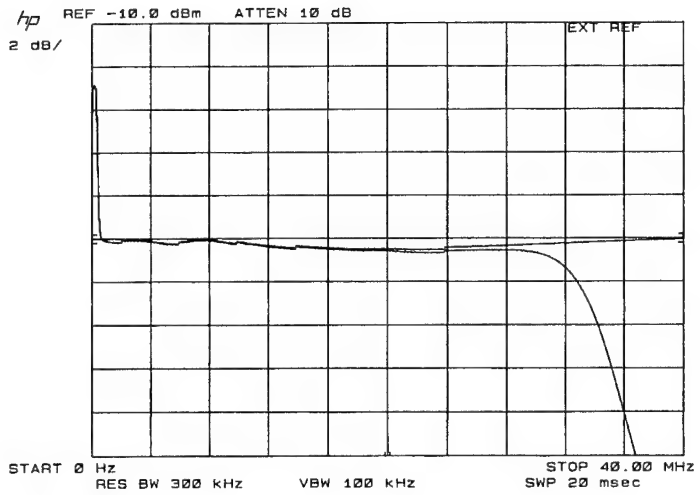

Figure 4.38 *In-band response of 33 MHz L.P. 9th order filter 22 mm air wound coils*

With the circuit returned to normal, the 17.7 mm coils were removed and replaced with the larger diameter 22 mm coils. Overall length of the filter and distance between coils was the same. The larger diameter coils will have greater mutual coupling. Figure 4.37 shows the further increase in the filter's characteristic impedance and in-band ripple. Figure 4.38, the in-band response, shows a further increase in the cut-off frequency.

4.2.5 Reducing the Effects of Mutual Coupling Between Toroids Through Shielding

The 9th order filter was constructed using toroidal coils (figure 4.27 coils (c)) in the same fully enclosed PCB box as used for the air wound coils, the same shunt capacitors are also used. L1, L4 were seven turns and L2, L3 were eight turns of 24SWG wire on Amidon T-50-6 toroidal formers. Figure 4.39 shows the Z_{11} plot figure 4.40 is the expanded in-band Z_{11} plot to 26 MHz, figure 4.41 is the frequency response to 40 MHz and figure 4.42 is the out-of-band response to 1 GHz. Comparing figures 4.39 to 4.42 the toroidal coils with 4.29 to 4.32 the air wound coils shows:-

- a slight increase in in-band insertion loss from the centre of the passband to the cut-off frequency due to power being absorbed within the toroidal material,
- a small decrease in the cut-off frequency when compared to the air wound coil filter due to mutual induction between the air wound coils and the shield slightly decreasing the air wound coils' inductance, and

- the lowest in the series of self-resonant frequencies of the toroidal coils are just above 1 GHz and are not displayed compared to the air wound coils which are seen below 1 GHz. This is due to the shorter length of wire when using inductance enhancing material. The plateau between 50 and 100 MHz is a result of the in-band distortion products generated by the spectrum analyser.

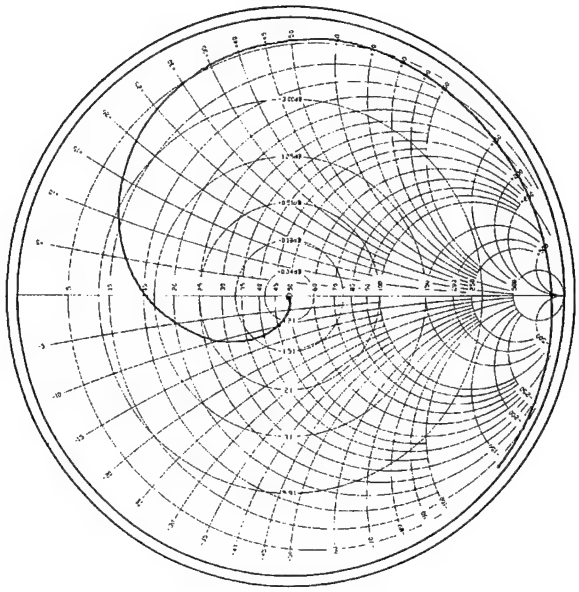

Figure 4.39 *Z_{11} plot 3 MHz to 50 MHz of the 33 MHz L.P. 9th order filter toroidal coils in P.C.B. enclosure*

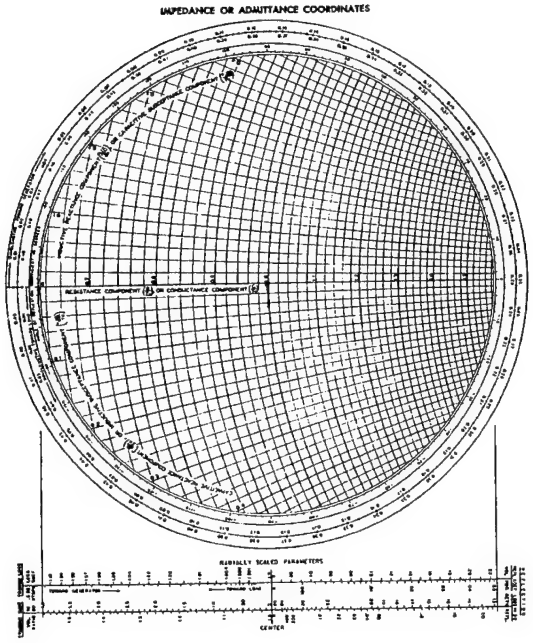

Figure 4.40 *Expanded Z_{11} plot 3 MHz to 26 MHz of the 33 MHz L.P. 9th order filter toroidal coils in P.C.B. enclosure*

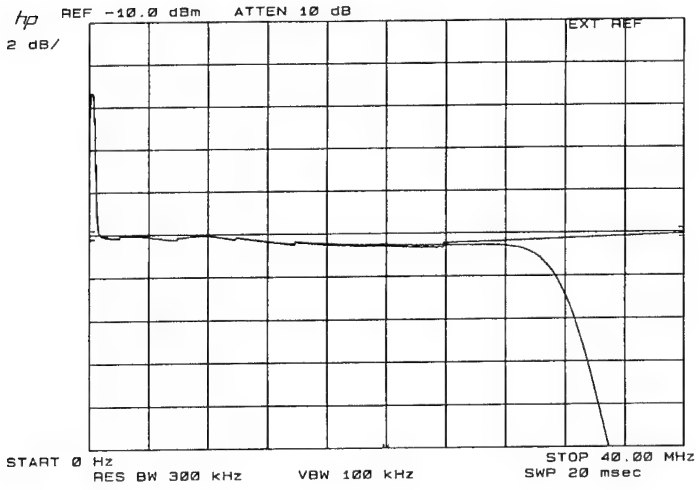

Figure 4.41 *In-band response of 33 MHz L.P. 9th order filter toroidal coils in P.C.B. enclosure*

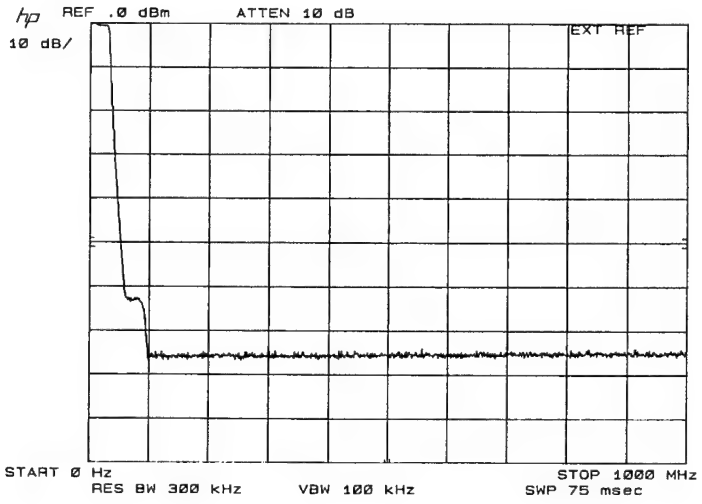

Figure 4.42 *Out-of-band response of 33 MHz L.P. 9th order filter toroidal coils in P.C.B. enclosure*

4.2.6 Reducing the Effects of Mutual Coupling Between Unshielded Toroids by Their Orientation

Figure 4.43 is the recommended unshielded layout for toroidal coils used in lowpass filters. The coils have been position in such a way that the mutual coupling between adjacent coils is kept to a minimum. Adjacent toroids are centrally located at right angles to one another. The toroidal windings of L2 and L4 are evenly displaced about imaginary line AB. This balances the positive and negative aspects of mutual coupling between adjacent toroids from both the coil windings and their one-turn-effects so their total sum is zero. Figures 4.44 to 4.47 are the filter's performance plots. The small loops in the response of figure 4.45 indicate that there is still some mutual coupling between toroids present. Note the gradual decrease in out-of-band attenuation with increasing frequency in figure 4.47. This is due to the capacitive coupling between toroids. Also notice in figure 4.45 the increase in through path resistance seen as a gradual progression along the R line on the Smith chart of the loops with increasing frequency. This increase in resistance is also due to capacitive coupling between toroids and is covered in more detail in *Section 4.2.8*.

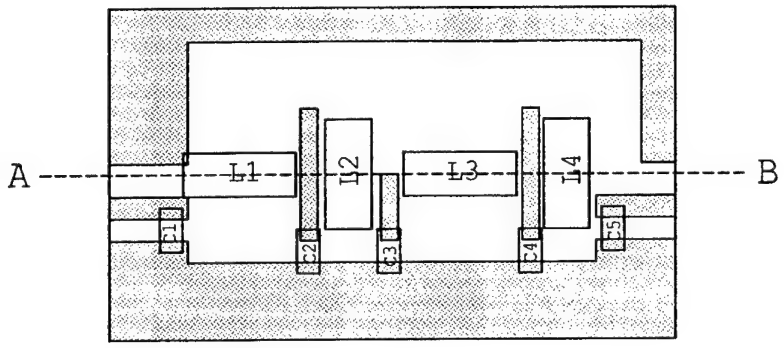

Figure 4.43 *Recommended P.C.B. layout for unshielded toroidal L.P. filter to cancel the effects of mutual coupling between toroids in close proximity*

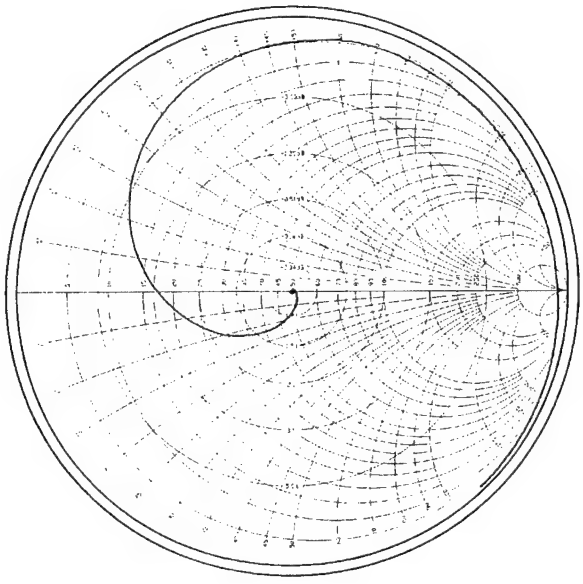

Figure 4 44 *Z_{11} plot 3 MHz to 50 MHz of the 33 MHz L.P. 9th order filter toroidal coils on P.C.B. layout*

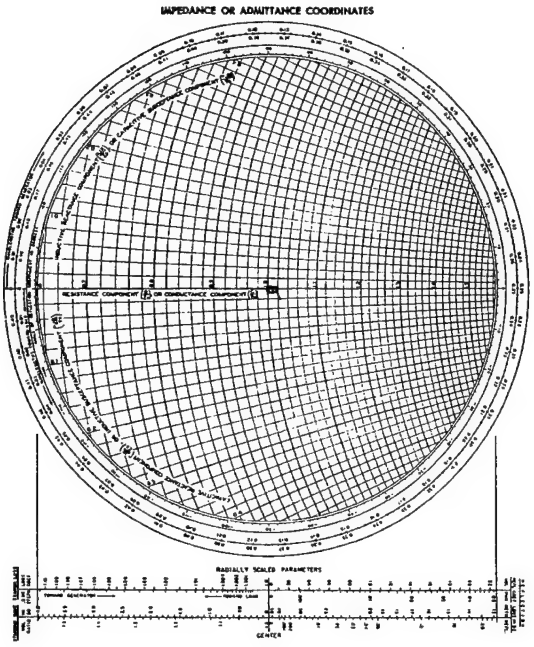

Figure 4.45 *Expanded Z_{11} plot 3 MHz to 26 MHz of the 33 MHz L.P. 9th order filter toroidal coils on P.C.B. layout*

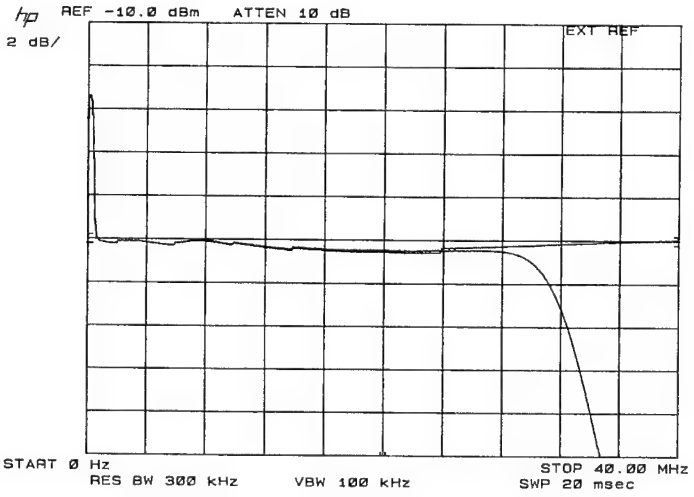

Figure 4.46 *In-band response of 33 MHz L.P. 9th order filter toroidal coils on P.C.B. layout*

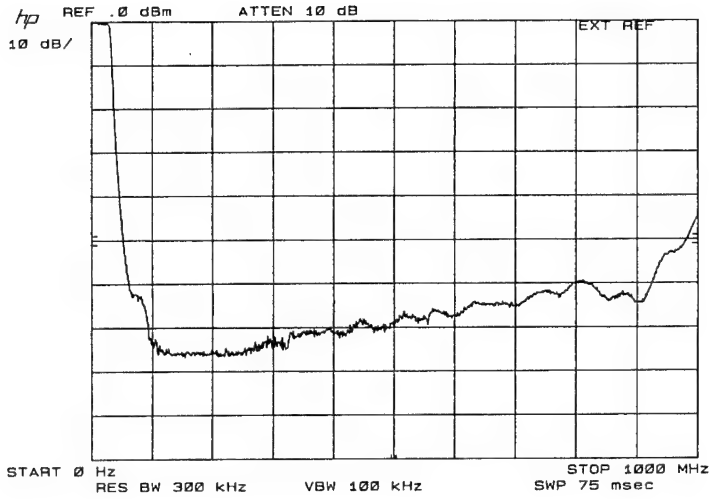

Figure 4.47 *Out-of-band response of 33 MHz L.P. 9th order filter toroidal coils on P.C.B. layout*

4.2.7 Variations in In-band Response of 33 MHz L.P. Toroidal Filter With Changes in the Sign of Mutual Inductance

Figure 4.48 is a diagram showing the component layout of the 33MHz toroidal filter. The toroids' axes were in-line and there was a 7 mm between toroids. The directions of both the toroidal winding helix and signal path were manipulated to change the sign of mutual coupling between toroids. The coils were adjusted to obtain the smallest possible in-band deviation from the designed characteristic impedance of 50 ohms. The *left hand rules for current carrying wire* and *induced currents* were used to derive the sign of mutual coupling between toroids. The following in-band Z_{11} plots from 3 MHz to 26 MHz were obtained.

- Figure 4.49:- The -3dB point was measured at 30.5 MHz, mutual inductance between adjacent toroids was negative and between the one turn effects positive. Coils L1, L4 and L2, L3 were removed and measured to confirm that the sign of the mutual inductance was indeed negative as predicted via the left hand rules. The coil's measured inductance was 340nH and 499nH respectively. They were higher, as expected, than that called for in the numerical design of figure 4.27. Negative mutual inductance reduces their apparent values when installed in the circuit.

- Figure 4.50:- The -3dB point was measured at 31.95 MHz, the mutual inductance between adjacent toroids was positive and between the one turn effects was negative.

- Figure 4.51:- The -3dB point was measured at 32.75 MHz, the mutual inductance between adjacent toroids was positive and between the one turn effects was also positive. Notice there is no in-band ripple, just a gradual increase in the filter's through path resistance with increasing frequency.

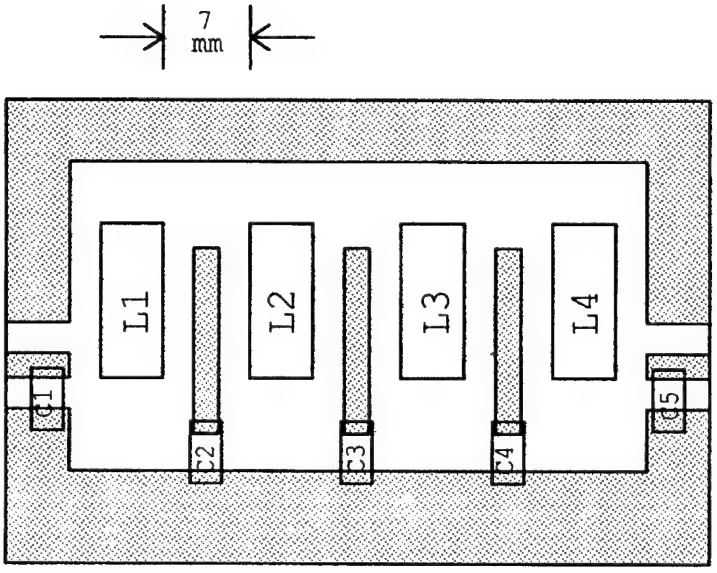

Figure 4.48 *P.C.B. component layout of 33 MHz L.P. filter with axes of toroids in-line*

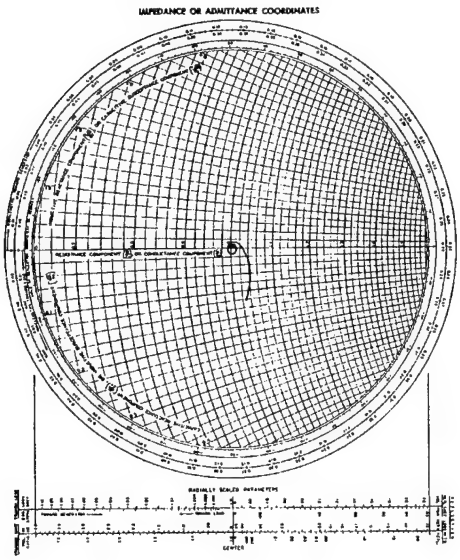

Figure 4.49 *Expanded Z_{11} plot 3 MHz to 26 MHz of the 33 MHz L.P. 9th order filter toroidal coils in-line with negative mutual induction between the toroidal windings and positive between their one-turn effects*

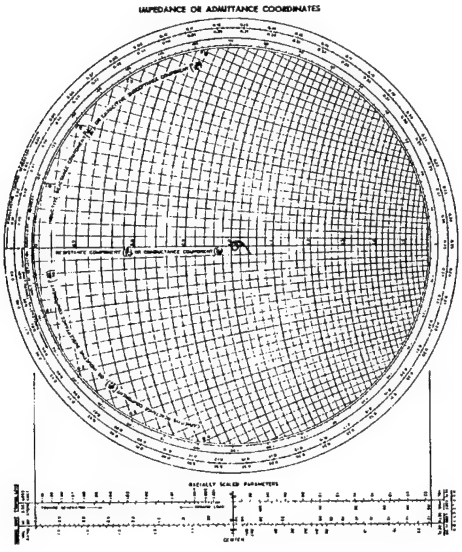

Figure 4.50 *Expanded Z_{11} plot 3 MHz to 26 MHz of the 33 MHz L.P. 9th order filter toroidal coils in-line with positive mutual induction between the toroidal windings and negative between their one-turn effects*

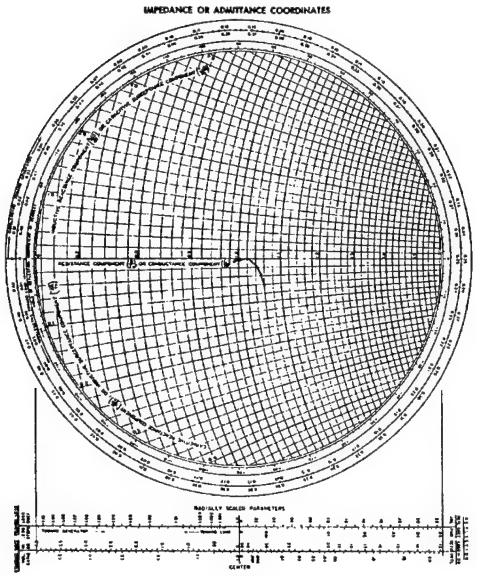

Figure 4.51 *Expanded Z_{11} plot 3 MHz to 26 MHz of the 33 MHz L.P. 9th order filter toroidal coils in-line with positive mutual induction between the toroidal windings and their one-turn effects*

4.2.8 Increase in a Toroidal Coil's Effective Series Resistance Through Capacitive Coupling with Other Toroids in the Signal Path

Any mutual coupling between the toroids would be expected to be seen as continuous overlayed small circles whose centres lie on a fixed position on the R line similar to figures 4.26, 4.33 and 4.37. Comparing figures 4.40 (toroidal filter in a fully enclosed shield) with figures 4.45, 4.49, 4.50 and 4.51 shows the unshielded toroidal filters have an increase in in-band through path resistance with increasing frequency. This is seen as a gradual progression of the continuous circles' centre along the R line to the right of the normalised impedance as the frequency is raised. Figure 4.51 has no mismatch circles and just shows the increase in resistance of the through path. The expanded Smith chart of figure 4.40 clearly shows that there is very little resistive component present in the toroids. There is no progression along the R line with an increase in in-band frequency. These same components, when removed from the shielded enclosure and mounted on an unshielded P.C.B. show an increase in resistance with frequency. If the resistive losses in the toroidal material are not to blame then something else is causing the increasing resistance with increasing frequency.

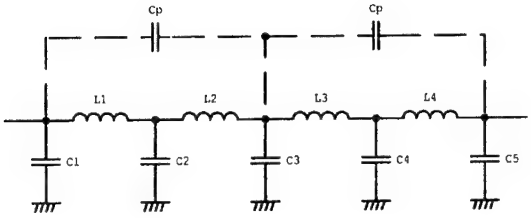

33MHz L.P. Filter

C1,C5 = 53pF	2 x 27pF in parallel
C2,C4 = 170pF	100pF and 68pF in parallel
C3 = 191pF	120pF, 68pF and 5.6pF in parallel
L1,L4 = 327nH	8T 26SWG T-50-6 Toroid
L2,L3 = 466nH	9T 26SWG T-50-6 Toroid
Cp = approximately 1pF	

Figure 4.52 *33 MHz lowpass 9th Order Toroidal Filter. Stray capacitive coupling is shown as Cp*

Capacitive coupling between the far ends of adjacent toroids forms a parallel resonant circuit whose frequency of resonance, which is in the stop band, approaches the filter's cut-off frequency. Figure 4.52 is the diagram of the toroidal L.P. filter in which the stray capacitive coupling between the far ends of adjacent toroids is shown as Cp. The parallel resonant frequency of L1 + L2 and the stray circuit capacitance Cp appearing across their far ends is approximately 157 MHz. The high dynamic impedance seen in series with the through path will be seen as a localised increase in the out-of-band rejection. The high attenuation of the filter order and test equipment limitations prevent this dip from being seen. However the real part of the low frequency outer skirt of this resonant circuit is seen in the upper part of the filter's in-band response as an increase in resistance with increasing frequency and can be as high as a few ohms. This is readily seen in the resistance component curve of figure 3.8, the universal resonance curve for a parallel resonant circuit. In the current examples, figures 4.49 to 4.51, total resistive losses seen in series with the four toroidal windings was as high as three ohms as the cut-off frequency was approached. The magnitude of the ohmic losses is proportional to Cp and inversely proportional to the difference between the passband -3dB frequency and the parallel resonant frequency. Any steps taken to reduce Cp will raise the parallel resonant frequency and lower the ohmic losses.

While the increase in resistance may be tolerated in receiver and low power circuits, it is not recommended where high power is used. Capacitive coupling between the toroids increases the filter's insertion loss by increasing the windings' effective series resistance which increases the energy dissipated as heat. Low permeability toroidal coils used in high power lowpass filters should be isolated from each other in fully enclosed shielding.

4.2.9 Designing and Building a 7th order 850 MHz Lowpass Filter.

This filter is very close to the technological limit for the construction techniques presented and therefore warrants a more in-depth discourse. The normalized values in the appendix were used to design the 7th order 850 MHz lowpass filter described in Figure 4.53.

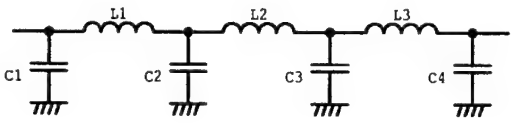

L1,L3 = 13.9nH 3T 0.41mm dia. ECW, COIL 2.8mm OD
L2 = 18.4nH 4T 0.41mm dia. ECW, COIL 2.8mm OD

C1,C4 = 2.34pF (a) 2.2pF 0603 CERAMIC CHIP CAPACITOR LS(C) = 1.2nH

C2,C3 = 7.02pF (a) 5.6pF 0603 CERAMIC CHIP CAPACITOR LS(C) = 1.2nH
(b) 6.8pF 0603 CERAMIC CHIP CAPACITOR LS(C) = 1.2nH

Figure 4.53 *850 MHz 7th order lowpass filter*

Fully enclosed shielding will be used to control the unwanted electric and magnetic coupling between the filter components. SMA connectors were chosen because of their superior performance as microwave frequencies are approached in lieu of BNC which have been used so far. A browse through catalogues from various SMA manufacturers shows the square PCB mount connector can easily be enclosed by a square shield. This connector has four earth pins, one from each corner of the square flange. These pins were cut-off with a sturdy pair of side cutters and trimmed flush with a file. The flange on the connector is 6.3 mm square. Equation (4.12) was used to calculate the OD of 2.8 mm for an air wound coil in a 50 ohm system for a square shield constructed around this flange. 0.41 mm enamel covered wire (ECW) wound on the shank of a 1.9 mm twist drill will give the required OD for the air wound coils. Reyner's equation (3.8) can now be used to calculate coil length and number of turns. The results are tabulated in *Table 4.2*.

Table 4.2 *Variables used in equation (3.8) to calculate required inductance. Dimensions are in inches and (millimetres).*

L (nH)	*D*	*l*	*n*	*t*
13.9	0.11″ (2.8 mm)	0.08″ (2.03 mm)	3	0.017″
18.4	0.11″ (2.8 mm)	0.12″ (3.05 mm)	4	0.017″

Equation (4.13) was used to calculate the required distance "*s*" of 0.0787" between end sections of the shield and the ends of the coils. This distance is required at both ends of the three coils giving a total of 0.47". The length of the filter, or distance between flanges of the two SMA connectors, can now be calculated from the total distance of "*s*" and the length "*l*" for the three coils from *Table* 4.2.giving:-

$$0.47+0.08+0.12+0.8=0.75''$$

The standard Philips low K capacitors that have been used previously in this text because of their small size and low distributed inductance are not suitable for this filter. The main body of the capacitors in the required capacitance range are 0.13" square being slightly larger than the diameter of the coils and having a component thickness of 0.075". The magnetic coupling between this capacitor and the air wound coil is considered too large for the proposed filter construction. The distributed inductance of these capacitors, although small, is also of concern over the frequency range of operation. Take for example the calculated value of 2.34pF for capacitors C1 and C4. A 2.2pF Philips capacitor with 2 mm lead lengths has a total estimated distributed inductance of 3.9nH. Using equation (2.4) to calculate C_{app} at 850 MHz returns an apparent value of 2.9pF. If a 6.8pF was chosen for C2 and C3 (7.02pF was calculated), again with 2 mm leads and the same estimated distributed inductance, it will have a C_{app} of 28pF at 850 MHz. Clearly the distributed inductance, which is to a large part a direct proportional function of a capacitor's length, has made these Philips capacitors unsuitable for this filter. Capacitors with smaller body lengths are required.

Small surface mount capacitors, particularly the 0603 size, are more suitable. They have a body length of 0.06" and are 0.03" square. The distributed inductance of these capacitors has been measured and found to be 1nH. Solder fillets at each end of the capacitor slightly increase the capacitor's length adding approximately 0.2nH resulting in a total of 1.2nH. Calculating C_{app} at 850 MHz for the 2.2pF and 6.8pF 0603 size capacitors with 1.2nH distributed inductance returns 2.38pF and 8.86pF respectively. The change in the 2.2pF capacitor to 2.38pF at 850 MHz is acceptable, however the increase in the 6.8pF to 8.86pF is

not and will be seen as a lowering of the filter's -3dB frequency. The next lowest preferred value below 6.8pF is 5.6pF and this has a C_{app} of 6.9pF at 850 MHz which is closer to the required 7.02pF. Equation (1.3) gives a characteristic impedance of 54.4 ohms for the filter using the 2.2pF and 5.8pF capacitors at low R.F. frequencies and 49.76 ohms at the filter's -3dB frequency of 850 MHz. This change in characteristic impedance with frequency will introduce a small ripple into the passband. The ripple will be seen on a Z_{11} Smith chart as a circle whose centre lies on the characteristic impedance of the filter and has a circumference that intercepts the chart's centre. The chart's centre is known, usually 50 ohms for a 50 ohm system, and the characteristic impedance of 54.4 ohms has already been calculated using equation (1.3). An expected in-band ripple of 0.03dB was calculated using equation (4.14) to find the maximum in-band SWR presented by the filter and then using this result in equation (4.1) to find the ripple in dB.

$$SWR = \frac{Z_o^{\,2}}{Z_T^{\,2}} \tag{4.14}$$

where:- Z_o = filter's characteristic impedance from equation (1.3) (Ω)
Z_T = filter termination impedances, normally 50 ohms (Ω)

Figure 4.54 describes the construction of the filter. It is easier to achieve crisp corners to the U shaped brass shim if the fold line is scored with a sharp blade and the shim folded away from the scored edge. All capacitors are soldered onto their respective partitions and connectors before assembly into the U shaped channel.

Figure 4.55 is the net list and simulated Z_{11} plot using ARRL's Radio Designer software. Note that distributed resistance has not been included in the analysis. The Z_{11} plot is therefore representative of a lossless filter's ideal response for the filter circuit described and is the reference by which measured plots are compared.

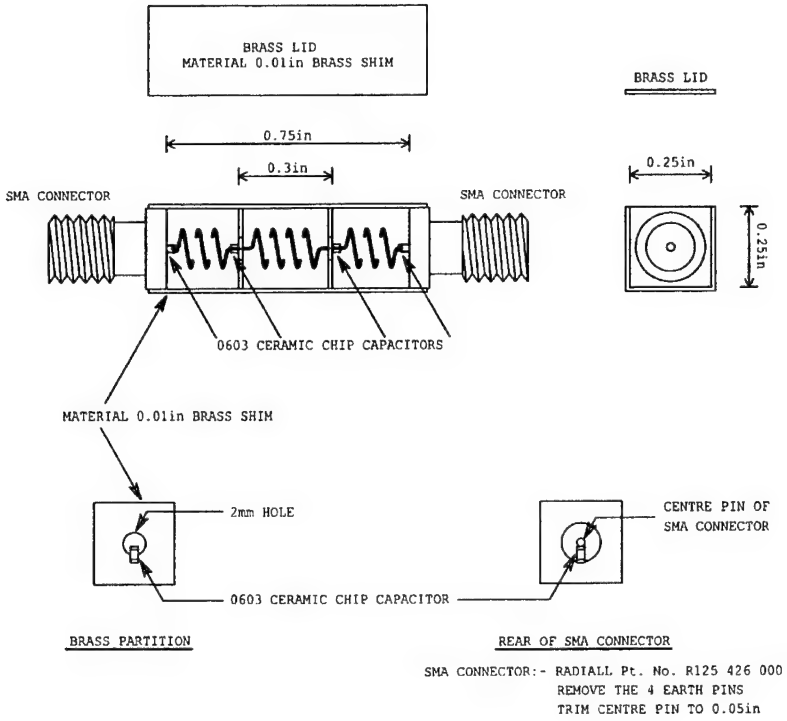

Figure 4.54 *Mechanical details of 850 MHz lowpass filter*

Figure 4.56 is the measured Z_{11} plot of the filter. Notice the impedance mismatch circle starting at the chart centre and forming a loop to the right of the centre indicating that Z_O of the filter is higher than 50 ohms as predicted. The loop diameter is not as large as in the simulation. This is due to the distributed resistance absorbing some of the forward and reflected wave as it traverses its way through the filter's components. This resistance is a product of the DC resistance of the wire, the proximity effects of the turns in the coils, the use of brass which has just over twice the resistivity of copper for the shielding material, and finally the decay in resistance of the coils' high dynamic resistance at parallel resonance. Simulation has shown these combined losses are about 0.1 ohm per coil at the filter's cut-off frequency. Figure 4.57 is the in-band through path loss. The top trace is the input level to the filter from the signal generator, the bottom the output from the filter. Notice the -3dB point at 850 MHz as predicted. The combined resistive loss is readily seen by comparing the measured Z_{11} plot of figure 4.56 with the measured in-band loss of figure 4.57 between the frequencies of 421 MHz and 650 MHz. 421 MHz on the Z_{11} is diametrically opposite to the 50 ohm point (chart centre) on the mismatch loop and is where the in-band ripple should maximize. Continuing up in frequency from here to 650 MHz brings us closer to the chart centre implying the losses should be decreasing.

Moving still higher in frequency takes us away from the chart centre area towards the -3dB point where the marker is. Examining the insertion loss on figure 4.57 clearly shows the losses continue to increase between these two frequencies and not decrease as predicted by the Z_{11}.

```
*
*
*850MHz LPF
*
*

BLK

SLC 1 0 C=2.2PF L=1.2NH
IND 1 2 L=13.9NH
SLC 2 0 C=5.6PF L=1.2NH
IND 2 3 L=18.4NH
SLC 3 0 C=5.6PF L=1.2NH
IND 3 4 L=13.9NH
SLC 4 0 C=2.2PF L=1.2NH

RES 4 0 R=50OH; 50 OHM TERMINATION

CKT: 1POR 1
END

FREQ
ESTP 1MHZ 1GHZ 300
END
```

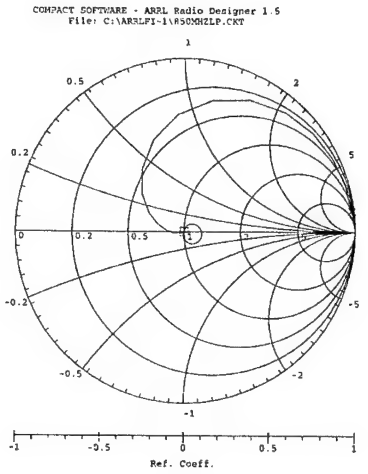

Figure 4.55 *ARRL Radio Designer net list and generated Z_{11} plot for the 850 MHz lowpass filter. Frequency range is 1 MHz to 1000 MHz*

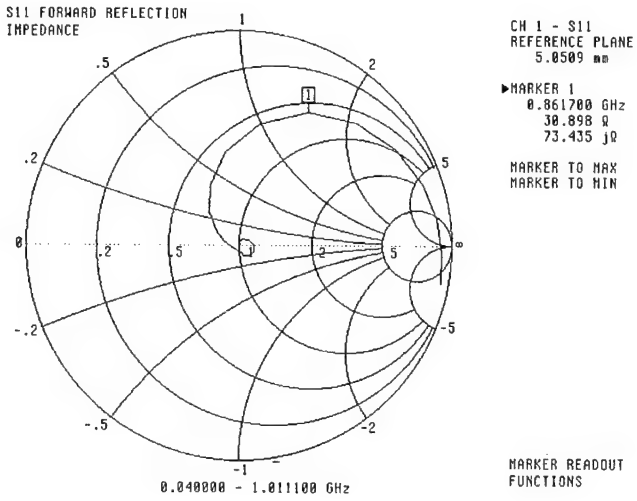

Figure 4.56 *Measured Z_{11} Plot of 850 MHz 7th Order Lowpass filter, 40 MHz (chart centre) to 1000 MHz using 2.2pF and 5.6pF capacitors*

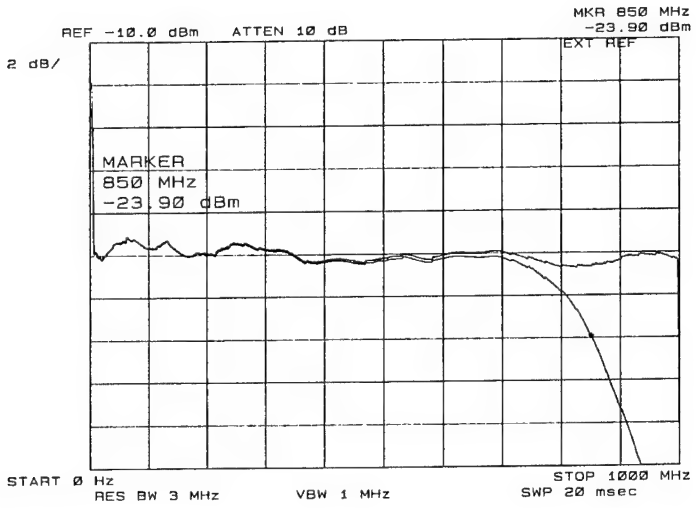

Figure 4.57 *Measured in-band insertion loss of the 850 MHz lowpass filter using 2.2pF and 5.6pF capacitors. Note vertical scale of 2dB/div*

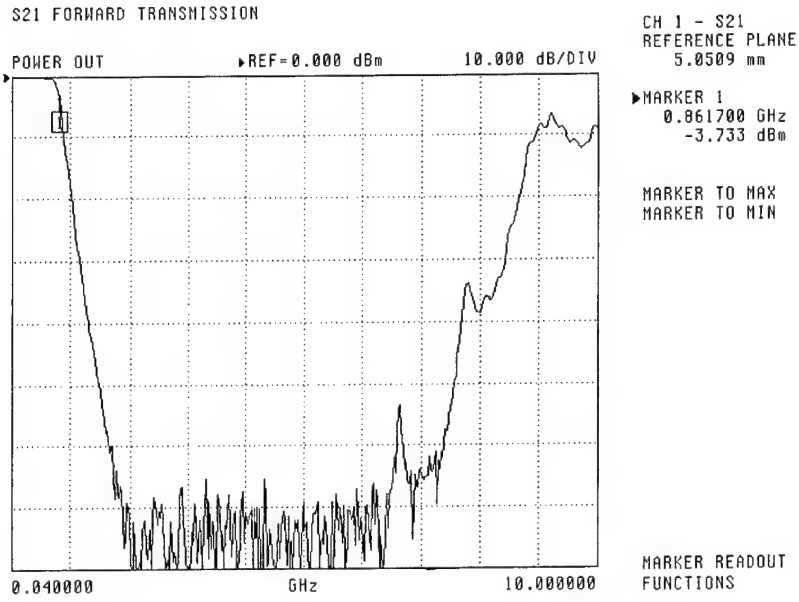

Figure 4.58 *Measured out-of-band insertion loss to 10 GHz of the 850 MHz lowpass filter using 2.2pF and 5.6pF capacitors*

An extra set of three coils was wound and their leads trimmed ready to install into the filter. The coils were then pulled by their leads to straighten the wire again in order to measure the length of wire in each coil. There was 28 mm of wire in L1 and L3 and 34.5 mm of wire in L2. These dimensions were then used in equation (4.16) to predict the spot frequencies where the coils become series resonant. The spacing between turns are normal for L1,L3 and towards large in L2. Values for the velocity factor v_f of 0.7 for L1,L3 and say 0.75 for L2 were chosen. *Table 4.3* lists the results of equation (4.16) and the measured spot frequencies for n=2. Listed also is the measured parallel resonant frequencies f_r for the coils.

Table 4.3 *Calculated (equation (4.16)) and measured (figure 4.58) spot frequency series resonances and the measured parallel resonant frequencies f_r of the in line coils in the 850 MHz lowpass filter.*

Coil	Wire Length (mm)	*vf*	*fr* (MHz)	n=2 (MHz)	n=3 (MHz)
L2	34.5	0.75	2500	6521 (cal) 6663 (meas)	9782 (cal)
L1,L3	28	0.7	3200	7500 (cal) 7784 (meas)	11250 (cal)

Figure 4.58 shows the gradual decrease in attenuation with increasing frequency from about 6.5 GHz upwards. This decrease in attenuation is due to the inductive reactance of the L_{app} associated with the shunt capacitors becoming a significant percentage of the filter's terminating impedance. The distributed inductance $L_{S(C)}$ of the 0603 capacitors used in shunt in this filter has been measured at 1.2 nH. Equation (2.5) was used to calculate L_{app} of both 2.2pF and 5.6pF capacitors at 9 GHz. The inductive reactance of the respective L_{app} for the two capacitors in question was then calculated at 9 GHz and found to be *j*60 ohms and *j*64 ohms. These results all appear in *Table 4.4*. Clearly these reactances are greater than the filter's terminating impedances and therefore the shunt capacitors cannot perform their intended function of shunting out-of-passband signals to ground. This lack of attenuation around 9 GHz has masked the expected response for n=3 of 9782 MHz for the coil L2.

Table 4.4 *Values of L_{app} from equation (2.5) and their reactance at 9 GHz for the 2.2pF and 5.6pF 0603 size ceramic chip capacitors used in shunt with the through path of the 850 MHz lowpass filter.*

True Capacitance	$L_{S(C)}$	L_{app}	X_{Lapp}
2.2pF	1.2 nH	1.058 nH	*j*60 ohms
5.6pF	1.2 nH	1.144 nH	*j*64 ohms

The following plots were included to show the effects of using a 6.8pF capacitor for C2 and C3. Don't be mislead by the almost perfect looking Z_{11} plot of figure 4.59. Comparing this plot with the in-band insertion loss of figure 4.60 and then comparing this last plot with figure 4.57 shows that the resistive losses have increased even further. Figure 4.60 shows the slope around the -3dB point is rounder and the cut-off frequency is slightly lower. Figure 4.61 highlights the effect the 6.8pF capacitance has on its $L_{S(C)}$ of 1.2nH. The L_{app} has increased slightly, lowering the frequency where the decrease in out-of-band attenuation begins to take effect.

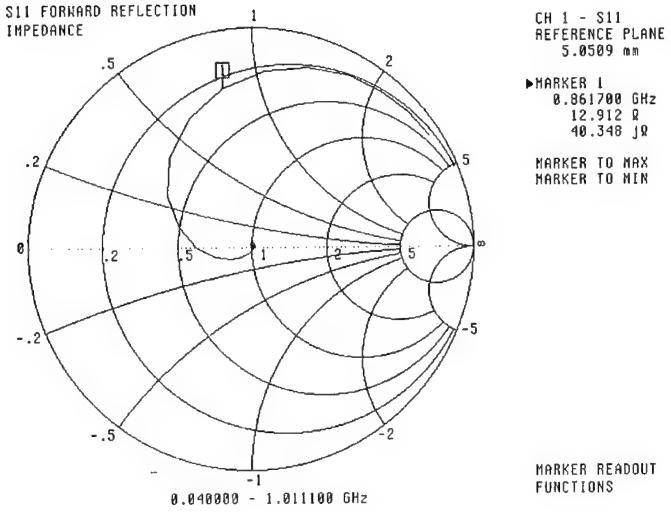

Figure 4.59 *Measured Z_{11} Plot of 850 MHz 7th Order Lowpass filter, 40 MHz (chart centre) to 1000 MHz using 2.2pF and 6.8pF capacitors*

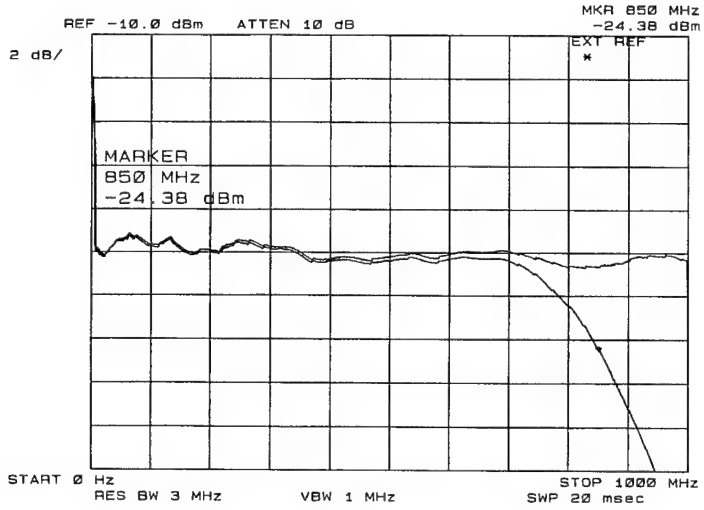

Figure 4.60 *Measured in-band insertion loss of the 850 MHz lowpass filter using 2.2pF and 6.8pF capacitors*

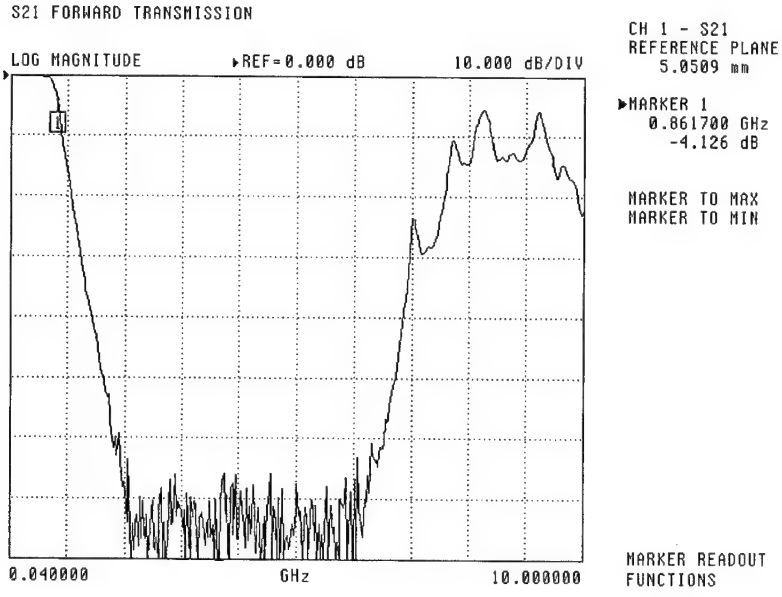

Figure 4.61 *Measured out-of-band insertion loss to 10 GHz of the 850 MHz lowpass filter using 2.2pF and 6.8pF capacitors*

4.2.10 Summarising Lowpass Filters

It is generally understood that the need for shielding in L.P. filters is to prevent out-of-passband signals from finding alternative paths around the filter's attenuating components. What is not generally understood is the need to isolate the magnetic flux of coils, especially air wound of large diameters, to prevent the effects of mutual coupling between them from affecting the passband response and cut-off frequency. Mutual coupling between coils can be reduced through:-

- attenuation of magnetic flux by distancing the coils as demonstrated in figures 4.25 and 4.26,
- the use of fully enclosed shielding to isolate the coils as demonstrated by comparing figure 4.29 and 4.39 with figures 4.33, 4.35, 4.37, 4.49, 4.50 and 4.51, and
- the use of inductance enhancing materials which provide a lower reluctance path to the magnetic flux thereby encouraging the flux to stay within the confines of the enhancing material. Caution should be used when using materials that have a low permeability as some flux lines will not be constrained and will extend beyond the core material. Figure 4.43 is the recommended PCB layout for toroidal cores in close proximity.

It may still be necessary to use Faraday shields to prevent stray capacitive coupling between the filter's components from affecting the in-band and out-of-band performance. Of the three methods described above, fully enclosed shielding is by far the most effective for both air wound and toroidal inductors. The type of material to be used in the construction of the enclosure is covered in section ***4.3 Shielding***.

4.3 Shielding

The traditional method of nulling the effects of unwanted magnetic coupling between two air wound coils in close proximity is to place the coils at right angles to each other. This method relies on the axes of both coils being orthogonal, on the same plane and having symmetry about the intersection of the two axes. This ensures that the sum of the induced voltages are zero and hence no induced current can flow. This is akin to the nulling of a bridge network. Just like a bridge network, a slight change in the orientation of the coils from the null point produces a large change in induced voltage. This method is not recommended for mobile equipment or high vibration environments. Also, it does not inhibit the capacitive coupling between coils. Another method is to keep the coils at least their diameter apart; 1.75 times the diameter has been shown to be very effective. Such a technique is impractical when designing compact equipment. These techniques are

centred on reducing the magnetic coupling between the two components and not the coupling to these components from external fields.

Total shielding of the electromagnetic fields at R.F. frequencies is generally carried out by surrounding the component to be shielded in a fully enclosed conducting medium that has a very low distributed resistance and possesses a very low relative permeability. The conducting medium acts as a Faraday shield and prevents any electric field component travelling further than the boundaries of the enclosure. The magnetic field component is not as easily attenuated and the choice of a shielding material with a very low relative permeability together with very low distributed resistance needs to be discussed. There are two basic methods of attenuating a magnetic field, diverting the course of the field, or cancelling it with an equal but opposite field.

4.3.1 Diverting the Course of the Field

Conducting materials that have a relative permeability greater than one attract magnetic lines of flux to them by offering a lower reluctance path than that of the surrounding medium, usually air. They have higher distributed inductance per unit length and higher resistivity than materials with a permeability of one. An enclosure made of tin-plated steel, for example, with its high permeability (approx. 1,000) would divert the magnetic lines of flux, both internal trying to get out or external trying to get in, around the contour of the shield. At R.F. frequencies the rate of change of flux would induce circulating eddy currents into the conducting enclosure. The induced circulating currents flowing through the high distributed inductance and resistivity of the shield will create voltage drops that modulate the ground reference of a through path signal as it travels through the circuitry within the enclosure. Also, the permeability of steel decreases as frequency increases to a point where at R.F frequencies its effectiveness as a magnetic shield is below that of copper. It is for this reason that ferrous based conducting materials should only be used at low frequencies and should be avoided in electromagnetic shielding at R.F. frequencies.

The filter described in figure 4.27 using coils (a) was constructed in the enclosure of figure 4.28 made of tin-plated steel. Figure 4.62 is the measured in-band insertion loss. Comparing the insertion loss of figures 4.31 (copper PCB enclosure) with 4.62 (tin-plated steel) shows the increase in insertion loss due to the increased resistivity in the current loops of the tin plate. Not all the energy induced into the tin plate enclosure is being returned to the in-line coils as would be the case in a perfectly conducting enclosure. Only the part that is not being dissipated as heat in the enclosure resistance is returned. This results in the observed increase in insertion loss. Figure 4.62 also shows an increase in the filter's cut-off frequency due to the enhanced negative mutual coupling to the through line coils by the large relative permeability of the tin-plated steel. Figure 4.63 is the out-of-passband response. Comparing this figure with figure 4.32 (PCB enclosure) will show the tin-plated enclosure has lowered the coils' parasitic resonant frequencies.

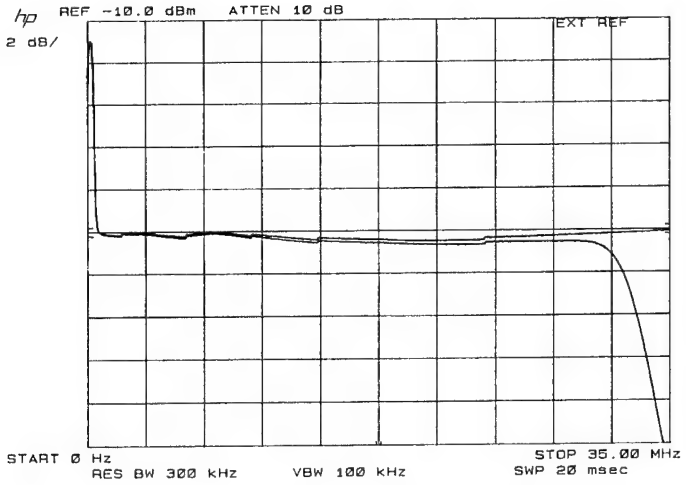

Figure 4.62 *In-band response of the 33 MHz L.P. 9th order filter 17.7 mm air wound coils in tin plate enclosure*

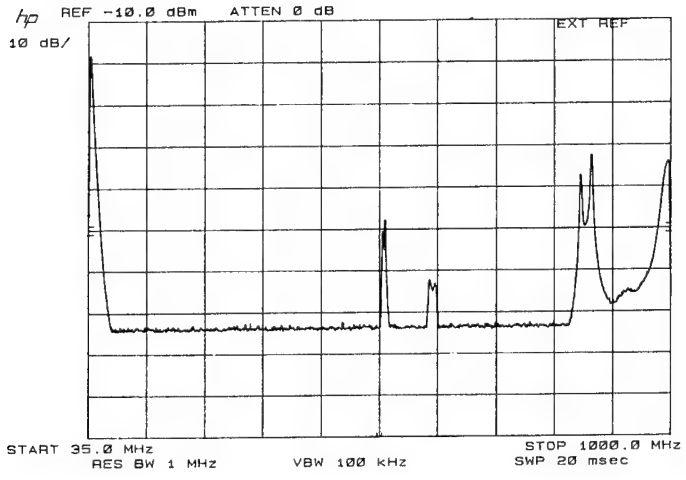

Figure 4.63 *Out-of-band response of the 33 MHz L.P. 9th order filter 17.7 mm air wound coils in tin plate enclosure*

4.3.2 Cancelling the Field With an Equal but Opposite Field

An enclosure made of copper has a permeability that is almost the same as air and therefore will not impede the flow of magnetic flux passing through it, nor will it divert it. If the copper forms a complete closed loop around the source of R.F. magnetic field, eddy currents will be induced into the copper. The direction of induced eddy currents will be in the opposite direction to the original current whose field induced it. Therefore the sense of magnetic field generated by the induced eddy current is in the opposite direction to the original field and can be used to cancel its effects.

4.3.3 Cancelling Fields Whose Direction of Travel are at Right Angles to the Axis of an Air Wound Coil

Figure 4.64 (adapted from ref. 29) is a cross sectional view of a single layered air wound coil fully enclosed by a copper shield in which 'G' is an element of wire at the centre of the coil and 'H' is an element of a side of the shield which is parallel with the coil axis. A current flowing out of the page through element 'G' will produce lines of magnetic flux centred on 'G' with a clockwise direction. If the current through 'G' was increasing the field centred on 'G' would be expanding that is, moving away from 'G'. This expanding field induces a current into element 'H' that will flow into the page. The magnetic field associated with the current in element 'H' is centred on 'H' and has a counter-clockwise direction. If there were no ohmic losses in the complete loop of which element 'H' is a part, then the magnetic field centred on 'H' would be equal but of opposite direction to the field centred on 'G' external to the shield. The complete loop for 'H' is formed by the four sides of the enclosure parallel to the coil axis. The two fields external to the shield would cancel thus providing a high degree of isolation. In the real world element 'H' has distributed resistance and a small amount of self-inductance which limits the current that can flow in the loop. The field centred on 'H' therefore does not quite have the same magnitude as 'G' external to the shield and leaves a portion of 'G' unchecked. Best possible shielding is obtained when the enclosure material has a very low distributed resistance and low self-inductance. The graph at the bottom of the figure 4.64 is representative of the magnitude and direction of the flux density. It can be seen that the flux external to the shield is almost equal but with opposite direction, their sum approximating zero. The field from 'H' internal to the shield is in the same direction to that centred on 'G' and induces a current into element 'G' that is in the same direction as the current flowing through it. This is negative mutual induction and has the effect of reducing the self-inductance of element 'G'.

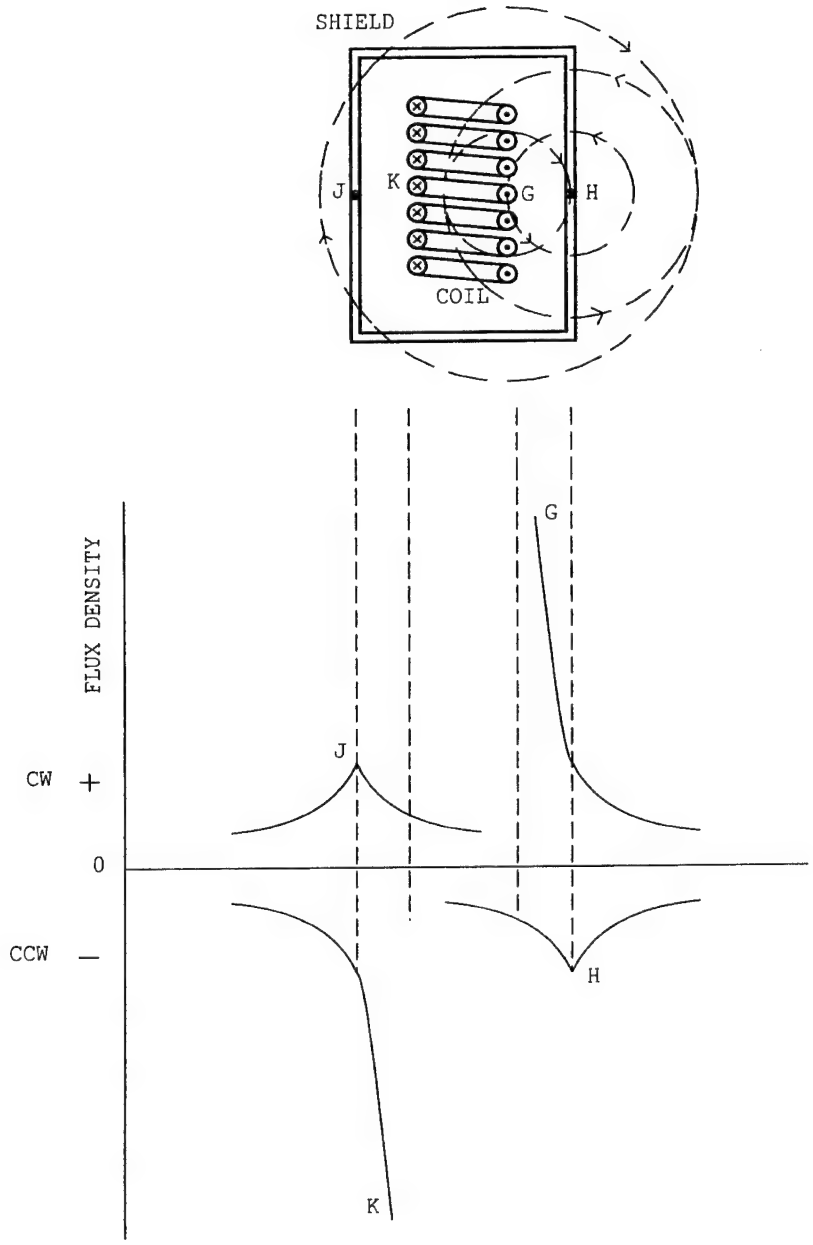

Figure 4.64 *Field strength distribution around element 'G' of a coil and element 'H' of the copper shield. Instantaneous R.F. currents and magnetic fields are shown*

4.3.4 Cancelling Fields Whose Direction of Travel are in-line with the Axis of an Air Wound Coil

Figure 4.65 is the same coil and enclosure as above where 'A' is an element of an end turn of the coil and 'E' is an element of the end section of the shield in-line with the coil diameter. The same increasing current is flowing as above and the field centred on 'A' generated by a current flowing out of the page has a clockwise direction and is expanding. The rate of change of flux induces a current into 'E' that is flowing into the page. Lines of flux centred on 'E' will have a counter-clockwise direction. Field lines external to the shield will be equal but of opposite direction and their effects cancel. This is shown in the graph at the bottom of figure 4.65. A similar analysis carried out on element 'B' which is on the opposite side of the same turn and lies on the diameter with 'A' will show the results in the graph at the top of figure 4.65. The current flowing in 'E' is into the page and the current in 'F' is out of the page. If a more detailed analysis were to be carried out it would be seen that the induced current into the shield flows in a circle whose centre lies on the axis of the air wound coil enclosed within the shield. It will also be seen that the direction of the circular current flow in the ends of the shield is opposite to the circular path the current follows as it travels through the helix of the coil. Figure 4.66 shows the circular path of the induced current in the end section of the shield. It can be seen that it is part of the total loop current circulating around the four sides of the enclosure. Positions of 'F', 'E' and 'H' are indicated.

The ability of the end sections of a shield to provide their own closed loop for the induced currents caused by fields whose direction of travel is in-line with the axis of the coil, indicates that only end sections of a shield are required if the air wound coils of a filter are mounted in-line on the same axis. By connecting these end sections to ground they also function as a Faraday shield reducing the capacitive coupling between the coils. The induced circular current in the end sections is zero at the point of the axis of the coil building to its maximum where the end section is the closest to the wire of the coil. Any electrical connection required through the shield to the coil should be made through the part of the end section that has minimum circulating current, that is, the part of the end section that lies on the axis of the coil. This ensures minimum disturbance to the circulating eddy currents and hence has minimum effect on the shield's effectiveness. This construction guide is valid for fully enclosed shielding or shielding employing only end sections.

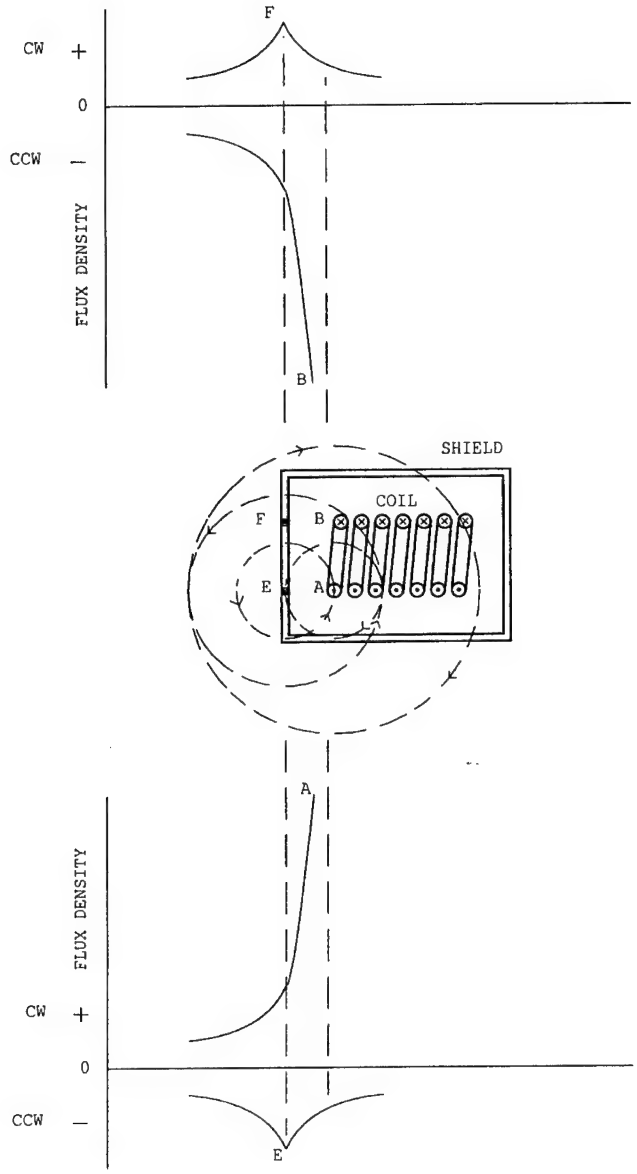

Figure 4.65 *Field strength distribution around element 'A' of a coil and element 'E' of the copper shield. Instantaneous R.F. currents and magnetic fields are shown*

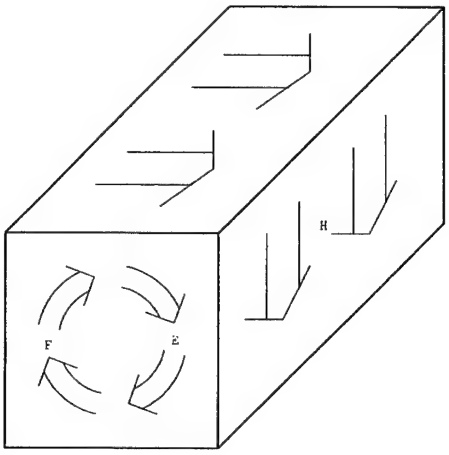

Figure 4.66 *Direction of instantaneous R.F. currents induced into a fully enclosed copper shield surrounding an air wound helical coil. Note the positions of 'E', 'F' and 'H' from the previous diagrams*

4.3.5 Summarising Shielding

The overall effect the conducting shield has on the coil is to lower its Q through energy lost in the resistive path of the induced circulating eddy currents in the shield, a decrease in inductance through negative mutual induction with the shield and, a decrease in the coil's self-resonant frequency by increasing the distributed capacitive coupling via the shield. The latter has the effect of increasing the coil's apparent inductance.

Materials to be used as shields placed around coils operating at R.F. frequencies should be non-magnetic with a very low resistivity. The shield can be considered as a closed single turn loop that has eddy currents induced into it by a traversing magnetic field. As such, steps should be taken to maximise the Q of the loop by keeping its resistive losses to a minimum. This ensures the external counter magnetic field generated by the eddy currents closely matches the field that produced it thereby neutralising its effects external to the enclosure and providing a high degree of isolation. The material most often used by this author when constructing prototype enclosures for filters is one ounce double sided tin plated PCB. When using this material, attention has to be paid to the construction to ensure a fully enclosed conducting path exists in the three planes of the internal walls.

4.4 Unwanted Resonances of Enclosures and Coils

Any fully closed conducting box can have several resonant modes, the frequencies of resonance being dependent upon the internal dimensions of the box. Also air wound coils can have standing waves developed across their length. Attenuation across the ends of a coil drops to low levels at spot frequencies where the electrical length equals half wavelength and multiples thereof. A lowpass filter constructed inside a fully enclosed shielded box will have a decrease in out-of-band attenuation at the enclosure resonant frequencies and at the in-line coils' half wavelength and multiples thereof. Very little attenuation occurs through the filter at these out-of-passband frequencies. Care needs to be taken in choosing the size of shielding enclosures to ensure the resonant modes of the enclosure and the half wavelength frequencies of coils do not coincide with any local transmitting equipment. This lack of adequate attenuation can generate spurious products in receivers limiting their spurious free dynamic range or provide insufficient attenuation to the upper harmonics of a transmitter connected to an aerial.

4.4.1 Enclosure Resonance

Equation (4.15), ref.31 pp430, can be used to calculate the frequencies at which the enclosure appears as a resonant cavity. Out of passband attenuation of L.P. filters can decrease to very low levels at these frequencies. The lowest frequency at which the enclosure will be resonant and have minimum attenuation between input and output is when $l = 0$, $n = 1$, $m = 1$.

$$f(l,m,n) = 300\sqrt{\left(\frac{l}{2d}\right)^2 + \left(\frac{m}{2b}\right)^2 + \left(\frac{n}{2a}\right)^2} \qquad (4.15)$$

where: $f(l,m,n)$ = resonant frequency of enclosure in MHz
l, m and n = a set of integers each corresponding to a different resonant frequency. Only one integer is allowed to be set to zero at any time.
a, b, and d = dimensions of the enclosure in meters (see figure 4.67)

It is extremely difficult to attenuate the passage of signals at the enclosure resonant frequencies; the internal electronic components only lower the resonant frequency. The only effective way would be to dampen the enclosure resonance by filling it with R.F. absorbing material. This would be counter-productive to any filter installed within, therefore prevention is the best course of action. The resonant frequencies of the enclosure will usually be in the microwave bands. If signals within this band are causing interference

to a receiver then a lowpass filter specifically designed to suppress this band constructed in a separate enclosure will need to be installed at the receiver's input.

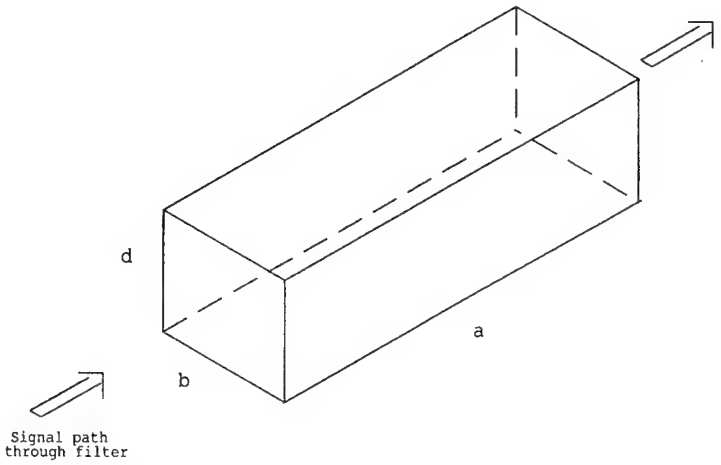

Figure 4.67 *Definitions of dimensions used in equation (4.15)*

4.4.2 Standing Waves in Air Wound Coils

All air wound coils wound with lengths of wire have distributed inductance from the wire length and through mutual coupling between elements of the wire being in close proximity to other elements on the same length of wire; put simply, mutual coupling between turns. Co-existing with this distributed inductance is distributed capacitance between turns. These two distributed elements form a distributed transmission line whose characteristic impedance is much higher than the standard 50 ohms impedance in common use. Standing waves can therefore develop along their length which makes the coil appear series resonant at a series of spot frequencies which are dependent on wire length, degree of mutual coupling between turns and the distributed capacitance both within the coil and to the installed environment. If the turns of the coil are compressed the distributed elements are increased and the distributed characteristic impedance decreases with a resulting decrease in spot frequency of the series of resonant frequencies. Likewise if the turns are stretched there is an increase in the frequency of the series of resonances.

If the distributed capacitance is kept reasonable, in keeping with good construction techniques, then the series of spot frequencies at which series resonance occurs can be

approximated to less than ten percent by equation (4.16). It is based on the well known equation for calculating frequency from the velocity of propagation divided by wave length and is offered as a guide to assist in predicting out-of-band filter performance. It shows the series of spot frequencies at which the attenuation through the coils used in the through path of a lowpass filter decreases to low levels. Also it can be used to approximate the upper frequency limit of a highpass filter where the largest shunt inductor first becomes series resonant. Equation (4.16) can be used for very low permeability toroidal coils only. As the toroidal coil's permeability is raised a correction factor based on the inductance increase of the one-turn-effect relative to free space needs to be applied. The shorter lengths of wire used when inductance enhancing material is employed raises the series of resonances to very high frequencies. Losses within the core material at these frequencies usually swamp the effects of the distributed high impedance transmission line.

$$f(n) \approx v_f \frac{n300}{2l} \tag{4.16}$$

where: $f(n)$ = approximate series resonant frequency of an air wound coil (MHz)
n = 2,3,4,5,6,7...etc.
v_f = velocity factor,
0.6 for close wound coils,
0.7 for normally wound optimum spacing, and
0.8 for coils with large spacing between turns
l = total length of wire in coil including lead length (metres)

Figure 4.68 is a plot showing the series of spot resonant frequencies for the 6.235μH air wound coil described in *Section 3.6*. It will be seen that there is relatively close agreement between the results of equation (4.16) and the measured response up to values of nine for n. Excessive amounts of distributed capacitance of an air wound coil, through turns being very close together and the coil in close proximity to shielding, will lower the series of resonant frequencies. Under these conditions equation (4.16) becomes inaccurate in proportion to the excess capacitance.

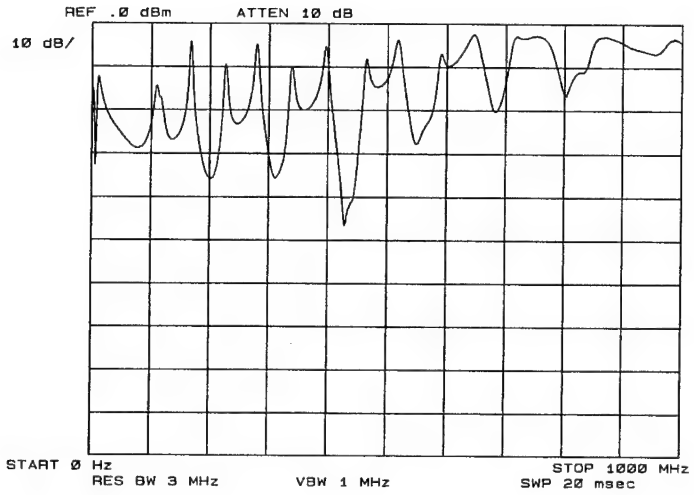

Figure 4.68 *High frequency response of the 6.235μH air wound coil showing the series resonances*

4.4.3 Out-of-Band Response of a Fully Shielded 32 MHz L.P. Filter Constructed With Air Wound Coils

Figure 4.69 is a plot of the out-of-band response up to 6 GHz of a 33MHz L.P. filter of figure 4.27 with coils (a). It should be noted that series resonances of the in-line air wound coils are predominantly seen. The first few resonances are effectively shunted to ground by the action of the shunt capacitors. As the frequency is raised the distributed inductance of the capacitors starts to predominate and becomes an appreciable percentage of the terminations, allowing coupling of signals at the coils' series resonant frequencies. It should be remembered that the physically small Philips miniature low k capacitors with very short lead lengths were used in this filter. If the physically larger 350 V silver mica capacitors were installed, the larger self-inductance of these capacitors would allow coupling of signals at lower series resonant frequencies than those shown in figure 4.69.

The enclosure of this filter (figure 4.28) is made of double sided PCB material soldered at all joints except for the lid which is held on by screws. The internal dimensions of the enclosure referenced to figure 4.67 are a=157 mm, b=40 mm and d=40 mm. There are three internal shields installed across the long dimension, one 35 mm from each end and one in the centre dividing the enclosure into four partitioned sections; two at 35x40x40 mm and two at 41x40x40 mm. These partitioned sections' dimensions are used to calculate the enclosure resonant frequencies. It is recommended that the lengths of the chambers not all

be identical. This helps to attenuate the passage of unwanted out-of-passband signals at microwave frequencies through the filter enclosure. Had all four chambers been made the same length, a fourth order spot frequency cavity filter would have been constructed at the chamber's resonant frequency.

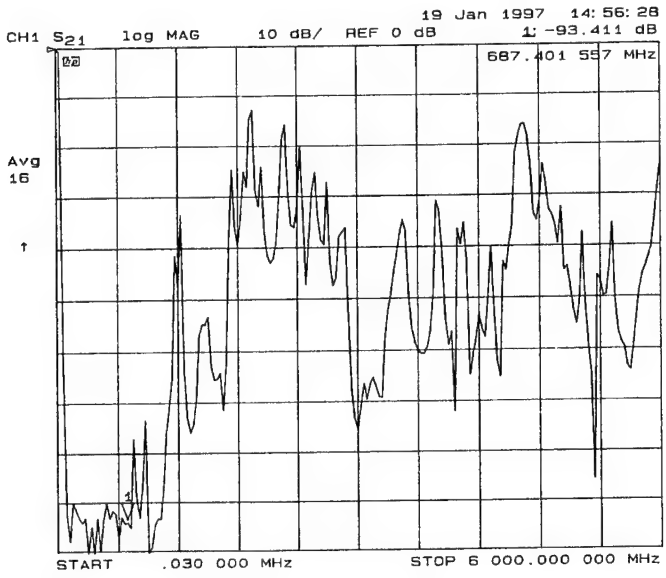

Figure 4.69 *Out-of-passband response to 6 GHz of the 33 MHz L.P. filter showing the various unwanted resonances*

5. ACKNOWLEDGMENTS

The sole responsibility for the accuracy of any technical writing lies with its author. Information obtained from references or discussions with colleagues is still the responsibility of the author for it was the author's decision to use or reject such information. With this in mind, this author wishes to acknowledge the contributions made to this document by the following people.

Angus Massie (Jr), for the many technical discussions which helped to clarify the reasons for the various observed responses of the many filters that were constructed.

Peter Wilinski, A friendly competition was agreed between Peter and this author as to who could build the better 33 MHz 9th order lowpass filter. An expanded central region of the Smith chart was needed to decide the winner. It should be noted that both completed filters in the contest were more than acceptable for any intended application. This author lost. Neither of us at the time understood why when similar construction techniques were used and both filters physically appeared the same. With endorsement from Peter, this author carefully measured every aspect of the winning filter to ascertain what gave it the edge. Close investigation revealed that Peter had slightly altered some of the capacitor values from the numeral design and had adjusted the in-line inductors to maintain the same cut-off frequency. This was further refined by this author using ARRL Radio Designer software and resulted in the normalised values for lowpass filters that appear in the appendix. This author then re-engineered his filter using the new normalised values maintaining the same diameter for his air-wound coils. While there was an improvement in the in-band response over both filters in the competition, there was still a small in-band through path residual inductance that could not be adjusted out. This residual inductance was smaller in the winning filter. Both filters had the same enclosure dimensions, the only difference being the diameter of the air wound in-line coils - the author's coils having a slightly smaller diameter. Various diameter coils were then tried and it was found that the residual through path reactance could be made to swing from slightly inductive through zero to slightly capacitive. This led this author to the development of equation (4.13) to counter the one-turn-effect of coils used in the through path of lowpass filters. Peter's coils were closer to the ideal ratio. The final filter was used as the reference filter in section *4.2.4 Reducing the Effects of Mutual Coupling Through Shielding*. It is unknown if this paper would have been written if this author had won the competition. What is known is it owes its existence to a friendly competition, this author losing and this author's desire to understand why he lost.

Angus Massie (Snr), for reviewing the document and his many suggestions during this process which helped to make it more readable.

6. REFERENCES

1. Hank Meyer, " *Accurate Single-Layer-Solenoid Inductance Calculations* " QST April 1992, Technical Correspondence, pp., 76-77. Corrections to this article appear in QST July 1992, pp.73.

2. A. H. Morton, " *Advanced Electrical Engineering* " Pitman Publishing Limited, London, ISBN 0-273-40172-6.

3. "*Skin Effect* " Wireless World, November 1953, pp., 537-541.

4. "*Radiotron Designer's Handbook* " Fourth Edition, Fifth Impression (1957), Amalgamated Wireless Valve Co. Pty.Ltd., Sydney, Australia.

5. Randall W. Rhea, (1994) " *HF Filter Design and Computer Simulation* " Noble Publishing, ISBN 1-884932-25-8.

6. Paul Lorrain and Dale Corson, (1970) " *Electromagnetic Fields and Waves* " second edition, ISBN: 0-7167-0331-9.

7. Robert Resnick and David Halliday, " *Physics* " Wiley International Edition, parts I and II.

8. Charles A. Coulson, (1958) " *Electricity* " fifth edition, University Mathematical Texts, published by Oliver and Boyd Ltd., Edinburgh, Great Britain.

9. Frederwick W. Grover, (1946) " *Inductance Calculations* " D. Van Nostrand Company Inc., 250 Fourth Avenue, New York.

10. Nelson M. Cooke and John Markus, " *Electronics and Nucleonics Dictionary* " McGraw-Hill Book Company, Inc.

11. V. G. Welsby, (1960) " *The Theory and Design of Inductance Coils* " second edition, Macdonald & Co. (Publishers) Ltd., 16 Maddox St., London, W.I

12. Simon Ramo, John R. Whinnery and Theodore Van Duzer, (1965) " *Fields and Waves in Communication Electronics* " John Wiley & Sons, Inc. LCCCN: 65-19477.

13. James K Hardy, (1979) " *High Frequency Circuit Design* " Preston Publishing Company, Inc., Reston, Virginia 22090. ISBN 0-8359-2824-1

14. R. G. Medhurst, " *H.F. Resistance and Self-Capacitance of Single-Layer Solenoids* " Wireless Engineer, February and March, 1947.

15. " *Iron-Powder and Ferrite Coil Forms* " Amidon Associates, Inc.. P.O. Box 956, Torrance, California 90508.

16. H. O. Granberg, " *Tables Simplify High-Power Lowpass Filter Design* " Microwaves & RF, May 1991, pp163.

17. " *Electronic Engineers' Handbook* " Third Edition, Donald G. Fink and Donald Christiansen editors, McGRAW-HILL, Inc.. ISBN 0-07-020982-0

18. M. G. Scroggie, (1971) " *Radio and Electronic Laboratory Handbook* " Eighth edition, ISBN 0-592-05950-2.

19. " *Designing High-Power Series Inductors and Shunt Capacitors* " Microwaves & RF, October 1987, pp 97-107.

20. Henry W. Ott, (1988) " *Noise Reduction Techniques in Electronic Systems* " second edition, ISBN 0-471-85068-3.

21. D. S. Evans, G. R. Jessop, (1976) " *VHF/UHF Manual* " 3rd edition, RSGB publication.

22. Frederick Emmons Terman, (1943) " *Radio Engineers' Handbook* " McGraw-Hill Book Company, Inc.

23. Charles S. Walker (1990) " *Capacitance, Inductance and Crosstalk Analysis* " Artech House, Inc., ISBN 0-89006-392-3

24. Brian C. Wadell (1991) " *Transmission Line Design Handbook* " Artech House, ISBN 0-89006-436-9

25. A. Kumar (1996) " *Antenna Design With Fiber Optics* " Artech House, ISBN 0-89006-759-7.

26. R. S. Hewes and G.R.Jessop (1985), " *Radio Data Reference Book* " R.S.G.B. ISBN-0-900612-67-3.

27. M.F. "Doug" DeMaw (1981), " *Ferromagnetic-Core Design and Application Handbook* " Prentice-Hall, Inc. ISBN 0-13-314088-1.

28. J. H. Reyner (1959), " *Radio and Electronics* " The New Era Publishing Co. Ltd., 45 Oxford Street, London, W.C.1

29. M. G. Scroggie (1963), " *Second Thoughts on Radio Theory* " Iliffe Books Ltd. Dorset House, Stamford St., London S.E.1

30. " *Reference Data for Radio Engineers* " (1975) Howard W. Sams & Co., Inc., Indianapolis, Indiana 46268. ISBN 0-672-21218-8

31. Peter A. Rizzi " *Microwave Engineering, Passive circuits* " (1988) Prentice-Hall, Inc. ISBN 0-13-586702-9

7. APPENDIX

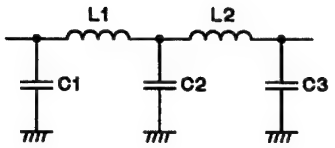

C1 = 0.719676 L1 = 1.675197
C2 = 1.96827 L2 = 1.675197
C3 = 0.719676

Normalised values for 5th order L.P. filter

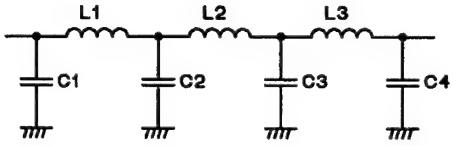

C1 = 0.6252397 L1 = 1.488474
C2 = 1.875719 L2 = 1.97253
C3 = 1.875719 L3 = 1.488474
C4 = 0.6252397

Normalised values for 7th order L.P. filter

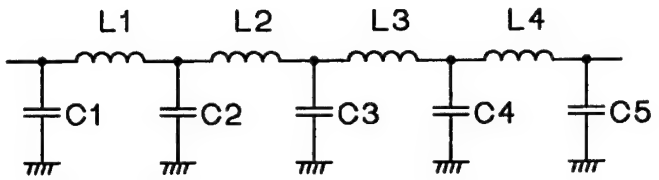

C1 = 0.5521	L1 = 1.359316
C2 = 1.761	L2 = 1.934266
C3 = 1.979957	L3 = 1.934266
C4 = 1.761	L4 = 1.359316
C5 = 0.5521	

Normalised values for 9th order L.P. filter

$$C = \frac{Cn}{2\pi f_o R} \qquad L = \frac{Ln\ R}{2\pi f_o}$$

f_o = cut-off frequency of filter (Hz)
Cn = normalised value of C (F)
Ln = normalised value of L (H)
R = termination resistance (ohms)

DISTRIBUTION LIST

Construction Techniques for Highpass and Lowpass Filters used in the 1 MHz to 1 GHz Frequency Range

W. Martinsen

AUSTRALIA

DEFENCE ORGANISATION

	No. of copies
Task Sponsor	
DGLD R1-3-A010	1
S&T Program	
Chief Defence Scientist FAS Science Policy AS Science Corporate Management Director General Science Policy Development	shared copy
Counsellor Defence Science, London	Doc Data Sheet
Counsellor Defence Science, Washington	Doc Data Sheet
Scientific Adviser to MRDC, Thailand	Doc Data Sheet
Scientific Adviser Joint	1
Navy Scientific Adviser	Doc Data Sht & Dist List
Scientific Adviser - Army	Doc Data Sht & Dist List
Air Force Scientific Adviser	Doc Data Sht & Dist List
Scientific Adviser to the DMO M&A	Doc Data Sht & Dist List
Scientific Adviser to the DMO ELL	Doc Data Sht & Dist List
Director of Trials	1
Systems Sciences Laboratory	
M. Woods EWRD/AR/180Labs	1
K. Goldsmith AOD/AMS/42Labs	1
Dr. C. Leat AOD/AMS/42Labs	1
Information Sciences Laboratory	
Chief of Intelligence, Surveillance & Reconnaissance Division	Doc Data Sht & Dist List
Research Leader, Secure Communications Branch	1
Head IA Group	1
W. Martinsen ISRD/IA/203Labs	10
I. Leach ISRD/IA/203Labs	1
A. Massie (Jr) ISRD/IA/203Labs	2
J. Arnold ISRD/IA/203Labs	1
J. Magarelli ISRD/IA/203Labs	1
A. Caldow ISRD/IA/203Labs	1
L. Richards ISRD/IA/203Labs	1
D. Taylor ISRD/IA/203Labs	1
P. Wilinski ISRD/IA/203Labs	1

C. Dolling ISRD/IA/203Labs	1
K. Gooley ISRD/RFP/200Labs	1
J. Lane ISRD/RFP/200Labs	1
M. Spooner ISRD/RFP/200Labs	1
S. Leak ISL/IND/MIN/205Labs	1
D. Miller EWRD/ESS/71Labs	1
L. Casey ISRD/IA/203Labs	1
DSTO Library and Archives	
Library Edinburgh	1 & Doc Data Sht
Australian Archives	1
Capability Systems Division	
Director General Maritime Development	Doc Data Sheet
Director General Land Development	1
Director General Aerospace Development	Doc Data Sheet
Director General Information Capability Development	Doc Data Sheet
Office of the Chief Information Officer	
Deputy CIO	Doc Data Sheet
Director General Information Policy and Plans	Doc Data Sheet
AS Information Structures and Futures	Doc Data Sheet
AS Information Architecture and Management	Doc Data Sheet
Director General Australian Defence Simulation Office	Doc Data Sheet
Strategy Group	
Director General Military Strategy	Doc Data Sheet
Director General Preparedness	Doc Data Sheet
HQAST	
SO (Science) (ASJIC)	Doc Data Sheet
Navy	
Director General Navy Capability, Performance and Plans, Navy Headquarters	Doc Data Sheet
Director General Navy Strategic Policy and Futures, Navy Headquarters	Doc Data Sheet
Air Force	
SO (Science) - Headquarters Air Combat Group, RAAF Base, Williamtown NSW 2314	Doc Data Sht & Exec Summ
Army	
ABCA National Standardisation Officer, Land Warfare Development Sector, Puckapunyal	e-mailed Doc Data Sheet
SO (Science), Deployable Joint Force Headquarters (DJFHQ) (L), Enoggera QLD	Doc Data Sheet
SO (Science) - Land Headquarters (LHQ), Victoria Barracks NSW	Doc Data & Exec Summ
Intelligence Program	

DGSTA Defence Intelligence Organisation	1
Manager, Information Centre, Defence Intelligence Organisation	1 (PDF version)
Assistant Secretary Corporate, Defence Imagery and Geospatial Organisation	Doc Data Sheet
L. Walton R6-5-21	1

Defence Materiel Organisation

Head Airborne Surveillance and Control	Doc Data Sheet
Head Aerospace Systems Division	Doc Data Sheet
Head Electronic Systems Division	Doc Data Sheet
Head Maritime Systems Division	Doc Data Sheet
Head Land Systems Division	Doc Data Sheet
Head Industry Division	Doc Data Sheet
Chief Joint Logistics Command	Doc Data Sheet
Management Information Systems Division	Doc Data Sheet
Head Materiel Finance	Doc Data Sheet

Defence Libraries

Library Manager, DLS-Canberra	Doc Data Sheet
Library Manager, DLS - Sydney West	Doc Data Sheet

OTHER ORGANISATIONS

National Library of Australia	1
NASA (Canberra)	1
Codan Pty. Ltd., 81 Graves St., Newton 5074, S.A.	1
Mini-Kits, P.O. Box 368, Enfield Plaza 5085, S.A.	1
Ebor Computing, (att. S.W. (Bill) Cumpston), 147 Henley Beach Rd., Mile End 5031, S.A.	1
Tomco Pty. Ltd., 17 Clarke St., Norwood 5067 S.A.	1
Daronmont Technologies, (att. P. Arthur), Innovation House, First Av., Technology Park, Mawson Lakes 5095. S.A.	1

UNIVERSITIES AND COLLEGES

Australian Defence Force Academy	
Library	1
Head of Aerospace and Mechanical Engineering	1
Hargrave Library, Monash University	Doc Data Sheet
Librarian, Flinders University	1

OUTSIDE AUSTRALIA

INTERNATIONAL DEFENCE INFORMATION CENTRES

US Defense Technical Information Center	2
UK Defence Research Information Centre	2
Canada Defence Scientific Information Service	e-mail link to pdf
NZ Defence Information Centre	1

ABSTRACTING AND INFORMATION ORGANISATIONS	
Library, Chemical Abstracts Reference Service	1
Engineering Societies Library, US	1
Materials Information, Cambridge Scientific Abstracts, US	1
Documents Librarian, The Center for Research Libraries, US	1
SPARES	5
Total number of copies:	**64**

DEFENCE SCIENCE AND TECHNOLOGY ORGANISATION
DOCUMENT CONTROL DATA

1. PRIVACY MARKING/CAVEAT (OF DOCUMENT)
N/A

2. TITLE

Construction Techniques for LC Highpass and Lowpass Filters used in the 1MHz to 1 GHz Frequency Range

3. SECURITY CLASSIFICATION (FOR UNCLASSIFIED REPORTS THAT ARE LIMITED RELEASE USE (L) NEXT TO DOCUMENT CLASSIFICATION)

Document	U
Title	U
Abstract	U

4. AUTHOR(S)

W. Martinsen

5. CORPORATE AUTHOR

Information Sciences Laboratory
PO Box 1500
Edinburgh, South Australia 5111 Australia

6a. DSTO NUMBER	6b. AR NUMBER	6c. TYPE OF REPORT	7. DOCUMENT DATE
DSTO-TN-0531	AR-012-994	Technical Note	October 2003

8. FILE NUMBER	9. TASK NUMBER	10. TASK SPONSOR	11. NO. OF PAGES	12. NO. OF REFERENCES
E 8709/8/17 Pt 1	ARM02/005	DGLD	130	31

13. URL on the World Wide

http://www.dsto.defence.gov.au/corporate/reports/ DSTO-TN-0531.pdf

14. RELEASE AUTHORITY

Chief, Intelligence, Surveillance and Reconnaissance Division

15. SECONDARY RELEASE STATEMENT OF THIS DOCUMENT

Approved for public release

OVERSEAS ENQUIRIES OUTSIDE STATED LIMITATIONS SHOULD BE REFERRED THROU GH DOCUMENT EXCHANGE, PO BOX 1500, EDINBUR GH, SA 5111

16. DELIBERATE ANNOUNCEMENT

No Limitations

17. CITATION IN OTHER DOCUMENTS Yes

18. DEFTEST DESCRIPTORS

High pass filters; Low pass filters; Radio frequency filters; Electron device manufacture; Off the shelf equipment

19. ABSTRACT

This technical note describes construction techniques for building passive LC highpass and lowpass filters whose intended use spans several octaves of bandwidth. It examines limitations in the frequency domain of the two basic components, inductors and capacitors, used to build these filters, the unwanted effects of the distributed reactance of opposite sign to the wanted within these components and the electro-magnetic coupling between these components when used to build a filter. The impact these unwanted characteristics have on the filter's overall performance is then examined. Recommendations are given on the various steps that may be taken to reduce these unwanted effects minimising the deviation from a filter's ideal performance.